AD NUMBER
ADB000431
LIMITATION CHANGES
TO: **Approved for public release; distribution is unlimited.**
FROM: **Distribution authorized to U.S. Gov't. agencies only; Test and Evaluation; OCT 1974. Other requests shall be referred to Army Ballistic Research Laboratory, Attn: AMXBR-SS, Aberdeen Proving Ground, MD 21005.**
AUTHORITY
usaardc ltr, 31 may 1978

AD

BRL R 1745

AD B000431

BRL

REPORT NO. 1745

WIND TUNNEL STUDY OF BASE DRAG REDUCTION BY COMBUSTION OF PYROTECHNICS

J. Richard Ward
Frank P. Baltakis
Steven W. Pronchick

October 1974

Distribution limited to US Government agencies only; Test and Evaluation; Oct 74. Other requests for this document must be referred to Director, USA Ballistic Research Laboratories, ATTN: AMXBR-SS, Aberdeen Proving Ground, Maryland 21005.

USA BALLISTIC RESEARCH LABORATORIES
ABERDEEN PROVING GROUND, MARYLAND

UNCLASSIFIED

SECURITY CLASSIFICATION OF THIS PAGE (When Data Entered)

REPORT DOCUMENTATION PAGE

READ INSTRUCTIONS BEFORE COMPLETING FORM

1. REPORT NUMBER: BRL REPORT NO. 1745
2. GOVT ACCESSION NO.
3. RECIPIENT'S CATALOG NUMBER
4. TITLE (and Subtitle): WIND TUNNEL STUDY OF BASE DRAG REDUCTION BY COMBUSTION OF PYROTECHNICS
5. TYPE OF REPORT & PERIOD COVERED
6. PERFORMING ORG. REPORT NUMBER
7. AUTHOR(s):

J. Richard Ward, Ballistic Research Laboratories
Frank P. Baltakis, Naval Ordnance Laboratory
Steven W. Pronchick, Naval Ordnance Laboratory

8. CONTRACT OR GRANT NUMBER(s)
9. PERFORMING ORGANIZATION NAME AND ADDRESS: USA Ballistic Research Laboratories, Aberdeen Proving Ground, Maryland 21005
10. PROGRAM ELEMENT, PROJECT, TASK AREA & WORK UNIT NUMBERS: 1W562604A600
11. CONTROLLING OFFICE NAME AND ADDRESS: U.S. Army Materiel Command, 5001 Eisehnower Avenue, Alexandria, Virginia 22333
12. REPORT DATE: OCTOBER 1974
13. NUMBER OF PAGES: 93
14. MONITORING AGENCY NAME & ADDRESS (if different from Controlling Office)
15. SECURITY CLASS. (of this report): UNCLASSIFIED
15a. DECLASSIFICATION/DOWNGRADING SCHEDULE
16. DISTRIBUTION STATEMENT (of this Report): Distribution limited to US Government agencies only; Test and Evaluation; October 1974. Other requests for this document must be referred to Director, USA Ballistic Research Laboratories, ATTN: AMXBR-SS, Aberdeen Proving Ground, Maryland 21005.
17. DISTRIBUTION STATEMENT (of the abstract entered in Block 20, if different from Report)

18. SUPPLEMENTARY NOTES
19. KEY WORDS (Continue on reverse side if necessary and identify by block number): Pyrotechnics, Base Drag REduction, Fumers and Combustion in Supersonic Flow
20. ABSTRACT (Continue on reverse side if necessary and identify by block number) jah

It is well known that tracer rounds have longer ranges than comparable non-tracer ammunition, and the ballistician seeks ways to degrade the tracer's ballistics to match the conventional round. Presumably the tracer reduces base drag by addition of heat and mass into the near wake of the projectile. Wind tunnel experiments conducted with well-defined gases at metered rates of injection showed that a hot, low-molecular weight gas would be the better drag

DD FORM 1473, 1 JAN 73 EDITION OF 1 NOV 65 IS OBSOLETE

UNCLASSIFIED

SECURITY CLASSIFICATION OF THIS PAGE (When Data Entered) reducer. It was also suggested that combustion in the near-wake could be advantageous. Fuel-rich mixtures of magnesium and inorganic oxidizers were investigated in this report as such gas generators (designated "fumers"). The excess magnesium in such mixtures is to be the hot, low-molecular weight gas. Wind tunnel tests were performed at the Naval Ordnance Laboratory to see if fuel-rich magnesium propellants reduced base drag. These tests showed reductions on the order of fifty percent in combination with oxidizers that burn slowly enough to be used in small arms applications. The base drag reduction was also proportional to the quantity of excess fuel in the mixtures. Ignition of mixtures containing over forty percent by weight magnesium was impossible for all oxidizers tested.

TABLE OF CONTENTS

LIST OF TABLES

LIST OF FIGURES

I. INTRODUCTION

A systematic look at new projectile shapes for small arms application was recently completed.[1*] This study concluded that a projectile with length to diameter ratio 5.5 was superior to conventional projectiles with length to diameter ratios near 3. These conclusions were subsequently verified experimentally.[2,3] A much further increase in effectiveness could be achieved if the base drag could be eliminated as shown in Figure 1 in which effectiveness is measured as remaining energy at a given range. Reduced time of flight and a flatter trajectory are two other advantages achieved with the lower drag projectiles. This report is concerned with a systematic approach to try to eliminate base drag with materials compatible with small arms ammunition.

II. SELECTION OF MATERIALS

Two recent reviews[4,5] on the reduction of base drag in supersonic flow by direct injection of heat and mass into the near wake both conclude the ejected gases should have the following characteristics:

1. low molecular weight
2. low ejection velocity
3. combustion in the near wake.

Obvious candidates from such considerations are fuel-rich solid propellants stored in the rear of the projectile. However, such materials must be able to be ignited by the combustion gases in the barrel; to continue burning in the rapid pressurization in the gun barrel and depressurization when the projectile exists the gun, to sustain combustion during projectile flight at which time the base pressure will be near atmospheric. These conditions ruled out conventional gun and rocket propellants, but not solid pyrotechnics. The pyrotechnics may also meet the conditions set above for the ejected gases, since Stevenson[6] reports the intensity of light emitted by a burning pyrotechnic is related to the amount of fuel burning in the wake. Other authors[7] noted a direct correlation between the quantity of excess fuel in a pyrotechnic and light intensity suggesting that fuel rich pyrotechnics may provide the after-burning sought. Tracer rounds have been observed to have lower total drag coefficients than corresponding conventional rounds[8,9]. The drag coefficient change varies with mach number and is less pronounced with boattailing, suggesting this change is associated with a change in the base drag.[10] A comparison between 20mm tracer and conventional round is shown in Figure 2. Thus, fuel-rich pyrotechnics were selected for investigation as "fumers" (a name chosen to distinguish these materials from conventional tracers).

**References are listed on page* 45.

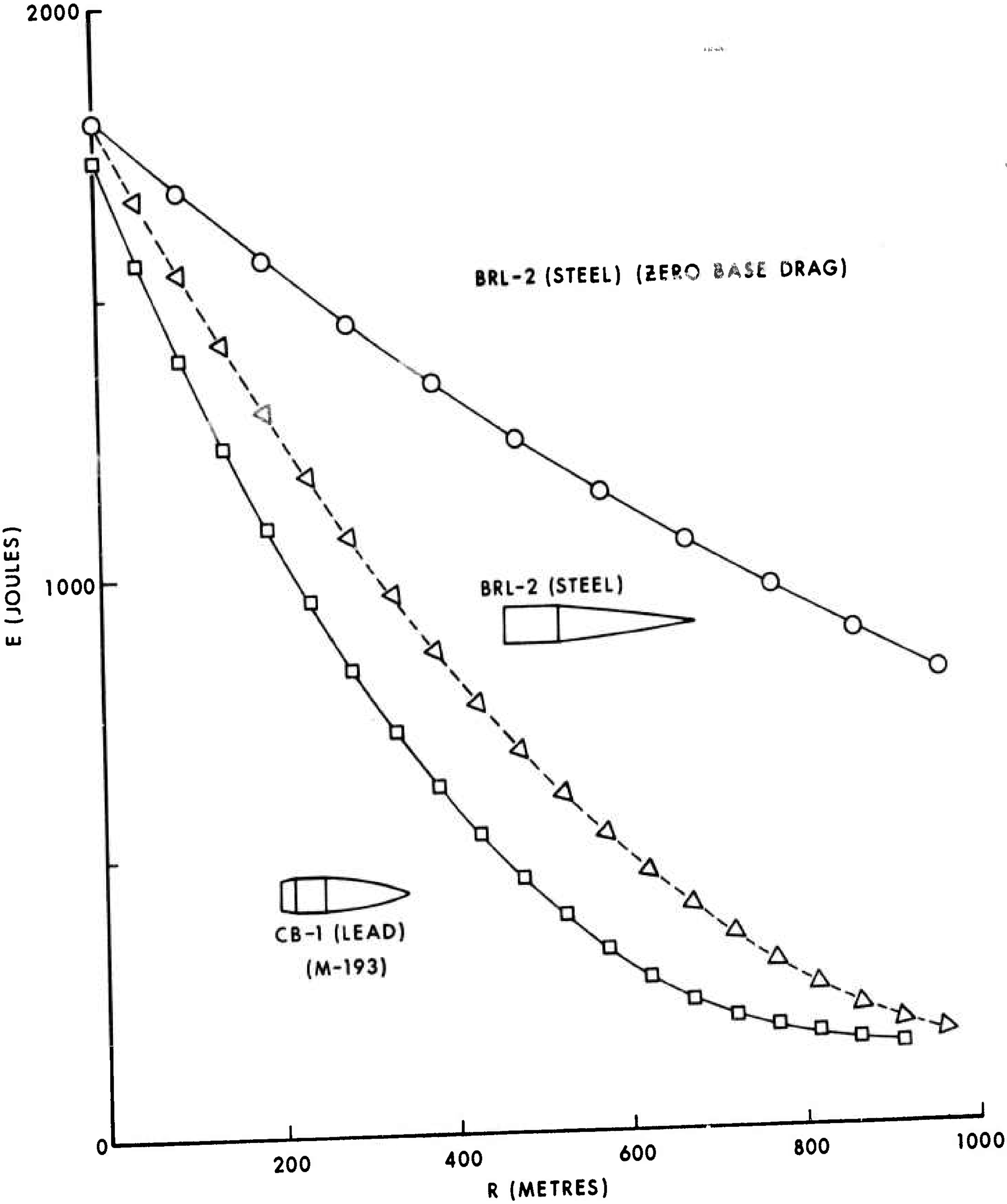

Figure 1. Remaining Energy vs Range for Idealized M-193 and an Improved Ballistic Shape Projectile

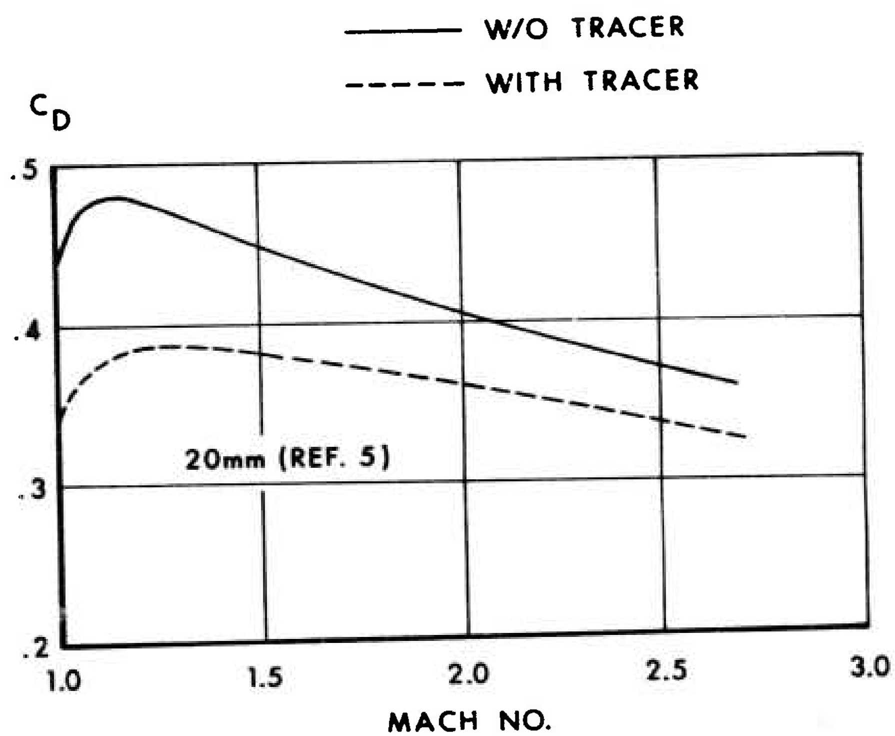

Figure 2. Drag Coefficient of 20mm Shell With and Without Tracer as a Function of Mach Number

To test fuel-rich pyrotechnics as fumers, wind tunnel tests were performed at the Naval Ordnance Laboratory's Hypersonic Tunnel. This tunnel could be preheated so that ambient temperature could be achieved in the test section and the wind tunnel model constructed for these tests could be spun to over 50,000 revolutions/minute. A wind tunnel test plan was constructed to test the following:

1. verify that the burning pyrotechnics change base pressure
2. correlate such an effect as a function of mach number, spin rate, fuel content, and the area of the burning surface in order to find the optimum mix.

The constituents used in these tests are listed in Table I; the wind tunnel test plan is listed in Table II.

III. EXPERIMENTAL

The study was conducted in a wind tunnel at freestream Mach numbers of 1.5, 2.0 and 2.5 at duplicated sea-level pressures and temperatures (at a reduced pressure at Mach 2.5). Special, centerbody-type nozzles of 6-inch exit diameter were designed and constructed for this program. The nozzles were installed in the NOL Hypersonic Tunnel System using a special settling chamber. Figure 3 illustrates the test setup.

The tests were conducted using an open-jet type test arrangement. The tunnel test cell pressure was controlled by means of an orifice at the diffuser inlet and it was maintained at approximately seventy percent of the static pressure of the test jet. The interaction of the upstream Mach line, emanating from the nozzle exit, and the model wake centerline was approximately 3.0, 4.5 and 6.2 model diameters for the Mach 1.5, 2.0 and 2.5 nozzles respectively.

To eliminate model support effects on the base pressure, the model was simulated by a cylindrical nozzle centerbody which was supported in the settling chamber upstream of the nozzle throat. The model was 1 inch in diameter and approximately 10.5 inches long (measured from the nozzle throat). It was instrumented with ten pressure transducers and one thermocouple. Figure 4 shows the instrumentation layout, Table III gives the location data.

As part of the facility calibration procedure, model base pressure distribution and Pitot pressure and total-temperature variation in the model wake region were also measured. A special plug with five static-pressure orifices was installed in the model base cavity (Figure 4) for the base pressure distribution measurements and a Pitot pressure rake containing 20 pressure probes and a temperature rake with 10 shielded thermocouples (Figure 5 and Table III) were used for the wake flow surveys.

Table I.

Wind Tunnel Experiments
At Naval Ordnance Laboratory

Capsule No.	Composition[a]	Mach No.	Spin Rate, rpm x 1000
1	R20C	2	0
2	R284	2	0
3	F1	2	0
4	F3	2	0
5	Fi3	2	0
6	F14	2	0
7	F1/F4 layered	2	0
8	F4	2	0
9	F4+6% binder[b]	2	0
10	F4+15% binder[b]	2	0
11	F4+20% binder[b]	2	0
12	Mg+20%[c]	2	0
13	30%	2	0
14	36.5	2	0
15	40	2	0
16	50	2	0
17	60	2	0
18	67.8	2	0
19	70	2	0
20	75	2	0
21	36.5 (1/4)	2	0
22	36.5 (1/2)	2	0
23	36.5 (3/4)	2	0
24	50 (1/4)	2	0
25	50 (1/2)	2	0
26	50 (3/4)	2	0
27	67.8 (1/4)	2	0
28	67.8 (1/2)	2	0
36	67.8 (3/4)	2	0
31	Mg 36.5	2	50
I	36 (1/2)	2	25
30	36 1/2 (1/2)	2	50
32	36 1/2 (3/4)	2	50
34	50	2	50
II	50	2	25
33	50 (1/2)	2	50
35	50 (3/4)	2	50
29	67.8	2	50
III	67.8	2	25
37	67.8	2	50
38	67.8	2	50

Table I.

Wind Tunnel Experiments
At Naval Ordnance Laboratory (Cont'd)

Capsule No.	Composition[a]		Mach No.	Spin Rate, rpm x 1000
39	Mg 36		2.5	50
40	36		2.5	25
41	36	(1/2)	2.5	50
42	36.5	(3/4)	2.5	50
43	50		2.5	50
44	50		2.5	75
45	50	(1/2)	2.5	50
46	50	(3/4)	2.5	50
47	67.8		2.5	50
48	67.8		2.5	25
49	67.8	(1/2)	2.5	50
50	67.8	(3/4)	2.5	50
51	Mg 36.5		1.5	50
52	36.5		1.5	25
53	36.5	(1/2)	1.5	50
54	36.5	(3/4)	1.5	50
55	50		1.5	50
56	50		1.5	25
57	50	(1/2)	1.5	50
58	50	(3/4)	1.5	50
59	67.8		1.5	50
60	67.8		1.5	25
61	67.8	(1/2)	1.5	50
62	67.8	(3/4)	1.5	50

[a] percent by weight

[b] calcium resinate

[c] binary mixtures of magnesium and strontium nitrate. Only the magnesium content in percent by weight is listed.

Table II.

Constituents of Pyrotechnic Mixes Used in the NOL Wind Tunnel Tests

Mix Designation	Constituent	Percentage by Weight
R20C	SrO_2	65.7
	CaRes[a]	6.0
	Mg	21.5
	PbO_2	3.4
	BaO_2	3.4
R284	Mg	28
	$Sr(NO_3)_2$	55
	PVC[b]	17
I-136	CaRes	10
	SrO_2	90
Fumer 1	Mg	8.1
	SiO_2	78.8
	C	4.0
	CaRes	9.1
Fumer 3	Al	27.1
	$Sr(NO_3)_2$	63.8
	CaRes	9.1
Fumer 4	Mg	33.2
	$Sr(NO_3)_2$	57.7
	CaRes	9.1
Fumer 13	Fumer 4	90
	gelatin	10
Fumer 14	Fumer 1	90
	gelatin	10

[a] calcium resinate

[b] polyvinylchloride

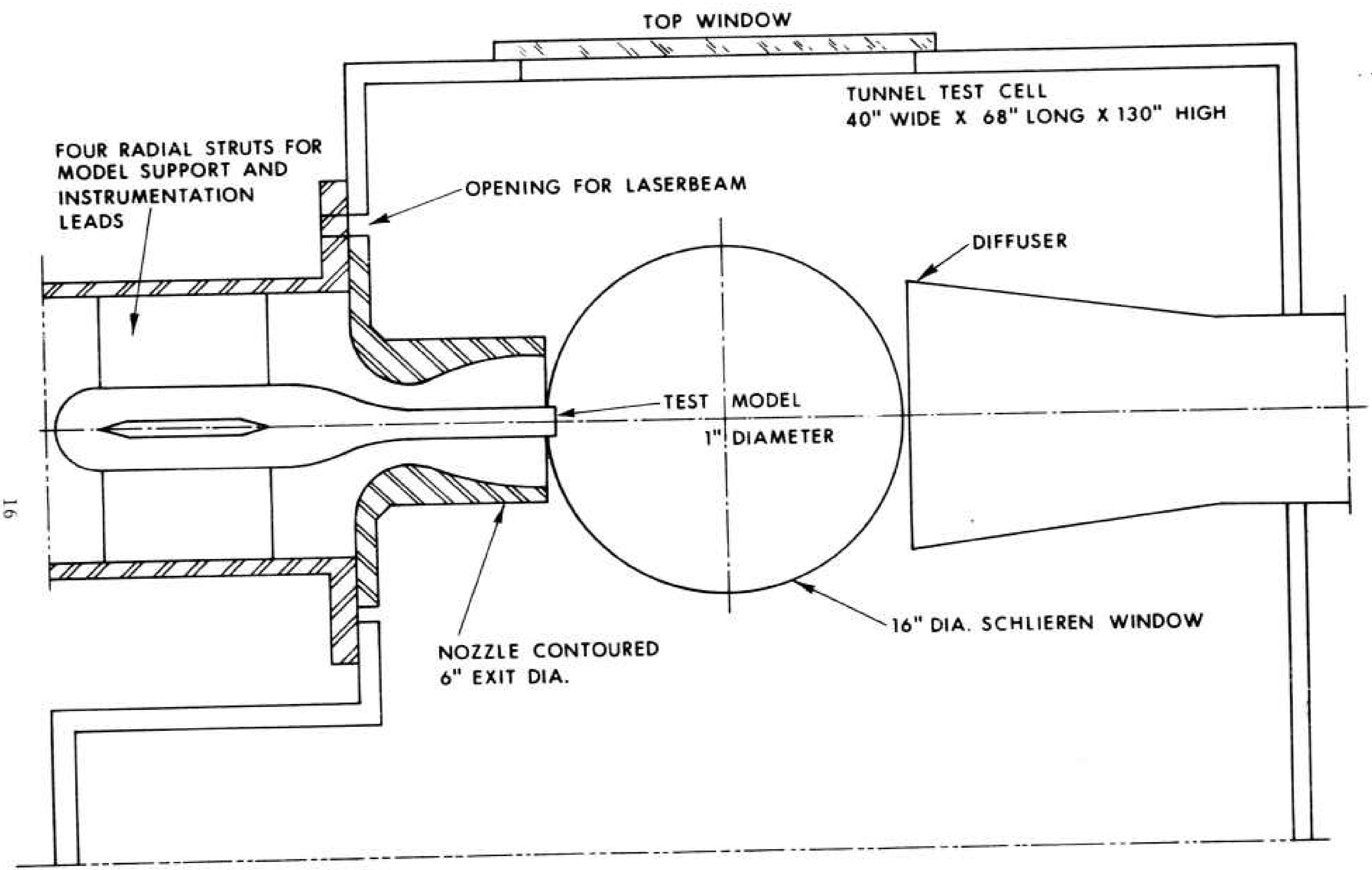

Figure 3. Wind Tunnel Test Set-up

Table III. Instrument Location Data[a]

Instrument	Roll Angle, θ deg	Axial Distance, X in	Radial Distance, R in	Orifice Diameter in
P1	60	0	0.45	0.046
P2	150	0	0.45	0.046
P3	240	0	0.45	0.046
P4	330	0	0.45	0.046
P5	120	-0.08	0.50	0.032
P6	300	-0.08	0.50	0.032
P7	210	-0.25	0.50	0.032
P8	180	-0.50	0.50	0.032
P9	30	-0.25	0.40	0.032
P10	0	-1.00	0.40	0.032
P11	0	0	0.115	0.046
P12	0	0	0	0.046
P13	180	0	0.115	0.046
P14	180	0	0.230	0.046
P15	180	0	0.115	0.046
P16	0	Xp	1.125	0.046
P17	0	Xp	0.875	0.046
P18	0	Xp	0.625	0.046
P19	0	Xp	0.375	0.046
P20	0	Xp	0.125	0.046
P21	0	Xp	0	0.046
P22	180	Xp	0.125	0.046
P23	180	Xp	0.250	0.046
P24	180	Xp	0.345	0.046
P25	180	Xp	0.500	0.046
P26	180	Xp	0.625	0.046
P27	180	Xp	0.750	0.046
P28	180	Xp	0.875	0.046
P29	180	Xp	1.125	0.046
P30	180	Xp	1.375	0.046
P31	180	Xp	1.625	0.046
P32	180	Xp	1.875	0.046
P33	180	Xp	2.125	0.046
P34	180	Xp	2.375	0.046
P35	180	Xp	2.625	0.046
TC1	210	0.06	0.45	
TC2	345	XTC	0.50	
TC3	345	XTC	0.25	
TC4	0	XTC	0	
TC5	165	XTC	0.25	
TC6	165	XTC	0.50	
TC7	165	XTC	0.75	
TC8	165	XTC	1.00	
TC9	165	XTC	1.25	
TC10	165	XTC	1.50	
TC11	165	XTC	1.75	

[a]Reference figures 4 and 5.

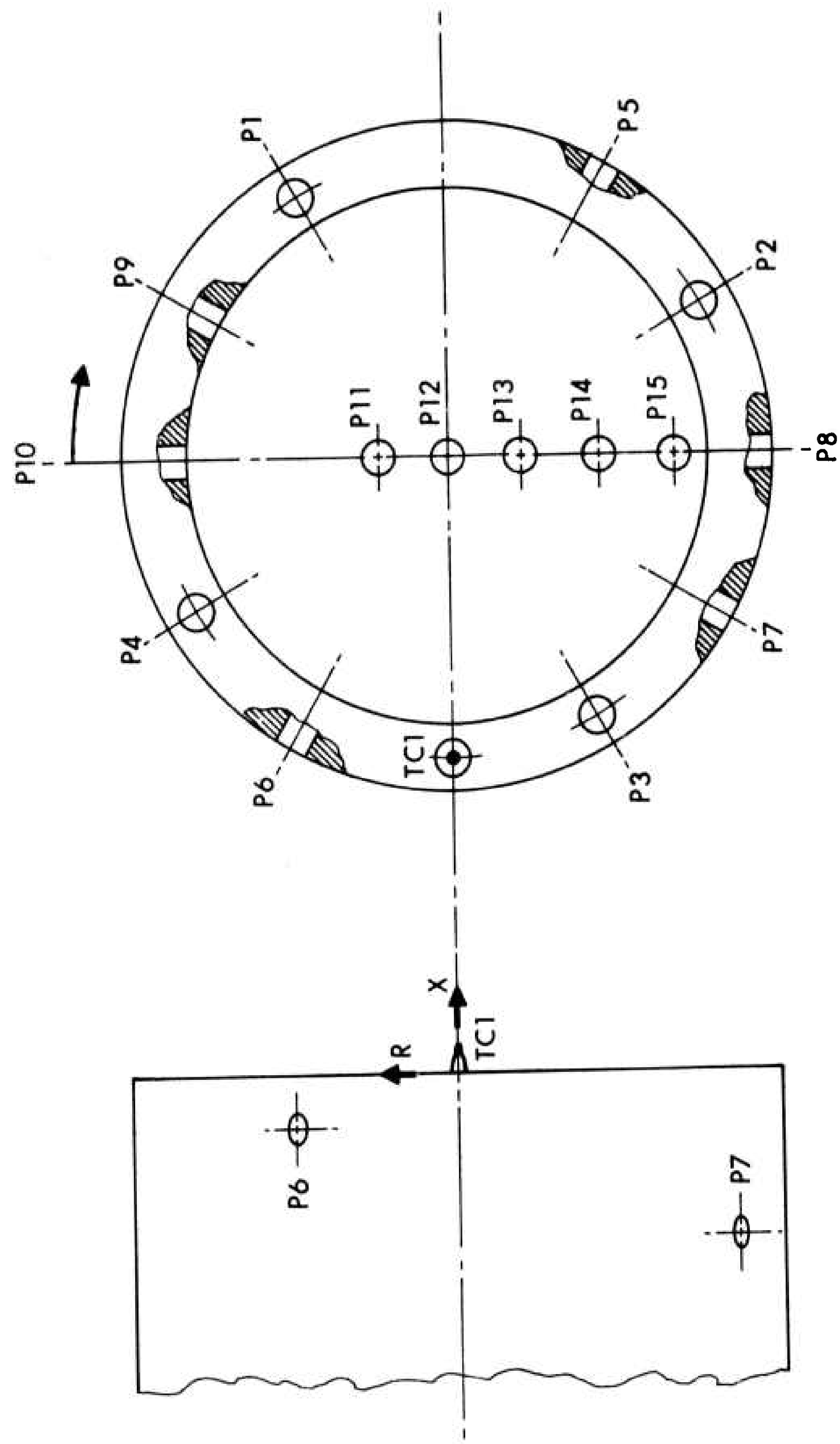

Figure 4. Model Instrumentation

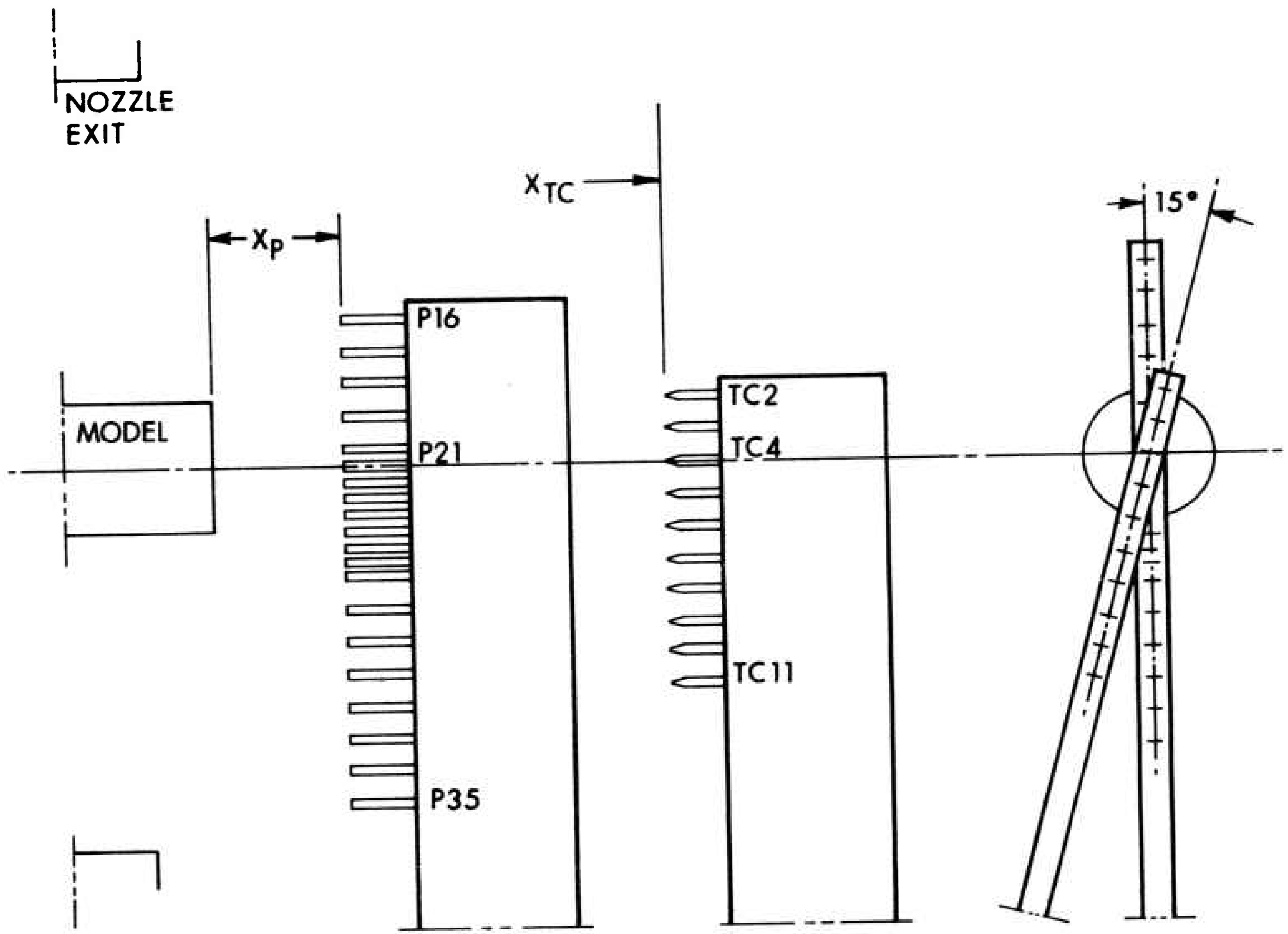

Figure 5. Pitot Pressure and Temperature Rakes for Wake Flow Surveys

The pressure orifice diameters ranged from 0.032 to 0.046 inch. On the model outer surface, and inside the cavity, locations P6 to P10, the orifice diameter was 0.032 inch. At the base, locations P1 to P4 and P11 to P15, it was 0.046 inch. The pitot pressure rake was made up of 0.063 in. O.D., 0.046 in. I.D. tubes spaced 1/4 or 1/8 inch apart. The temperature rake was made of chromel-alumel thermocouples of .06-inch diameter wire shielded with a .095 O.D., .0625 I.D., vented stainless-steel tubing. The temperature rake was positioned 4.125 inches downstream of the Pitot rake and rotated 15 degrees relative to the Pitot rake. The pitot pressure - temperature rake assembly was moved to different axial positions during the flow calibration tests. The rakes were also used during the combustion tests during which it was located six inches downstream of the model base (six inches to the Pitot rake.) A photograph of the test section with the rakes is shown in Figure 6.

With exception of P11 to P15 each orifice was connected to a separate pressure transducer (strain gage type, Statham) for continuous measurement. Pressures at orifices P11 to P15 were connected to a single transducer through a scanner-type valve in order to obtain a more precise relative variation across the model base. The output of the pressure transducers and of the thermocouples were recorded on magnetic tape using the Hypersonic Tunnel analog-to-digital recording system.

The pyrotechnics were presse into hollow, steel cylinders, one of which is shown in Figure 7. A pressing pressure of 240 MN/m^2 (35,000 psi) was used for all samples. The flow area restric ors were steel washers sized to reduce the flow by 25, 50, or 75 percent respectively. An air turbine, illustrated in Figure 8, served to provide the required spin rates. The turbine air was ducted in an exhausted through the model support struts. The turbine spin rate was measured with a magnetic-type pickup and it was recorded on tape along with the model pressures.

The photographic instrumentation included a schlieren system with a 35mm and a 70mm camera, a 16mm color-film camera, and a TV camera (Figure 9). The schlieren system with its light beam in the horizontal plane viewed the flow field through the tunnel side windows. The 16mm and the TV cameras viewed the test area through the tunnel top window. The 35mm pulse-type camera was operated at 10 pictures per second (pps), the 70mm camera at approximately 1 pps, and the 16mm camera at 24 pps. The TV camera was used to monitor the test section events.

The pyrotechnics were ignited with a 250-watt Westinghouse CO_2 laser. The arrangement of the laser is shown in Figure 9. The light beam diameter at the plane of impingement on the propellant was about 3/8-inch. Continuous mode was used with the exposure ranging from two to five seconds.

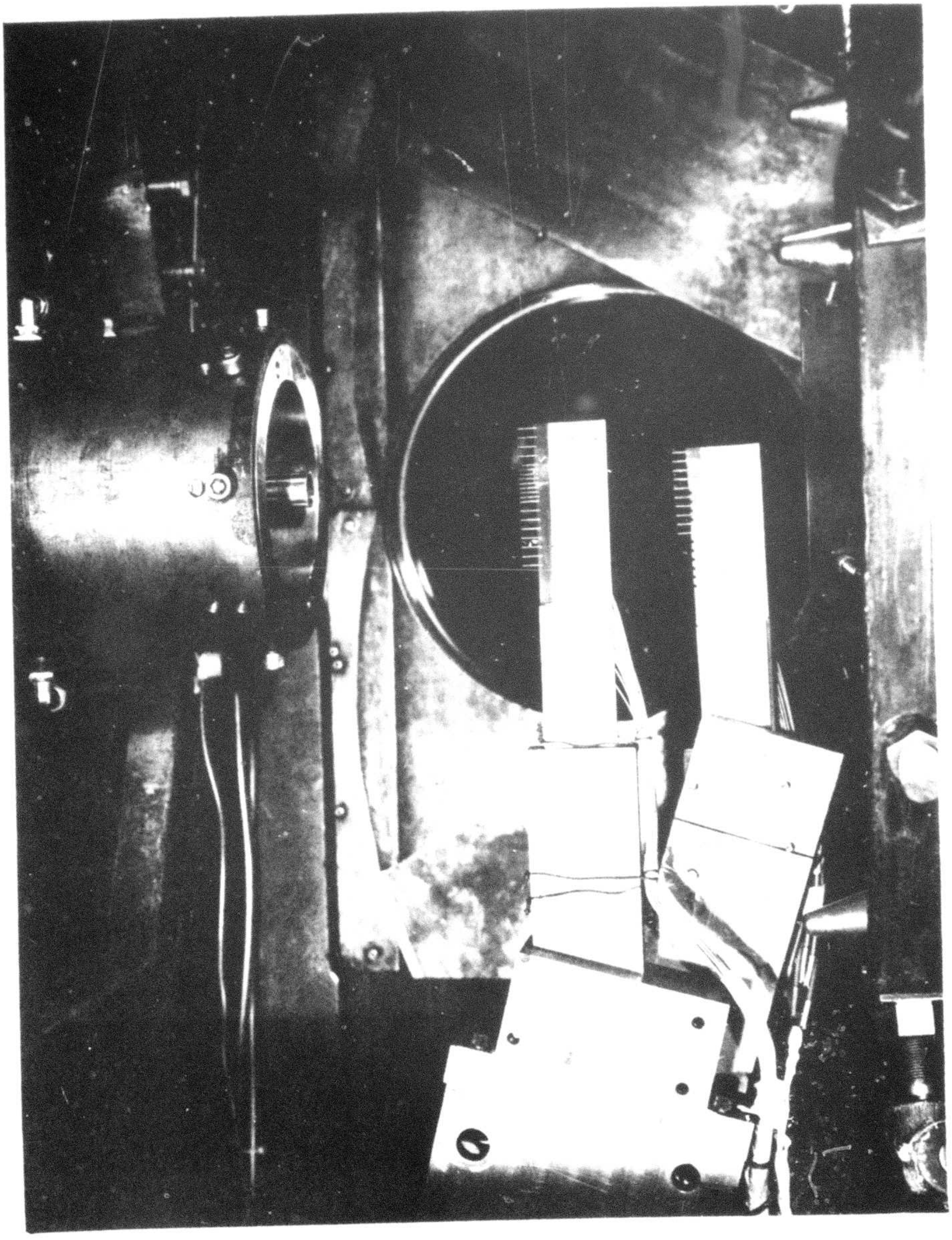

Figure 6. Photograph of the Test Area

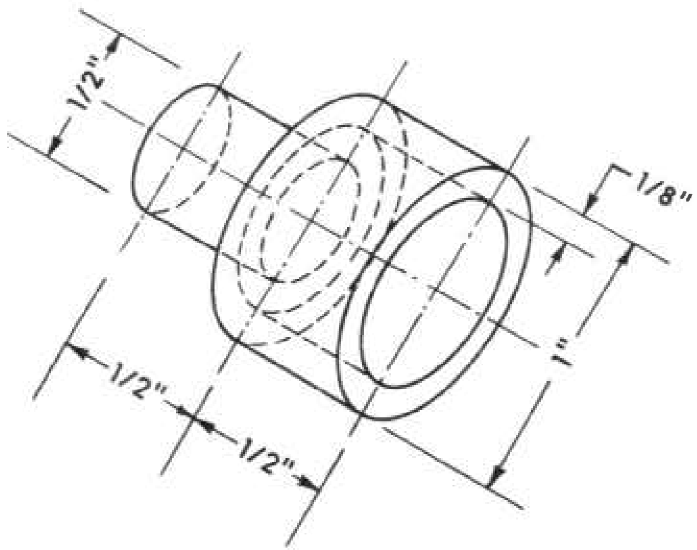

Figure 7. Steel Capsules for Wind Tunnel Test Samples

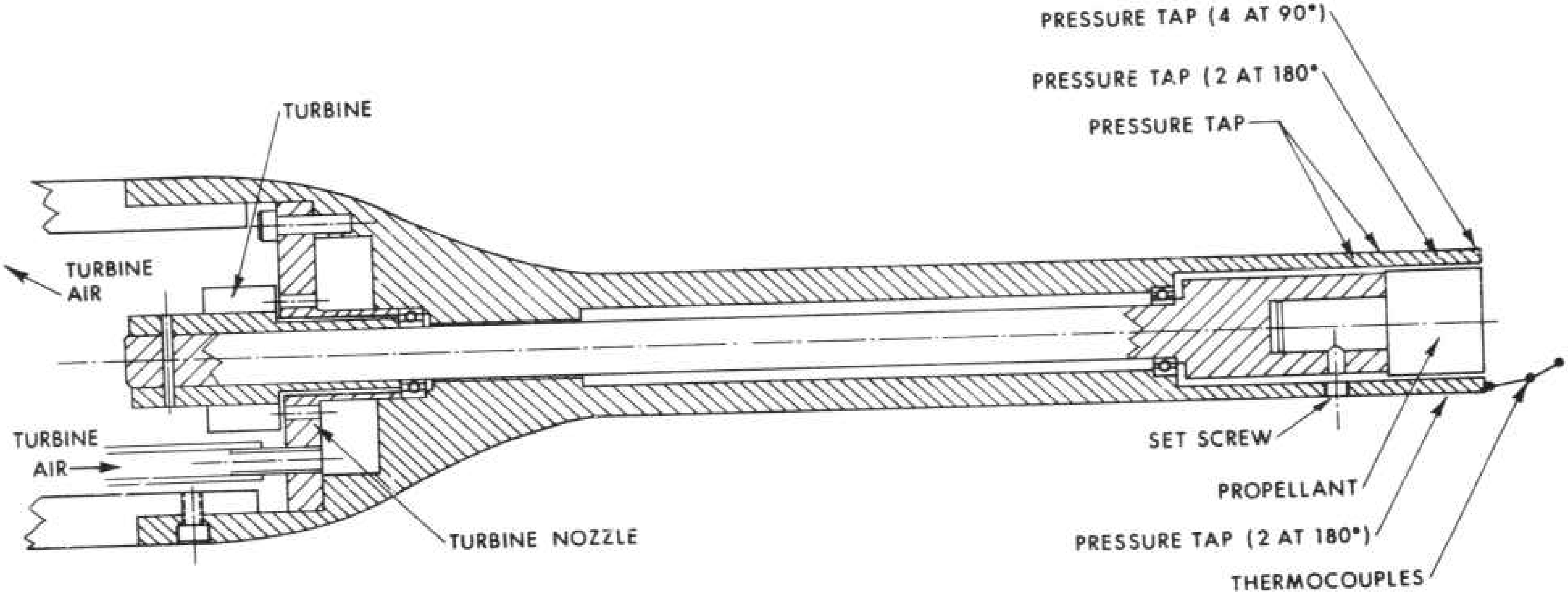

Figure 8. Test Model Configuration

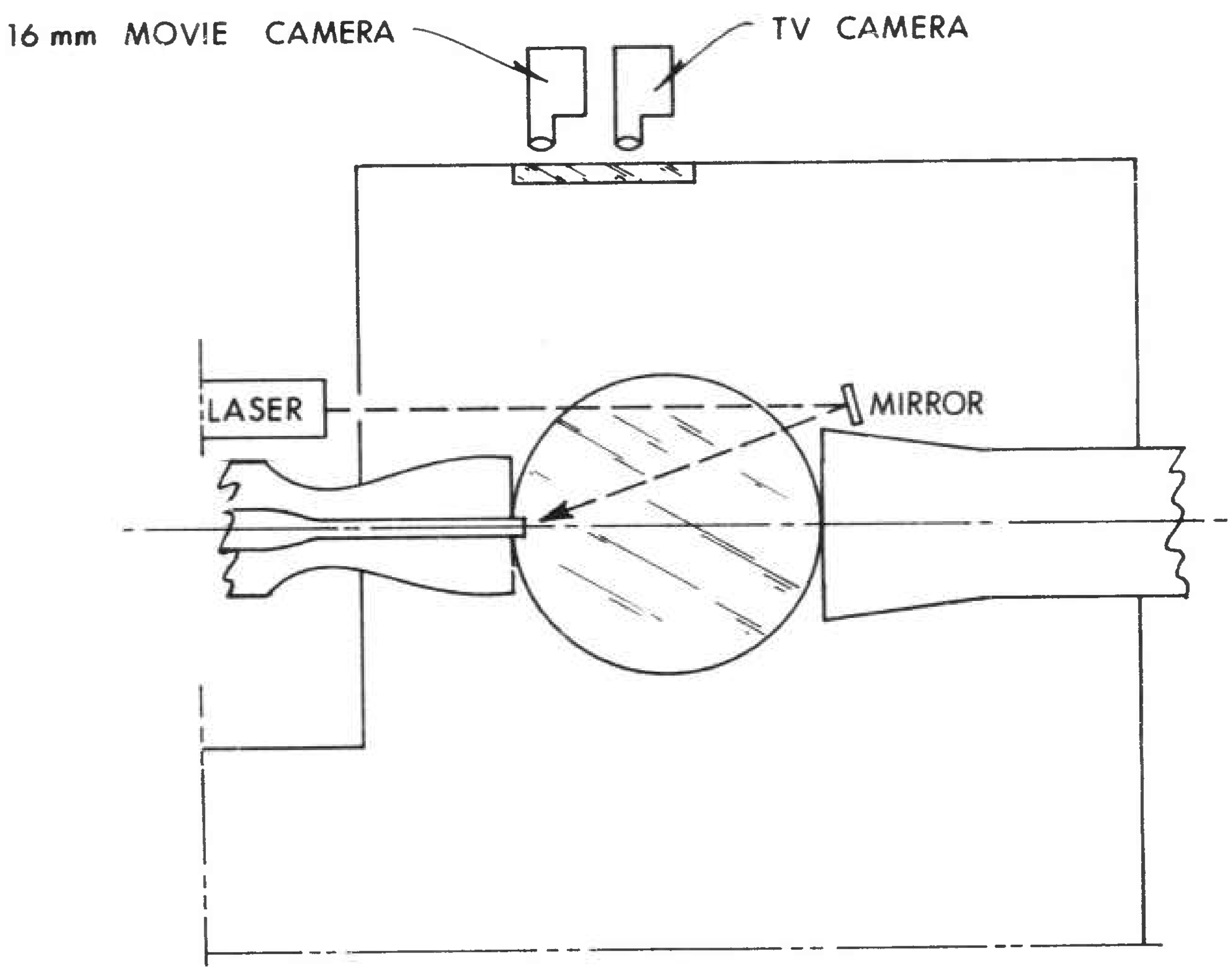

Figure 9. Photographic and Laser Ignition Set-up

IV. RESULTS

A. Initial Runs-Flow Calibration

Three nozzles were constructed with nominal Mach numbers 1.5, 2, and 2.5 respectively. The first runs were made to calibrate the nozzles and to insure that the base pressure and free stream pressure region were unaffected by reflections from the nozzles. In addition we wished to see the effect of the presence of the Pitot rake on the near-wake region. The Pitot rake (Figure 5) was used for these surveys. The rake was held in the vertical centerplane with probes extending 1.12 inches above and 2.75 inches below the centerline for all the tests.

The Mach number profiles at the nozzle exit were uniform containing only slight deviations. The Mach number measured for each nozzle was 1.56, 1.98, and 2.56 respectively. Schlieren photographs (Figures 10-12) also show the flow to be free of strong non-uniformities or disturbances at the nozzle exit. Series of Mach waves visible on the photographs are due to small imperfections in the nozzle contour or to discontinuities such as openings for the spin mechanism screws on the centerbody. The Mach 1.5 nozzle contains one somewhat more pronounced disturbance. Its influence on base pressure is estimated to be one or two percent. Static pressures measured on the centerbody (P7 and P8) are in good agreement with the static pressures from the Pitot measurements. The surface pressure measured at stations P5 and P6 is expected to be influenced by the base flow and to be slightly lower.[5]

The base pressure data, radial distribution, and its variation with the axial rake position are summarized in Figures 13-15. To avoid interfering with base pressure data, the axial rake remained six inches or more behind the model during the base burning tests. This limited severely the planned surveys of downstream pressure and temperature with burning.

B. Base-Burning Runs

A summary of all the runs for which base burning data was obtained is shown in Table IV. A glance at Table I shows that it was not possible to follow the test sequence originally planned, since it was not possible to ignite magnesium-strontium nitrate mixes with more than thirty percent magnesium. Two important exceptions were noted. When the fuel capsules were heated to approximately 470K, the 36.5/63.5 binary $Mg/Sr(NO_3)_2$ mixes could be ignited. The temperature of the capsule is estimated to have been 390K at the time of ignition. These runs will be referred to as preheated under the remarks column in Table IV. It was also found that the presence of the area restrictors aided ignition. A similar effect was noted during actual 7.62mm fumer firings.[11] Since successful ignition had been achieved for every candidate mix proposed in the test series with a fifty-watt CO_2 laser[12], it was thought that part of

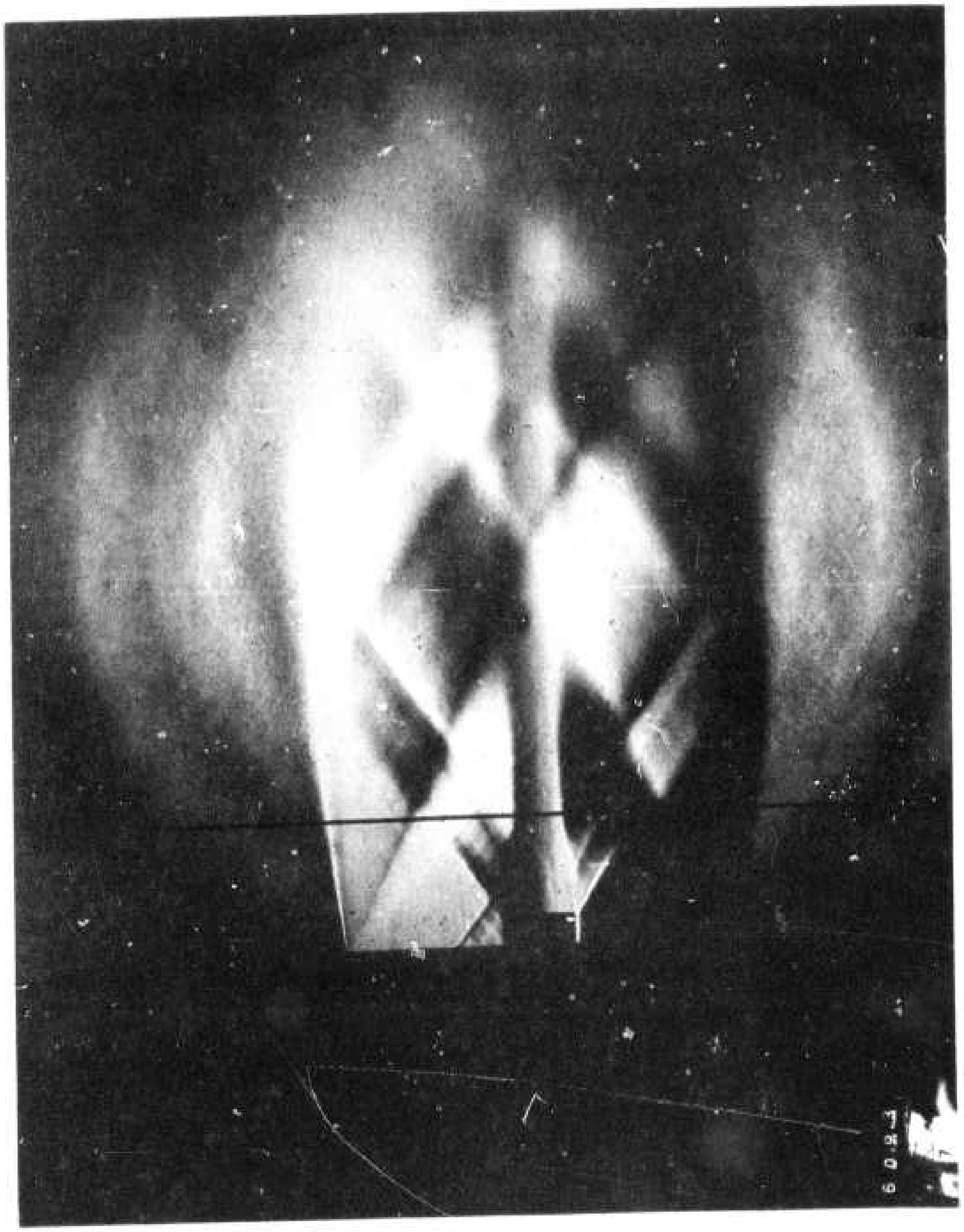

Figure 10. Schlieren Photograph of Flow Without Combustion, M=1.5

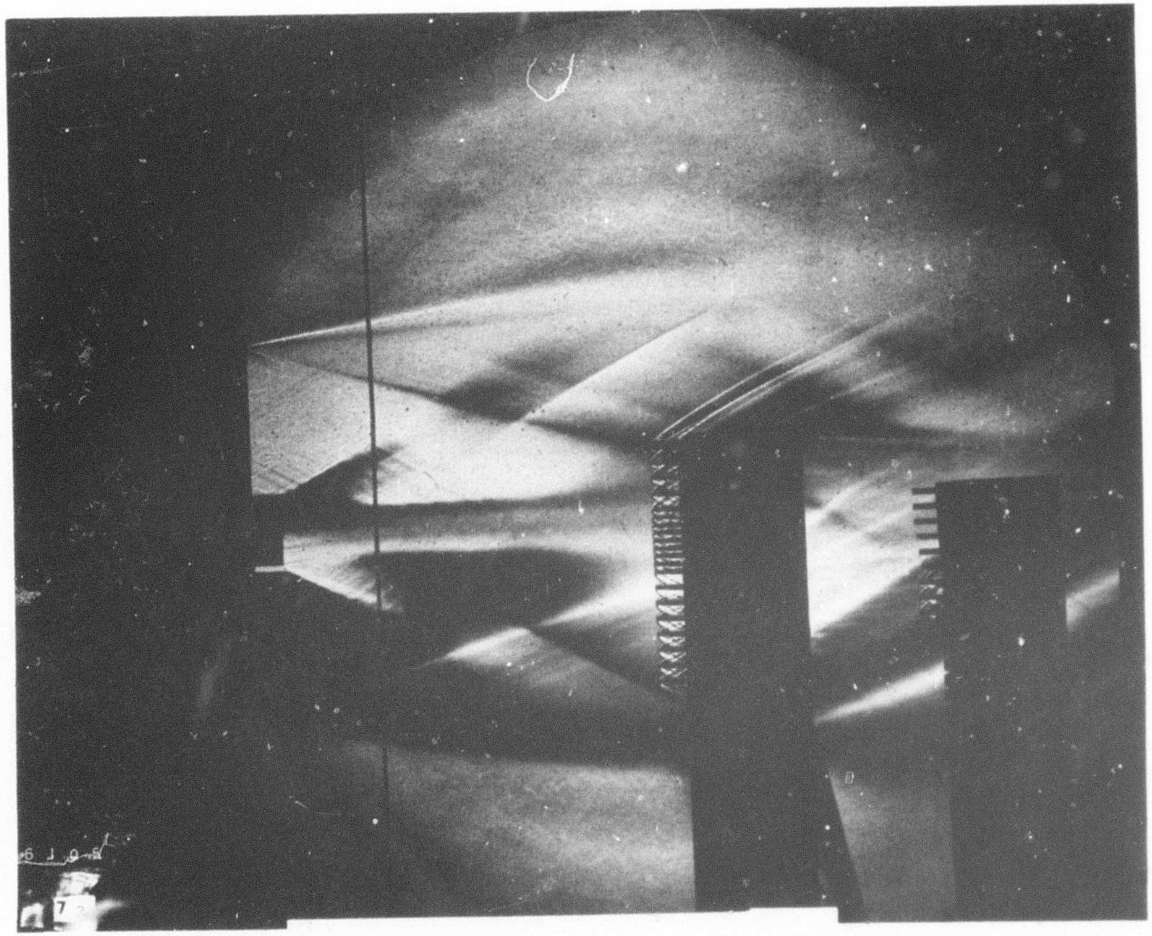

Figure 11. Schlieren Photograph of Flow Without Combustion, M=2

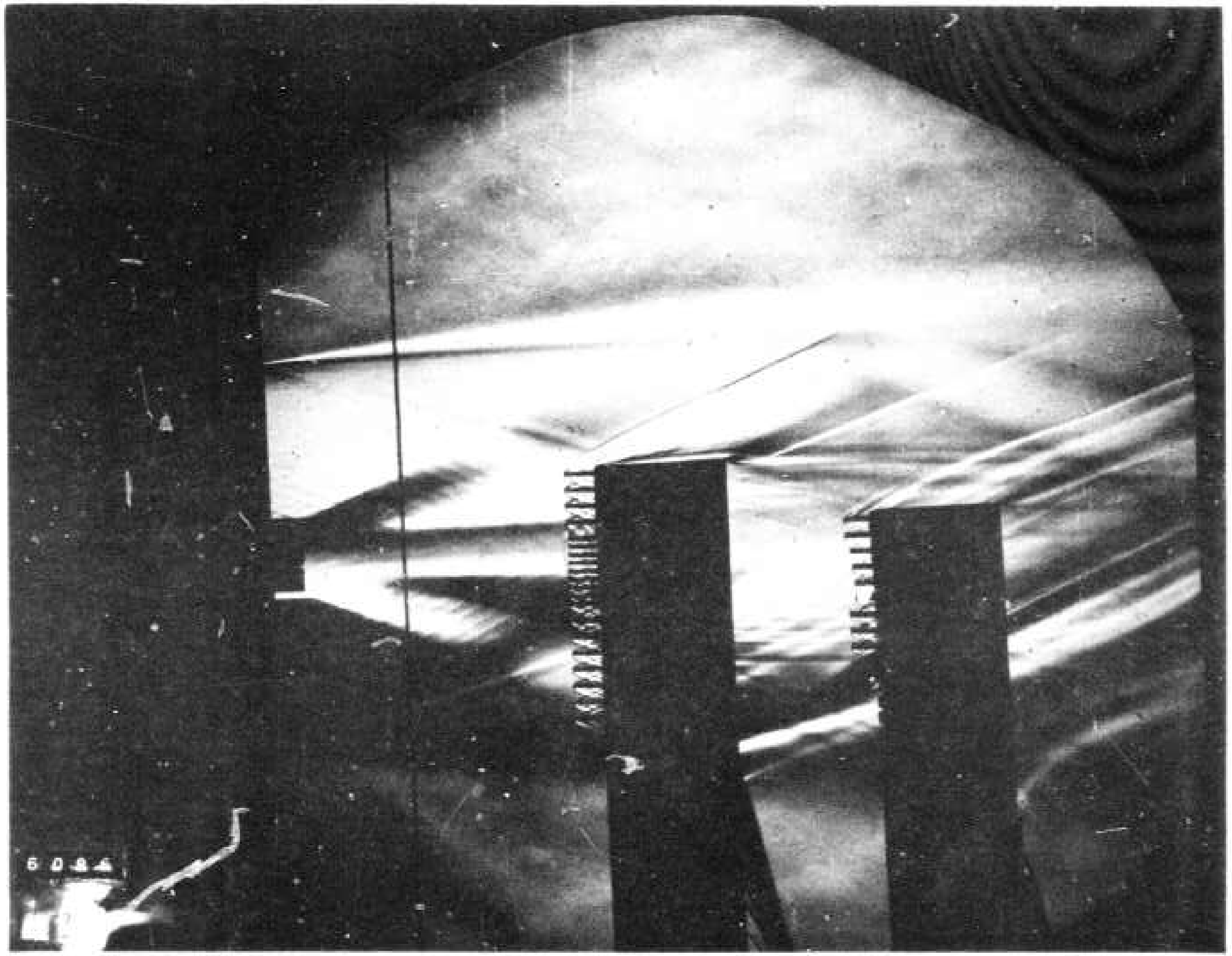

Figure 12. Schlieren Photograph of Flow Without Combustion, M=2.5

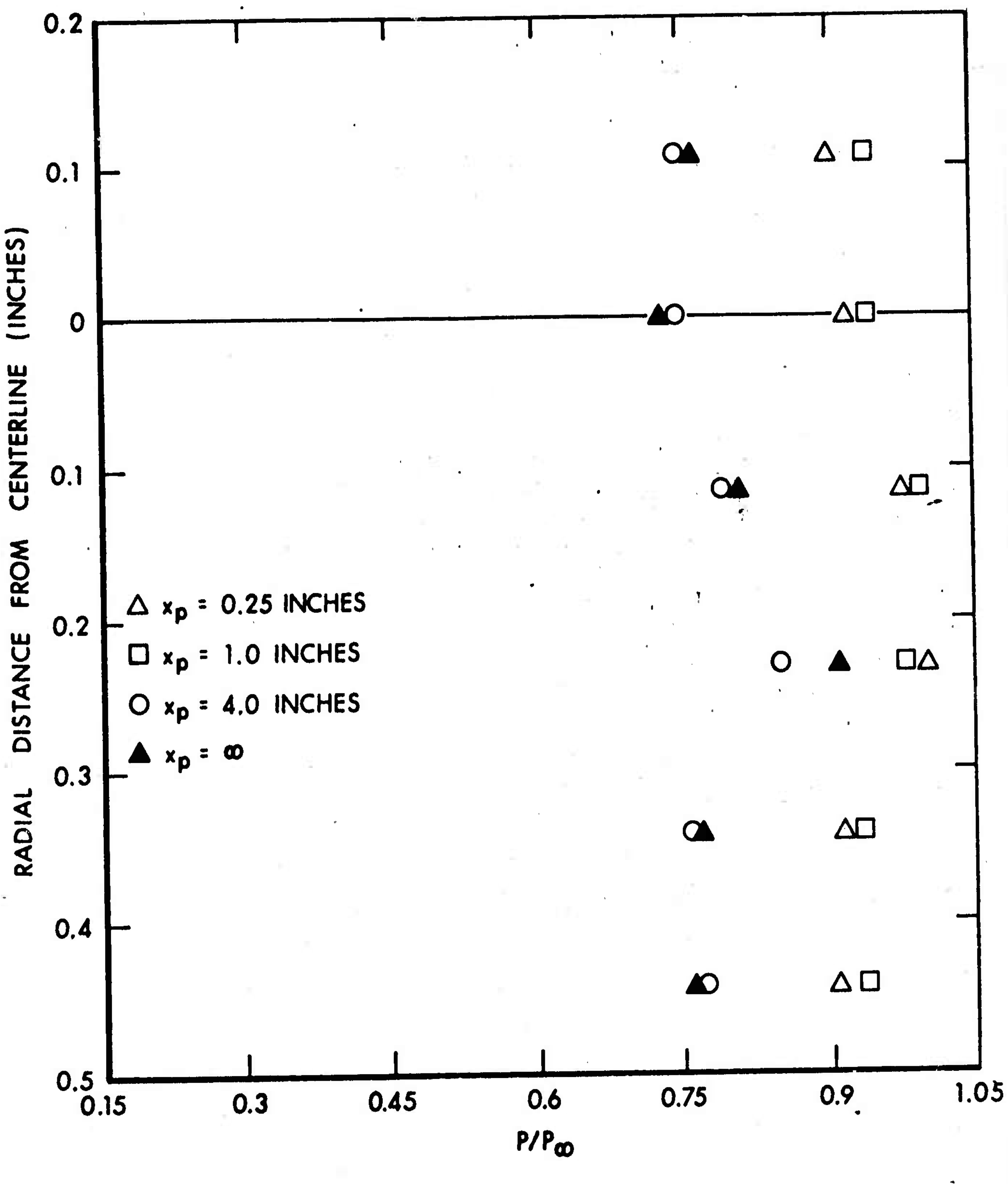

Figure 13. Radial Base Pressure Variation for M=1.56 Nozzle

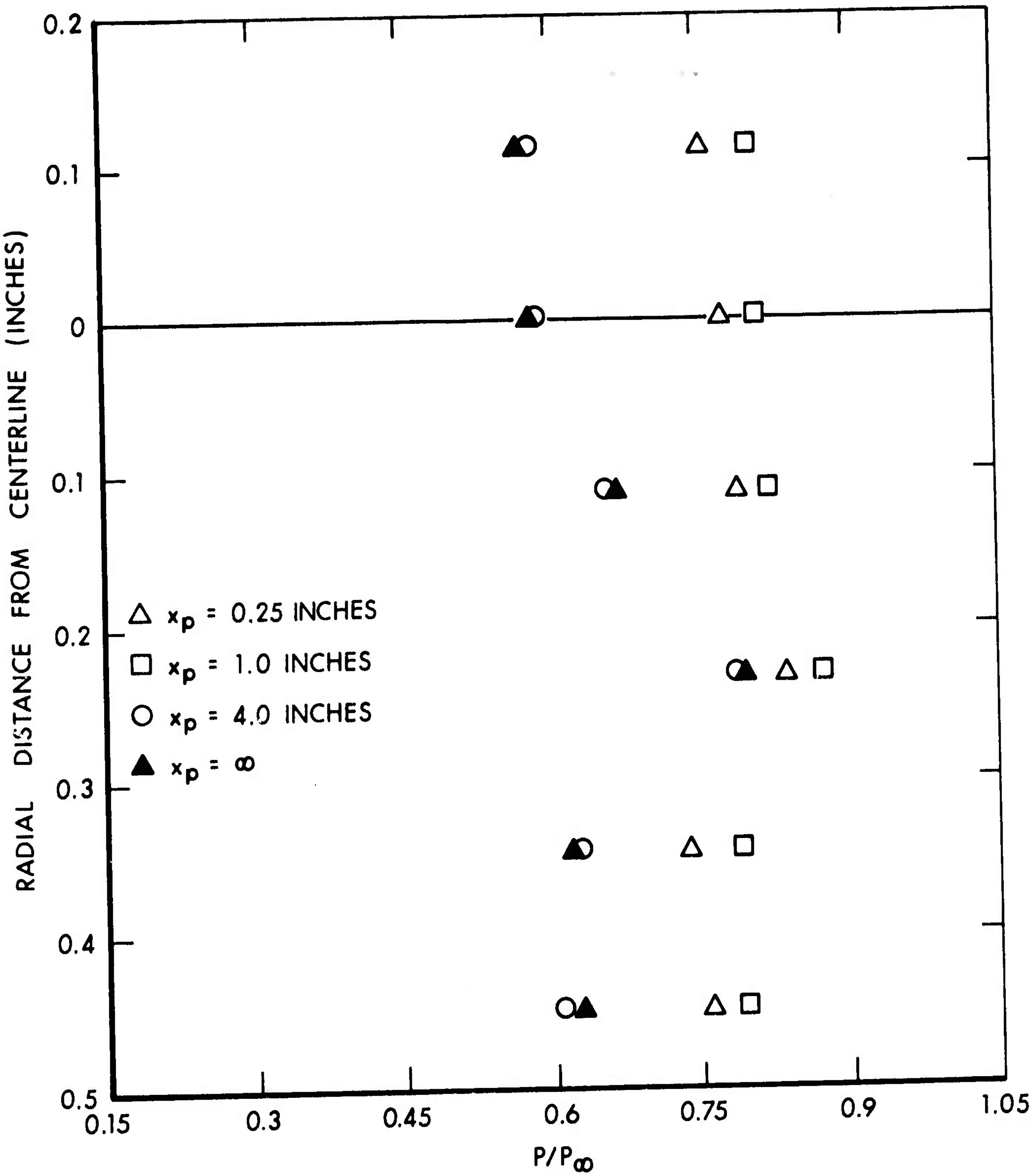

Figure 14. Radial Base Pressure Variation for M=1.98 Nozzle

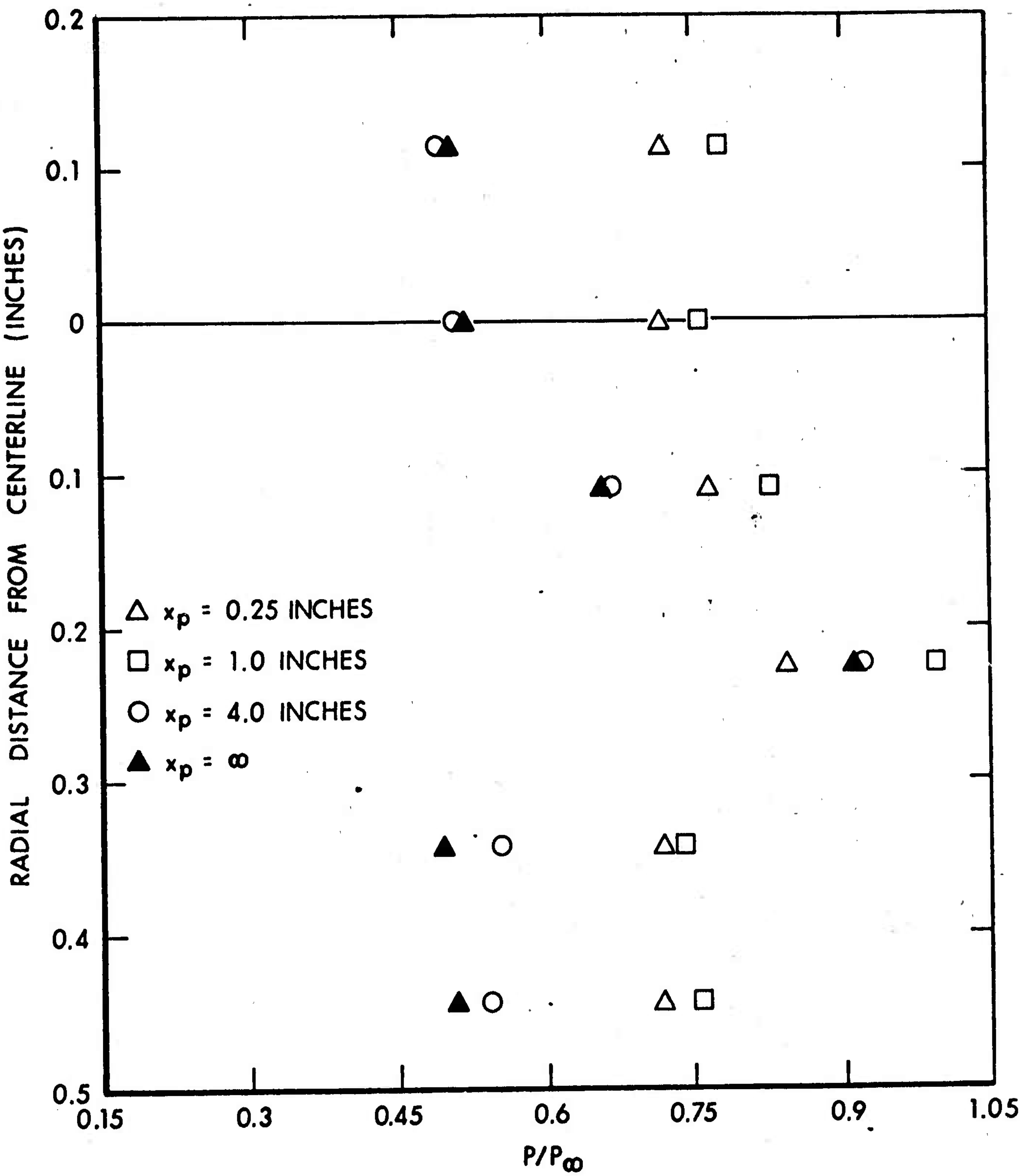

Figure 15. Radial Base Pressure Variation for M-2.56 Nozzle

Table IV. Summary of Base Burning Tests

Run No.	Mach No.	P_o, MN/m^2	T_o, K	Pyrotechnic	Spin Rate RPM	Area Restriction	Remarks
1	1.98	0.837	482	R20C	0	0	No slag
2	1.98	.815	484	R-284	0	0	Large slag deposit
3	1.98	.817	480	F-1	0	0	No slag
4	1.98	.838	482	F-3	0	0	No ignition
5	1.98	.803	499	F-13	0	0	Burning not sustained
6	1.98			F-14	0	0	No slag, no data
7	1.98	.820	505	F-1/F-4	0	0	No slag
8	1.98	.801	503	F-4	0	0	Burning not sustained
801	1.98	.786	504	F-4	0	0	Repeat of Run 8, same result
9	1.98	.791	490	F-4+6% binder	0	0	Large slag deposit
10	1.98	.800	498	F-4+15% binder	0	0	More slag than on Run 9
11	1.98	.828	493	36.5% Mg/63.5% $Sr(NO_3)_2$	0	25%	Laser failed to operate
1101	1.98			36.5% Mg/63.5% $Sr(NO_3)_2$	0	25%	No ignition
1102	1.98			36.5% Mg/63.5% $Sr(NO_3)_2$	0	25%	No ignition
12	1.98	.811	494	36.5% Mg/63.5% $Sr(NO_3)_2$	0	50%	Area restrictor melted, no slag
13	1.98	.813	493	36.5% Mg/63.5% $Sr(NO_3)_2$	0	75%	Same as Run 12
14	1.98	.828	494	50% Mg/50% $Sr(NO_3)_2$	0	0	No ignition
15	1.98	.810	490	50% Mg/50% $Sr(NO_3)_2$	0	50%	No ignition
16	1.98	.817	491	36.5% Mg/63.5% $Sr(NO_3)_2$	0	0	Partial ignition
17	1.98	.875	496	67.8% Mg/32.2% $Sr(NO_3)_2$	0	0	No ignition
18	1.56	.443	451	20% Mg/80% $Sr(NO_3)_2$	0	0	Partial ignition
1801	1.56	.436	461	20% Mg/80% $Sr(NO_3)_2$	0	0	Graphite applied to surface, partial ignition
19	1.56	.390	458	30% Mg/70% $Sr(NO_3)_2$	0	0	Partial ignition
1901	0			30% Mg/70% $Sr(NO_3)_2$	0	0	No airflow; full combustion
30	1.56	.278	456	36.5% Mg/63.5% $Sr(NO_3)_2$	0	0	Partial ignition

Table IV. Summary of Base Burning Tests (Cont'd)

Run No.	Mach No.	P_o, MN/m^2	T_o, K	Pyrotechnic	Spin Rate RPM	Area Restriction	Remarks
21	1.98	0.489	483	20% Mg/80% $Sr(NO_3)_2$	0	0	Layer of R20C added; only R20C burned
22	1.98	.494	487	36.5% Mg/63.5% $Sr(NO_3)_2$	0	0	Layer of R20C added; only R20C burned
23	1.98	.494	487	36.5% Mg/63.5% $Sr(NO_3)_2$	0	75%	Partial ignition
24	1.98	.475	482	36.5% Mg/63.5% $Sr(NO_3)_2$	0	75%	No ignition
25	1.98	.661	492	36.5% Mg/63.5% $Sr(NO_3)_2$	0	50%	No ignition
26	1.98	.706	489	36.5% Mg/63.5% $Sr(NO_3)_2$	0	0	No ignition
2601	0	.710	489	36.5% Mg/63.5% $Sr(NO_3)_2$	0	0	No airflow; full combustion
27	1.98	.709	489	36.5% Mg/63.5% $Sr(NO_3)_2$	0	50%	Fuel preheated to about 120K
28	1.98	.701	493	20% Mg/80% $Sr(NO_3)_2$	0	0	Preheated; partial ignition
29	1.98	.747	494	36.5% Mg/63.5% $Sr(NO_3)_2$	0	75%	Preheated
30	1.98	.343	444	36.5% Mg/63.5% $Sr(NO_3)_2$	0	0	No ignition
31	1.56	.326	443	20% Mg/80% $Sr(NO_3)_2$	0	0	Partial ignition
3101	0	.211	448	20% Mg/80% $Sr(NO_3)_2$	0	0	No airflow, ignition
32	1.56	.232	451	36.5% Mg/63.5% $Sr(NO_3)_2$	0	0	Partial ignition
33	1.56	.349	455	36.5% Mg/63.5% $Sr(NO_3)_2$	0	0	Partial ignition
34	1.56	.345	455	40% Mg/60% $Sr(NO_3)_2$	0	0	Preheated; partial ignition
35	1.56	.347	457	36.5% Mg/63.5% $Sr(NO_3)_2$	0	50%	Preheated
36	1.56	.723	402	36.5% Mg/63.5% $Sr(NO_3)_2$	0	75%	Preheated
37	1.56	.731	508	50% Mg/50% $Sr(NO_3)_2$	0	50%	Preheated; no ignition
38	1.98	.743	513	36.5% Mg/63.5% $Sr(NO_3)_2$	0	0	Preheated; burned with delay
39	1.98	.712	513	50% Mg/50% $Sr(NO_3)_2$	0	50%	Preheated; no ignition
40	1.98	.886	580	36.5% Mg/63.5% $Sr(NO_3)_2$	0	0	Preheated; no ignition
41	1.98	.846	535	F-4 + 20% binder	0	0	Ignition after a long delay

Table IV. Summary of Base Burning Tests (Cont'd)

Run No.	Mach No.	P_o, MN/m^2	T_o, K	Pyrotechnic	Spin Rate RPM	Area Restriction	Remarks
42	2.49	0.849	539	36.5% Mg/63.5% $Sr(NO_3)_2$	0	0	Preheated
43	2.49	.906	556	36.5% Mg/63.5% $Sr(NO_3)_2$	40,000 10,000	0	Preheated
44	2.49	.902	569	36.5% Mg/63.5% $Sr(NO_3)_2$	50,000	0	Preheated; no ignition
45	2.49	.881	546	67.8% Mg/32.2% $Sr(NO_3)_2$	0	0	No ignition
46	2.49	.883	562	67.8% Mg/32.2% $Sr(NO_3)_2$	0	0	No ignition; capsule lost
47	2.49	.875	572	67.8% Mg/32.2% $Sr(NO_3)_2$	49,000	0	No ignition
48	2.49	.836	531	36.5% Mg/63.5% $Sr(NO_3)_2$	50,000	0	No ignition
49	2.49	.803	516	36.5% Mg/63.5% $Sr(NO_3)_2$	65,000	0	No ignition
50	2.49	.839	495	R-20C	62,000	0	Capsule lost during run
51	1.98	.780	494	R-20C	0	0	Spinning stopped before ignition
52	1.98	.811	493	R-20C	0	0	Spinning stopped before ignition
53	1.98	.834	491	R-20C	62,000	0	Capsule lost before ignition
54	1.98	.787	493	R-20C	30,000	0	Laser beam off target
55	1.98	.794	494	50% R-20C/50% F-4	0	0	Capsule protrudge .20 in Only R-20C burned
56	1.98	.804	489	R-20C	32,500	0	
57	1.98	.820	494	I-136	0	0	Slow burning. Large amount of slag remaining
58	1.98	.806	493	20% Mg/80T SrO_2	0	0	Metallic slag remaining
59	1.98	.808	495	30% Mg/70% SrO_2	0	0	Capsule protruding .025"
60	1.98	.492	470	40% Mg/60T SrO_2	0	0	No ignition
61	1.98	.369	449	10% R-20C/90% F-4	0	0	F-4 did not burn until air pressure was reduced
62	1.56	.367	449	R-20C	0	0	Negligible slag
63	1.56	.383	449	R-20C	43,500	0	
64	1.56	.346	448	40% Mg/60% SrO_2	0	0	No ignition
65	1.56			50% Mg/50% SrO_2	0	0	No ignition

the problem was the presence of the supersonic flow. Run 1901 was made with no flow, and as indicated in Table IV, the mix immediately ignited. It was noted that mixes with strontium peroxide as the oxidizer ignited more readily and burned steadily. Thus, additional capsules were made up with T20C mix to test the effect of spin on base drag reduction, and a series of binary magnesium-strontium peroxide mixes to test the effect of the magnesium content. Also added was a "dark fumer", I-136, to the test. This mix uses the binder, calcium resinate, as the fuel; it contains no magnesium. It also emits no visible light when used as a tracer.

The pressure-time histories for the runs for which complete or partial combustion occurred are shown in Appendix A. The data are presented with the base pressure normalized to the free-stream static pressure. A few seconds of pre-and post-combustion pressure history are shown for each run. The pre-combustion pressure is steady and the value in close agreement with the base pressure measured during the flow calibration tests. The increase due to combustion is step-type for runs for which the fuel ignited quickly and burned steadily. For a number of runs the fuel ignited slowly or non-steadily and the increase in base pressure was slow and not always steady. On Run 10 the fuel ignited with a very long delay necessitating tunnel flow shutdown before completion of combustion. On Run 61 the fuel ignited and burned a few seconds after the layer of a special igniter-mix was burned.

At the end of burning the base pressure returned to the pre-combustion value for the runs for which the fuel burned clean, without leaving a heavy layer of slag. In some cases, particularly capsules with area restrictors, the slag protruded outside the base cavity causing the post-combustion base pressure to read higher (Runs 35, 36 and 42). On Run 63, due to spin-induced vibrations, the capsule moved axially protruding from the base cavity and causing the pre-combustion pressure to read higher.

The pressure-time histories in Appendix A were prepared from measurements at station P2. Pressures at other stations (P1, P3, P4) were essentially the same except for the effects of slag formation.

The data from these runs are presented in Table V. The base drag coefficient is related to the measured base pressure, free stream pressure, air velocity, and air temperature by the following equation:

$$C_{Db} = \frac{(P_\infty - P_b)}{1/2\rho_\infty U_\infty^{\,2}} \quad . \qquad (1)$$

Samples of schlieren photographs taken with the 70mm camera are shown in Appendix B. Gross effects may readily be seen on such features as the extent of the flame, the effect of spin on the flame-wake interaction (runs 42 <u>vs</u> 43, runs 62 <u>vs</u> 63), and the effect of combustion on the wake neck location.

Table V. Summary of Test Results for Runs with Sustained Combustion[a]

Run No.	M	$(P_b/P_\infty)_i$	$(P_b/P_\infty)_{max}$	$(C_{Db})_i$	$(C_{Db})_{min}$	mass, g	tb, sec	P_∞, $P_a \times 10^{-4}$ [b]	T, K
1	1.98	0.601	0.807	0.145	0.070	10.8	2.7	11.0	270
2	1.98	.601	.731	.146	.098	8.1	8.7	10.8	271
3	1.98	.604	.729	.144	.099	10.6	5.1	10.8	267
5	1.98	.609	.636	.143	.133	7.0	3.3	10.6	280
7	1.98	.605	.715	.144	.104	9.2	2.6	10.8	283
9	1.98	.608	.739	.143	.095	8.2	7.7	10.4	274
10	1.98	.609	.716	.142	.104	8.0	-	10.6	279
12	1.98	.609	.750	.142	.091	8.9	5.5	10.7	277
13	1.98	.606	.731	.144	.098	8.6	5.4	10.7	276
27	1.98	.624	.768	.137	.085	5.0	5.1	9.38	274
29	1.98	.623	.764	.137	.086	8.2	4.8	9.24	276
35	1.56	.768	.866	.135	.079	8.5	5.4	8.69	311
38	1.98	.615	.768	.140	.085	8.4	4.4	9.52	281
42	2.49	.522	.764	.110	.054	8.2	5.2	5.26	259
43[c]	2.49	.543	.807	.105	.045	8.3	-	5.03	239
51	1.98	.609	.893	.143	.072	-	2.5	10.6	289
52	1.98	.620	.802	.139	.072	-	2.6	11.1	277
56[d]	1.98	.615	.859	.140	.052	-	0.8	10.4	276
57	1.98	.612	.672	.141	.120	-	4.3	10.5	277
58	1.98	.613	.789	.141	.077	-	1.7	10.6	274
59	1.98	.616	.864	.140	.050	-	1.0	10.8	277
61	1.98	.613	.789	.141	.077	-	-	10.6	277
62	1.56	.765	.920	.139	.047	9.4	2.7	9.21	302
63[e]	1.56	.764	.967	.138	.019	9.4	0.7	9.16	302

[a] Spin rate zero unless otherwise noted.

[b] 1 MPa = 145 psi

[c] Spin rate varied during run from 40,000 to 10,000 rpm

[d] Spin rate 32,500 rpm

[e] Spin rate 43,500 rpm

Table VI. Effect of the Combustion of Standard Pyrotechnic on Base Pressure (M = 1.98, Static)

Mix	$(P_B/P_\infty)_i$	$(P_B/P_\infty)_{max}$	$\%C_{D_b}$ reduction	tb,sec	m,g
R20C	0.601	0.807	50	2.7	10.8
R284	0.601	0.731	32	8.7	8.1
F-1	0.604	0.729	32	5.1	10.6
F-1/F4	0.605	0.715	28[a]	2.6	9.2

[a]Mix extinguished before it had all burned. We presume only the F-1 burned.

Results of the wake survey proved inconclusive, since the rake was positioned six inches downstream to avoid interfering with the base pressure measurements which were the prime concern in this first series of tests.

V. DISCUSSION

The first stated objective was to verify experimentally that the "tracer effect" is a base pressure change. The results clearly affirm that indeed it is. Table VI extracts the pertinent test data from the previous section. Table VI also points out that the pyrotechnic mix producing the greatest pressure change burns fastest.

To assess this more quantitively, one can compute the specific impulse for the sample as shown below:

$$FSI = \frac{A \int_0^{tb} (P_{b_t} - P_{bn}) \, dt}{m} , \qquad (2)$$

where FSI = the fumer specific impulse,
A = area of the base,
tb = burning time,
P_{b_t} = base pressure at time t during burning,
P_{bn} = base pressure no burning,
m = mass .

This expression may be evaluated in the wind tunnel experiment from integrating the pressure-time history and using previously determined values for the area and the fumer mass. In standard international units, the FSI has units of newton-second/kilogram. For applications where one is volume limited, a more appropriate figure of merit would be the "volumetric impulse," obtained by multiplying the FSI by the density of the fumer. For the standard mixes in Table VI the FSI in standard international units are:

R20C	3200	(330)
R284	6300	(640)
F-1	3200	(330)

The numbers in parentheses are the fumer specific impulse in conventional engineering units (pound force-second/pound mass).

The effect of spin was the most dramatic as evidenced from both Table V and VII. The effect of spin on burning time and base pressure is illustrated in Figure 16 where pressure-time histories for spin and non-spin R20C are superimposed. The burning time of R20C is decreased by one-fourth at 43,500 rpm, but the faster burning, spinning R20C increases the base pressure more than the unspun mix. This increase is

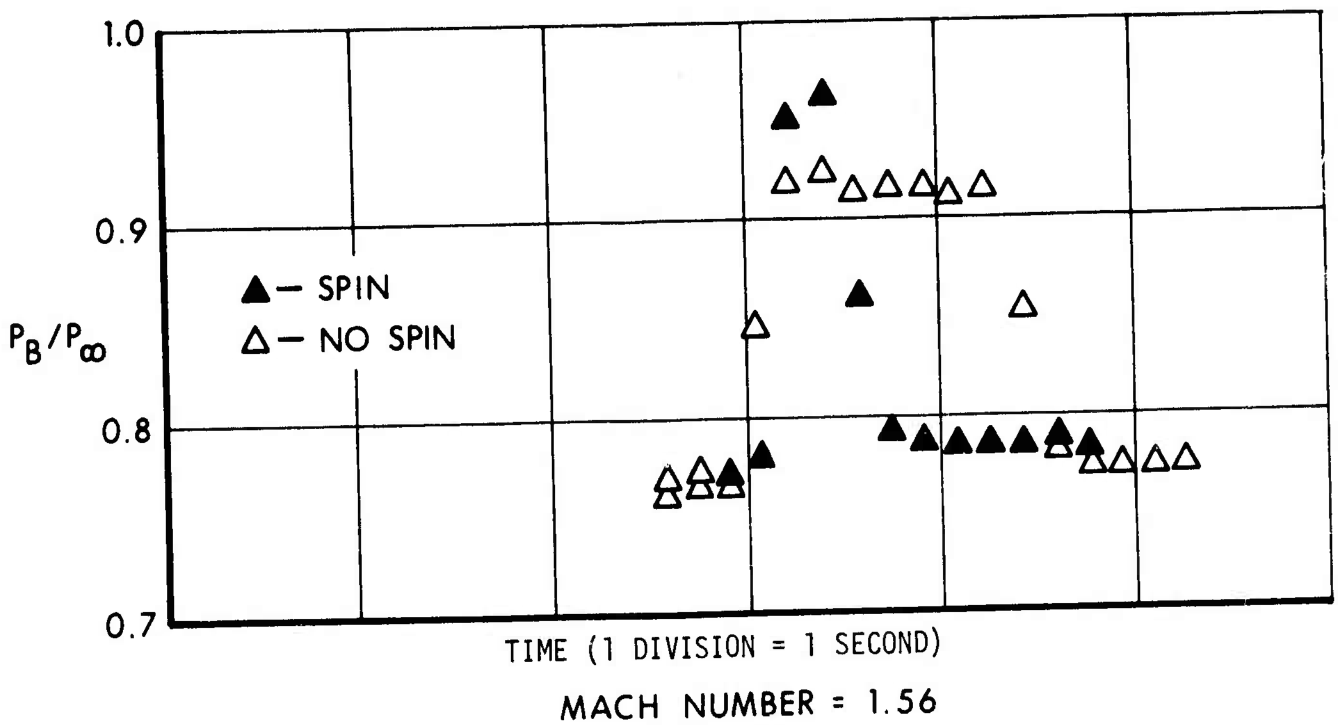

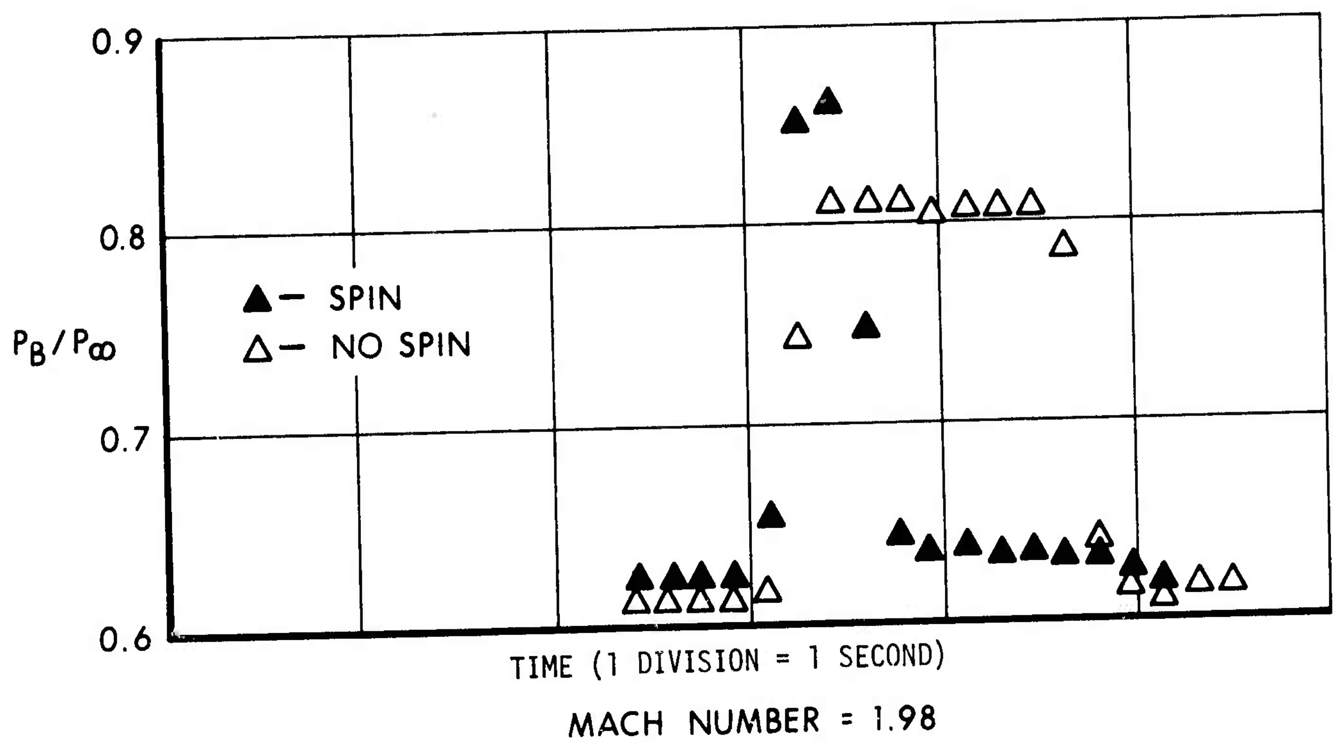

Figure 16. Comparison of Base Pressure vs Time Curve for Spun and Unspun R20C

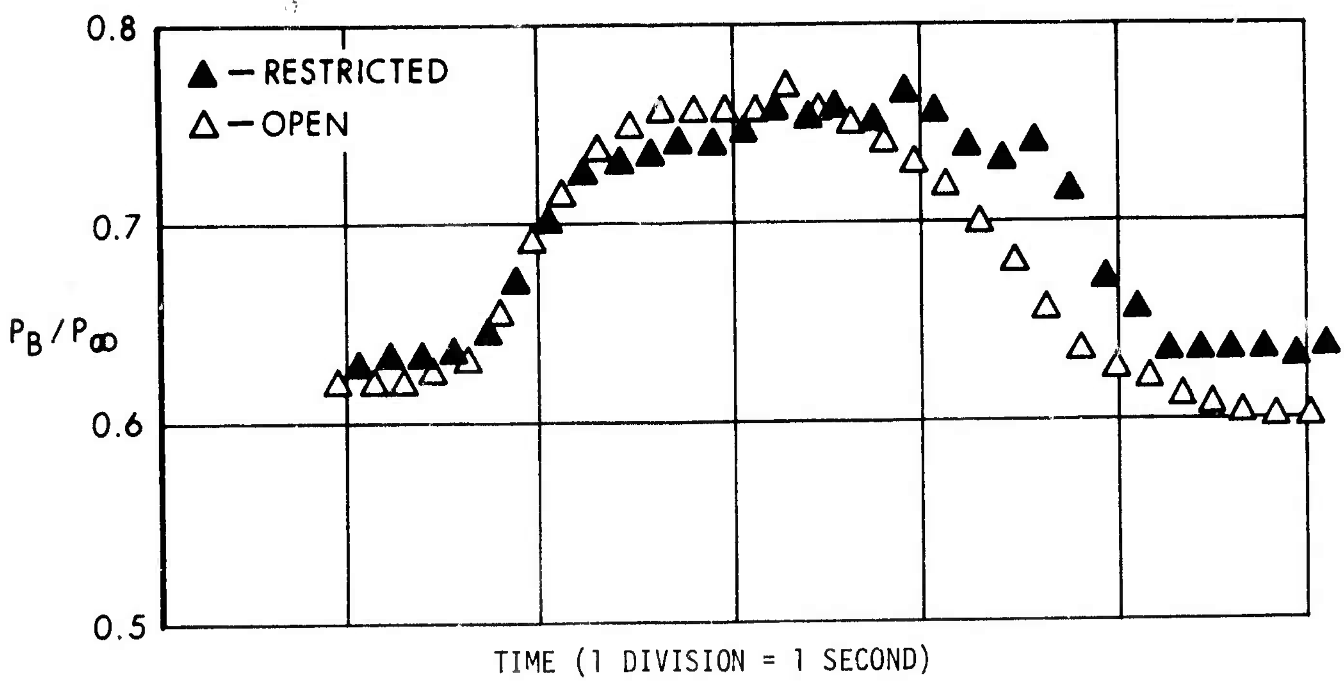

MACH NUMBER = 1.98, 50% AREA RESTRICTION

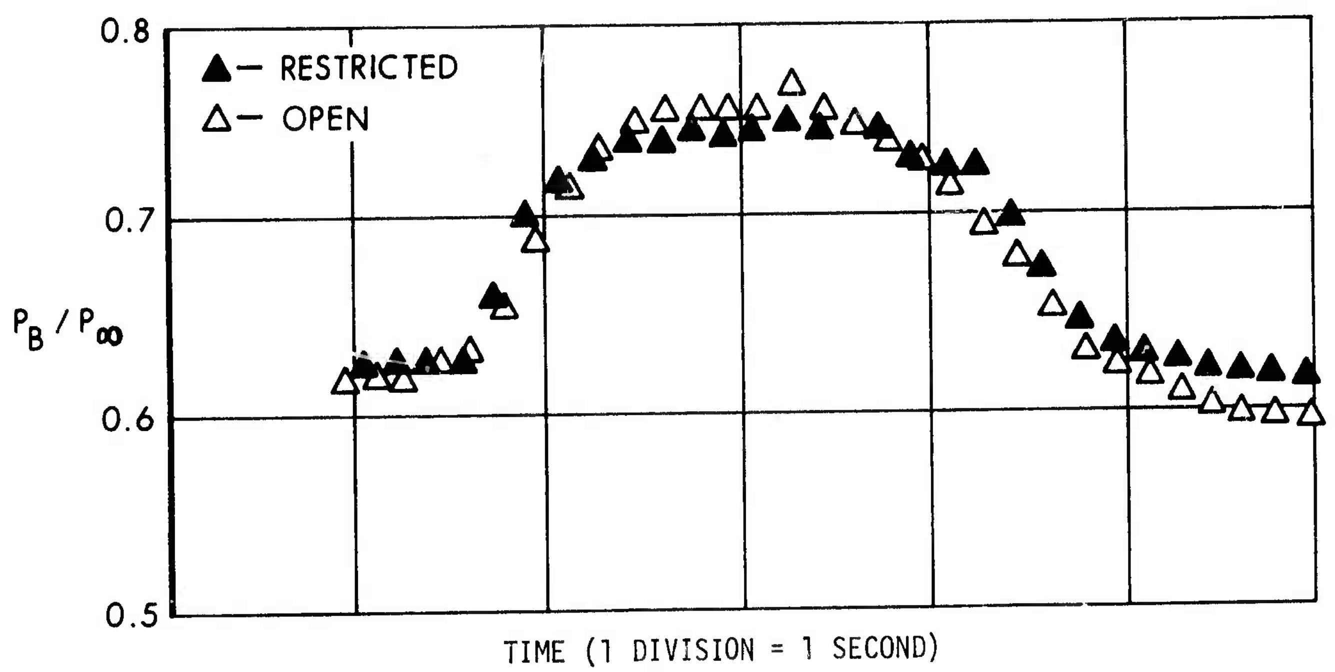

MACH NUMBER = 1.98, 75% AREA RESTRICTION

Figure 17. Comparison of Pressure vs Time Curve for Capsules with Area Restrictors

Table VII. Fumer Specific Impulses for Pyrotechnics Tested as Fumers

Run No.	Mix	Mach No.	%Area Restricted	Isp,n-sec/kg
1	R20C	1.98	-	3200
2	R284	1.98	-	6300
3	F-1	1.98	-	3200
9	F-4+6% binder[a]	1.98	-	3300
12	stoich $Mg/Sr(NO_3)_2$[b]	1.98	50	3600
13	"	1.98	75	4100
27	"	1.98	50[c]	4800
29	"	1.98	75[c]	3450
35	"	1.56	50[c]	1400
36	"	1.56	75[c]	1800
38	"	1.98	-[c]	4550
42	"	2.49	-[c]	4000
62	R20C	1.56	-	2000
63	R20C	1.56	-[d]	750

[a]calcium resinate

[b]36.5/63.5 percent by weight binary mix

[c]preheated to around 500K

[d]spin rate 43,500 rpm

not sufficient to overcome the reduced burn time as far as the fumer specific impulse is concerned so we would predict R20C to be a particularly poor fumer. Such results were observed in firing tests.[6] The coverage of the spin effects is not as extensive as it was originally intended because the capsules with area restrictors were not balanced.

The effect of the flow area restrictors on burning time and base pressure change are shown in Figure 17. As noted in the remarks column in Table IV, the area restrictors melted, so the only conclusion we draw from these tests is that steel washers used in the projectile as flow restrictors will not affect fumer performance. An unexpected result from the use of the area restrictors was that the mixes with the area restrictors were easier to ignite. This, too, was noted during the actual firing tests.[6] Reliable ignition of F-1 was achieved only when area restrictors were employed.

One series for which no data were obtained was the effect of magnesium content on drag reduction (Runs 12-20 Table I). As was pointed out in reference 7, previous wind tunnel experiments designed to test the effect of various gases ejected into the wake on base pressure concluded that the ideal base drag reducing fumer would be a hot, low-molecular weight gas that burned in the near-wake with the air present there. These authors speculated the excess magnesium in a fuel-rich magnesium-containing pyrotechnic might provide the sought for hot low-molecular weight gas that would burn in the wake and be, therefore, an ideal fumer candidate. Since this hypothesis was one of the chief objectives of the tests, we prepared a series of capsules using strontium peroxide as the oxidizer. We chose this oxidizer since we could more easily ignite it than strontium nitrate mixes and because the stoichiometric binary mixture contained a relatively low concentration of magnesium (17%), so we were confident we could ignite some capsules with excess magnesium. As Table V indicates, we burned successfully the 20/80 and 30/70 binary mixes, but were unsuccessful with the 40/60 and 50/50 mixes. Nonetheless, the predicted trend of increasing drag reduction with an increasing amount of excess magnesium appeared as shown in Table VIII. We also included data for F-1 which also uses strontium peroxide as the oxidizer as well as I-136 which contains no magnesium.

Table VIII. Effect of Fuel Concentration (M_∞=1.98)

Mix	$\%\Delta C_{Db}$	tb, sec
F-1 (8.1% Mg)	32	5.1
20/80 Mg/SrO_2	46	1.7
30/70 Mg/SrO_2	65	1.0
I-136	15	4.3

These runs also show how we can design fumers using binders and different oxidizers by comparing the percent drag reduction and burning time of R20C and the 20/80 Mg/SrO_2 mix as shown below

	$\%\Delta C_{Db}$	tb, sec
20/80 Mg/SrO_2	46	1.7
R20C	50	2.7

The addition of different fuels (carbon and calcium resinate) and different oxidizers (PbO_2 BaO_2) increases the burning time while keeping the drag reduction nearly constant. This is precisely what we must do in the future in a systematic manner to achieve the optimum fumer for a given application. We are not starting from scratch. Caven and Stevenson[6] point out that the visibility of a tracer is a function of the excess magnesium in the flame. Thus, existing tracer compositions will be good starting points to try to find optimum fumers. However, this also implies that one is not likely to find a "dark" fumer that will be effective.

Future experiments will try to optimize base drag reduction with burning time. Since these tests indicate that burning magnesium in the near-wake is an especially effective drag-reducer, one needs a way to increase the burning times of such compositions. Two approaches are possible. One is to increase the particle-size of the magnesium. Another approach is the use of flame retardants such as oxamide. These materials have been shown to reduce burning rates by endothermic decomposition at the surface, thereby reducing the surface temperature. Hopefully one will be able to use such coolants with the energetic peroxides which appear to be the oxidizers easiest to ignite.

VI. CONCLUSIONS

1. The so-called "tracer effect" results from a increased base pressure.

2. Center-perforated washers assist the igniton of pyrotechnics. The ignition of pyrotechnics is more difficult in the supersonic flow than under static conditions.

3. The center-perforated steel washers used to restrict the area through which the pyrotechnic combustion gases may flow into the wake melted and had no effect on base pressure compared to the capsules with no washers.

4. Spinning dramatically increased the fumer burning rate and base drag reduction. It does not appear that the increased base drag reduction compensates for the reduced burning time.

5. A trend indicating that the base drag reduction is proportional to the amount of magnesium in the composition was evidenced.

ACKNOWLEDGMENT

The authors wish to thank Theresa Elmendorf and Walter Puchalski of Frankford Arsenal for supplying the steel capsules and for pressing the fumer samples, respectively.

REFERENCES

1. L. C. MacAllister, B. J. Reiter, B. B. Grollman, and A. E. Thrailkill, "A Compendium of Ballistic Properties of Projectiles of Possible Interest to Small Arms," BRL Report No. 1532, February 1971. (AD#882117)

2. M. J. Piddington, F. H. Oertel, E. L. Herr, and W. J. Bruchey, "Experimental Ballistic Properties of Selected Projectiles of Possible Interest in Small Arms(U)," BRL Memorandum Report No. 2194, June 1972 (Confidential). (AD #521618L)

3. F. H. Oertel and B. R. Dunetz, "A New Projectile Concept for Small Arms Application(U)," BRL Memorandum Report No. 2230, September 1972 (Confidential). (AD #523414L)

4. J. E. Bowman and W. A. Clayden, "Reduction of Base Drag by Gas Ejection," RARDE Report 4/69, December 1969.

5. S. N. B. Murthy and J. R. Osborn, "Base Flow Data With and Without Injection: Bibliography and Semi-Rational Correlations" BRL Contract Report No. 113, August 1972.

6. J. J. Caven and T. Stevenson, "Pyrotechnics for Small Arms Ammunition," Frankford Arsenal Report R-1968, July 1970.

7. J. R. Ward and R. K. Pahel, "Fuel-Rich Magnesium-Oxidizer Mixes as Drag-Reducing Fumers," BRL Memorandum Report No. 2336, October 1973. (AD #771171)

8. M. J. Piddington, "Aerodynamic Characteristics of the 7.62mm NATO Ammunition M-59, M-80, M-61, M-62," BRL Memorandum Report No. 1883, March 1967. (AD #815788)

9. M. J. Piddington, "Aerodynamic Properties of a 20mm HE-T Projectile for the VRFWS," BRL Memorandum Report No. 2000, July 1969.

10. R. Sedney, "Review of Base Drag," The Fluid Dynamic Aspects of Ballistics, AGARD Conference Proceedings, No. 10, September 1966, pp 211-240.

11. R. Kwatnoski, Frankford Arsenal Report, in press.

12. J. R. Ward, R. K. Pahel, and K. J. White, "Laser Ignition of Pyrotechnic Compositions Being Tested as Drag-Reducing Fumers," BRL Memorandum Report No. 2308, April 1973. (AD #765415)

APPENDIX A.

PRESSURE-TIME CURVES FOR BURNING RUNS

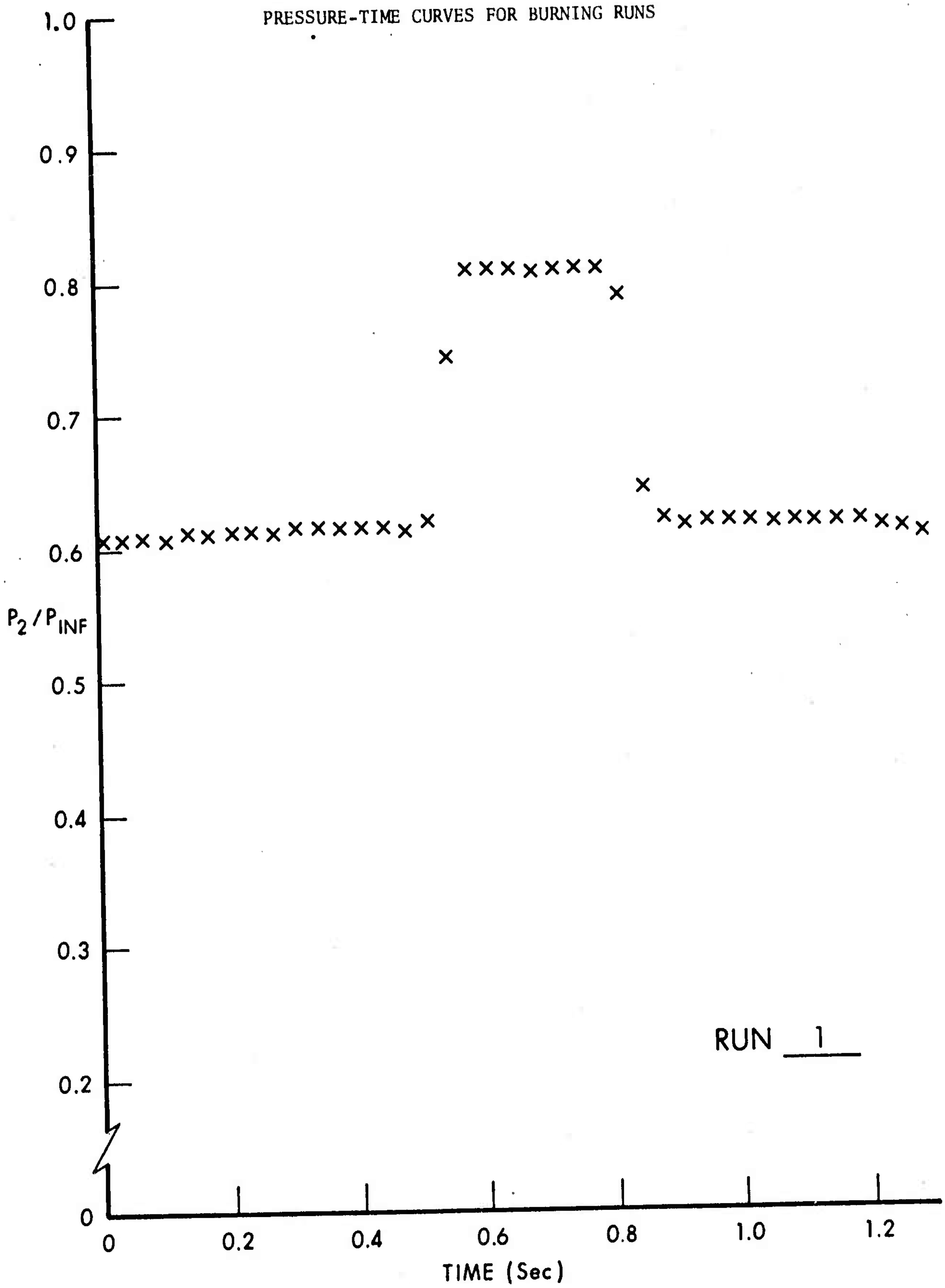

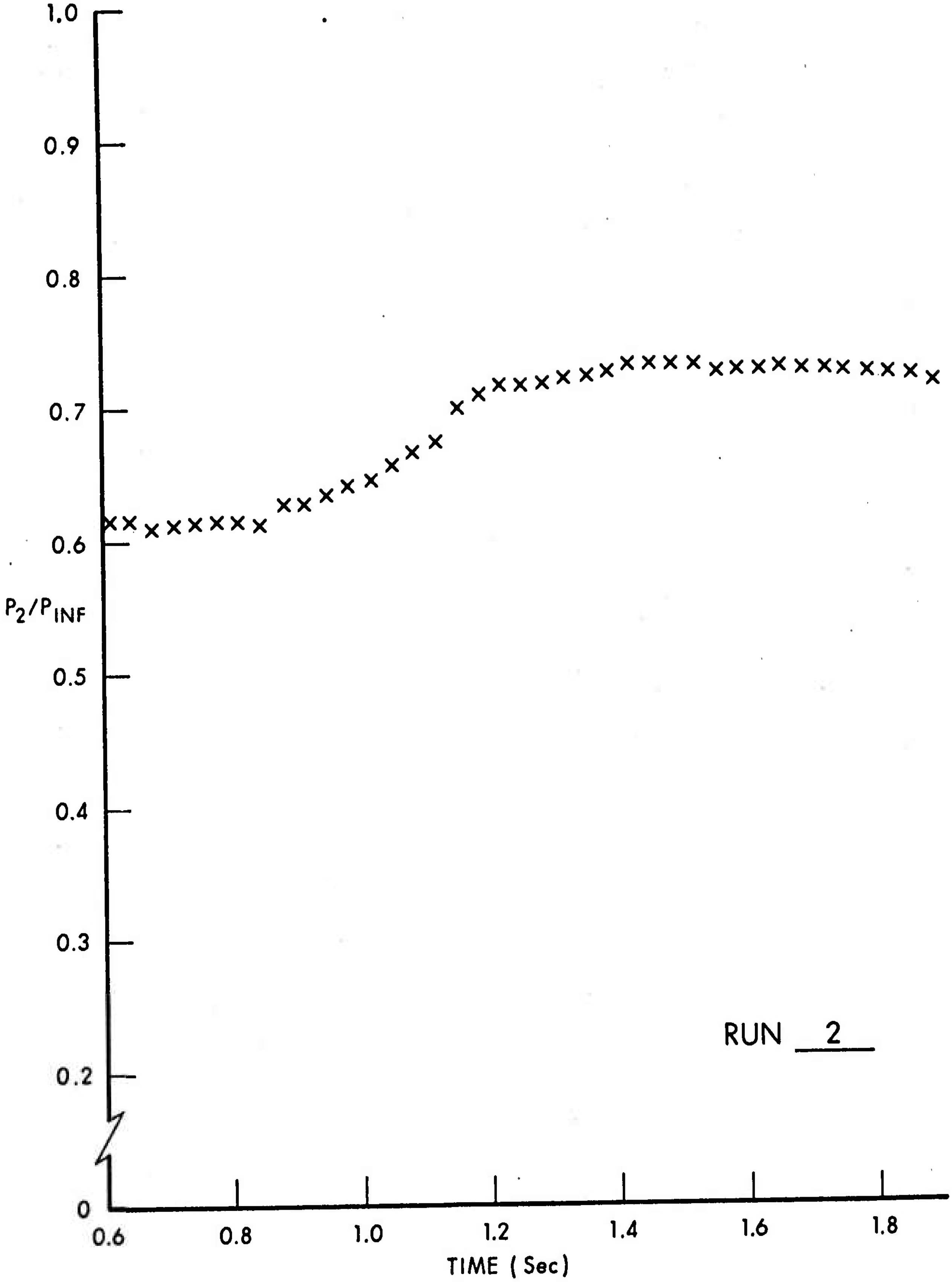
1.0
0.9
0.8
0.7
0.6
P_2/P_{INF}
0.5
0.4
0.3
0.2
0
0.6
0.8
1.0
1.2
1.4
1.6
1.8
TIME (Sec)
RUN 2

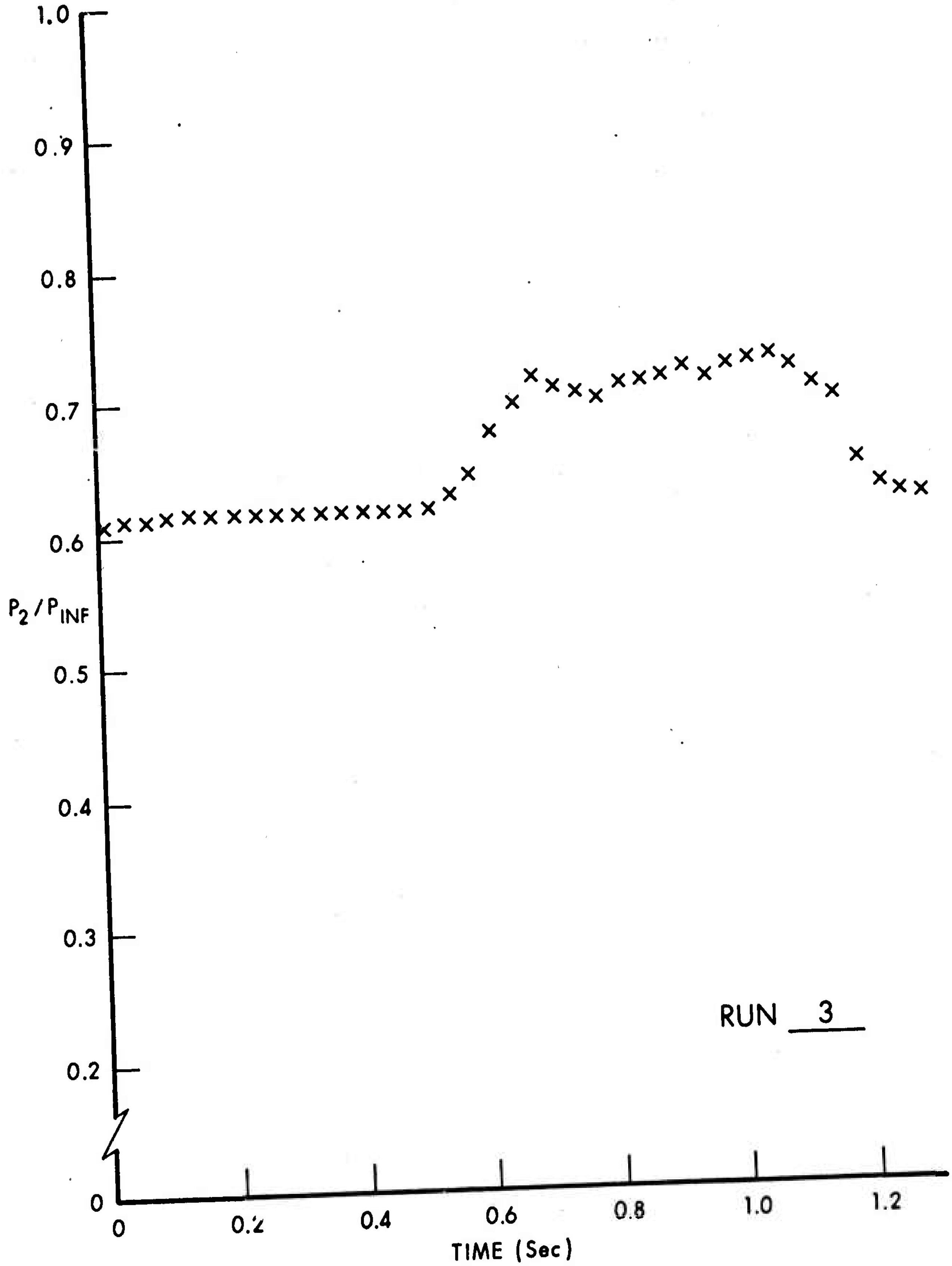
1.0
0.9
0.8
0.7
0.6
P_2/P_{INF}
0.5
0.4
0.3
0.2
0
RUN 3
0
0.2
0.4
0.6
0.8
1.0
1.2
TIME (Sec)

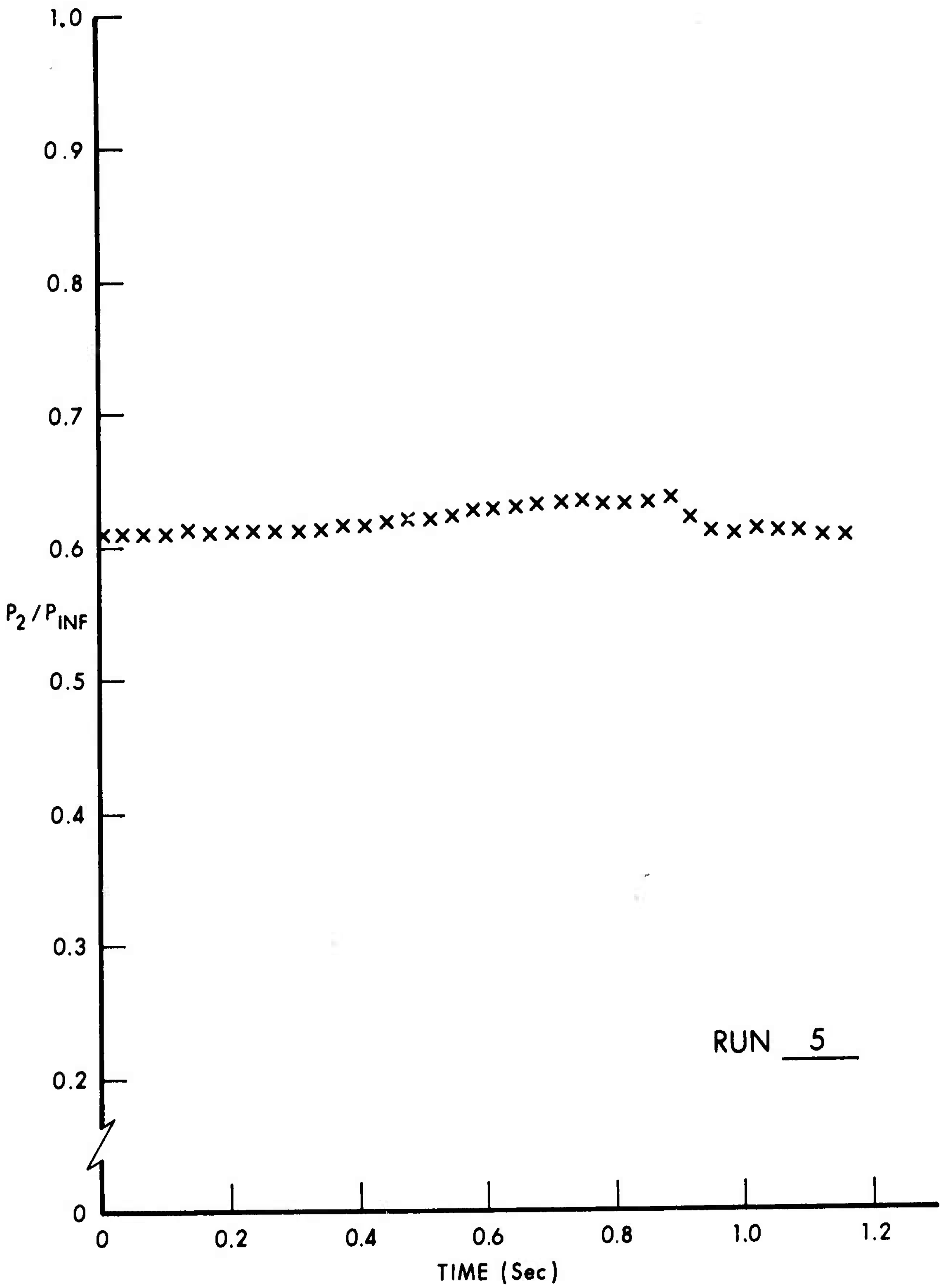
1.0
0.9
0.8
0.7
0.6
P_2 / P_{INF}
0.5
0.4
0.3
0.2
0
0
0.2
0.4
0.6
0.8
1.0
1.2
TIME (Sec)
RUN 5

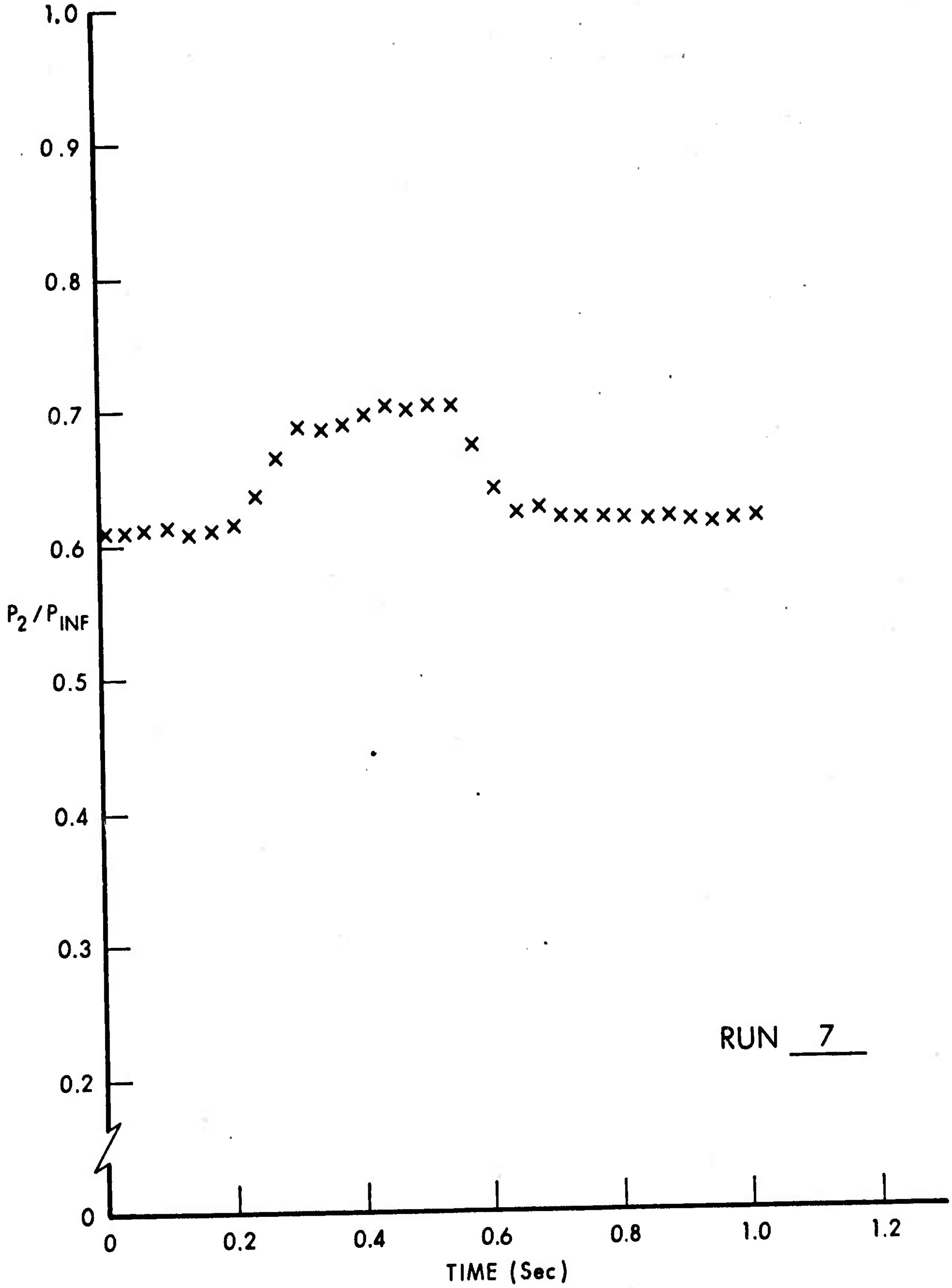
1.0
0.9
0.8
0.7
0.6
P_2/P_{INF}
0.5
0.4
0.3
0.2
0
RUN 7
0
0.2
0.4
0.6
0.8
1.0
1.2
TIME (Sec)

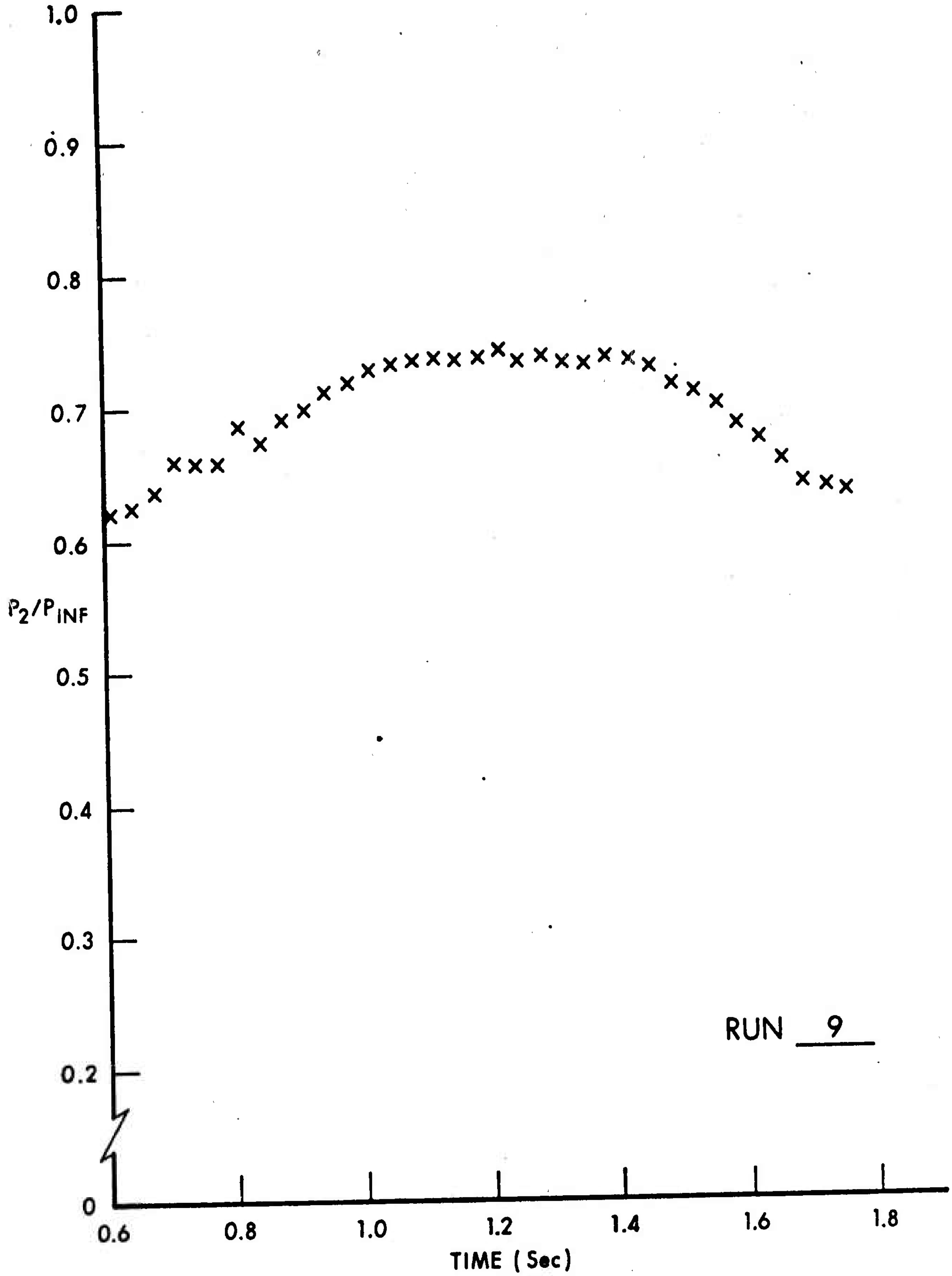
1.0
0.9
0.8
0.7
0.6
P2/PINF
0.5
0.4
0.3
0.2
0
RUN 9
0.6
0.8
1.0
1.2
1.4
1.6
1.8
TIME (Sec)

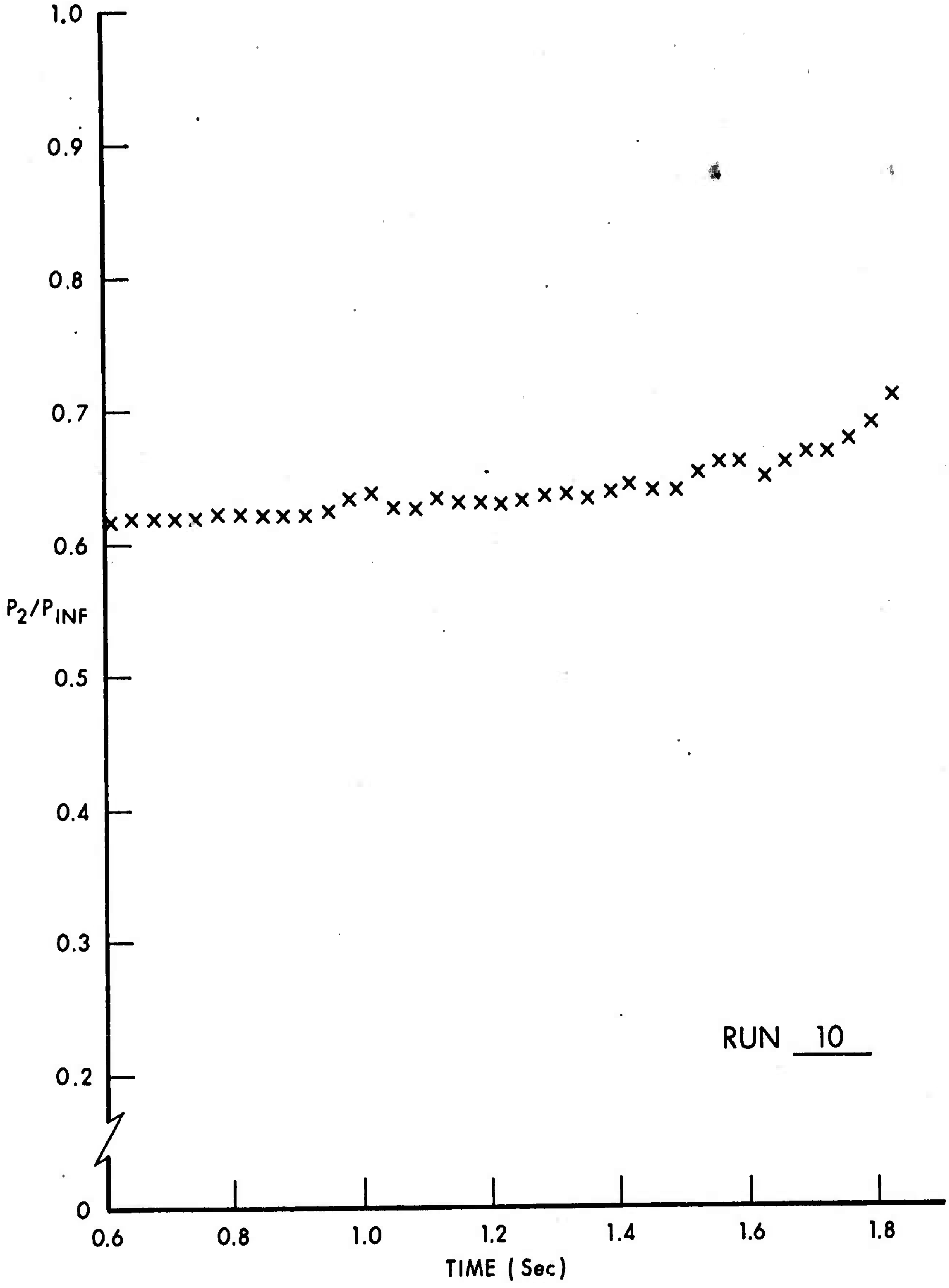
1.0
0.9
0.8
0.7
0.6
P2/PINF
0.5
0.4
0.3
0.2
0
0.6
0.8
1.0
1.2
1.4
1.6
1.8
TIME (Sec)
RUN 10

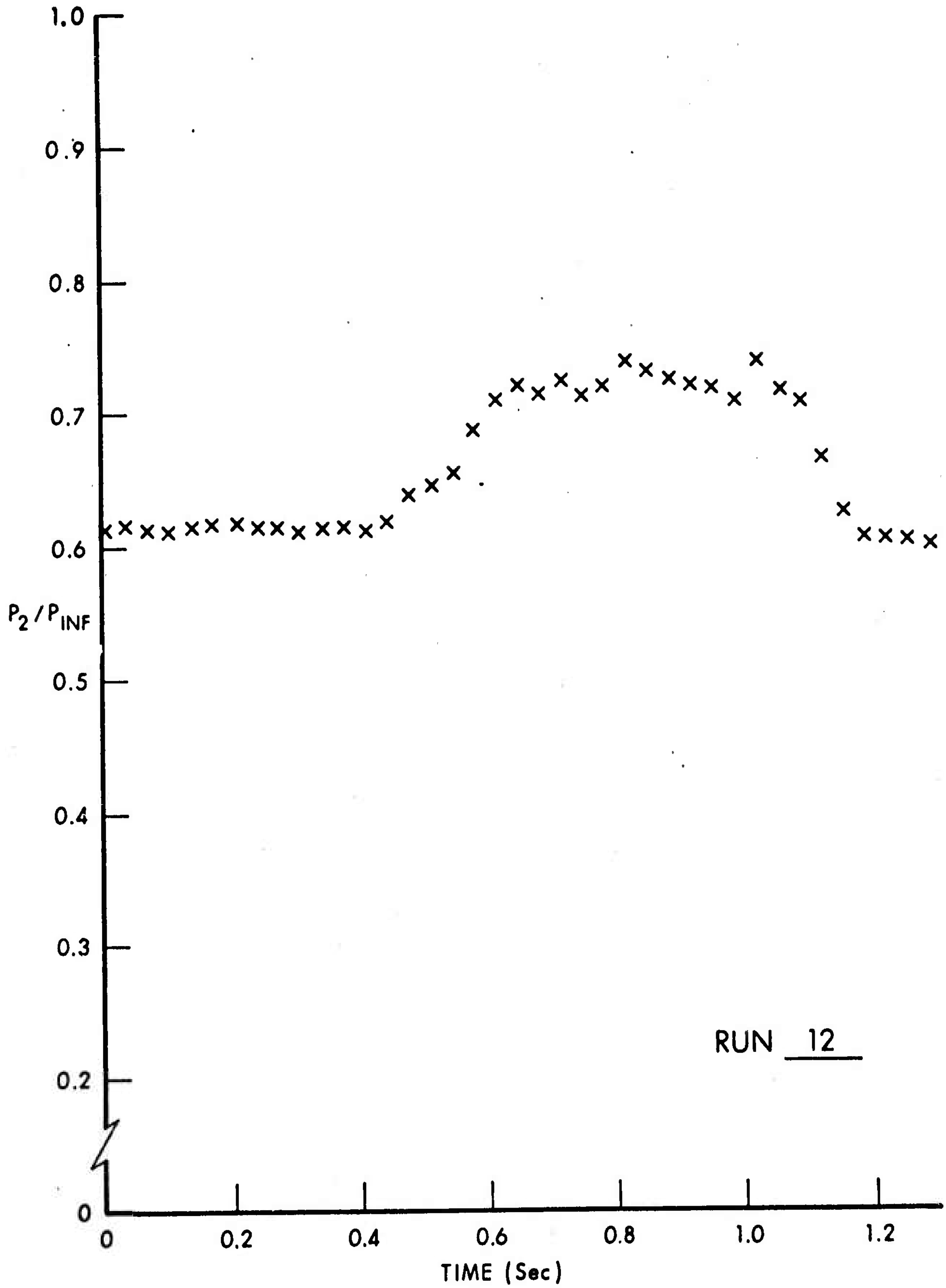
1.0
0.9
0.8
0.7
0.6
P2 / PINF
0.5
0.4
0.3
0.2
0
RUN 12
0
0.2
0.4
0.6
0.8
1.0
1.2
TIME (Sec)

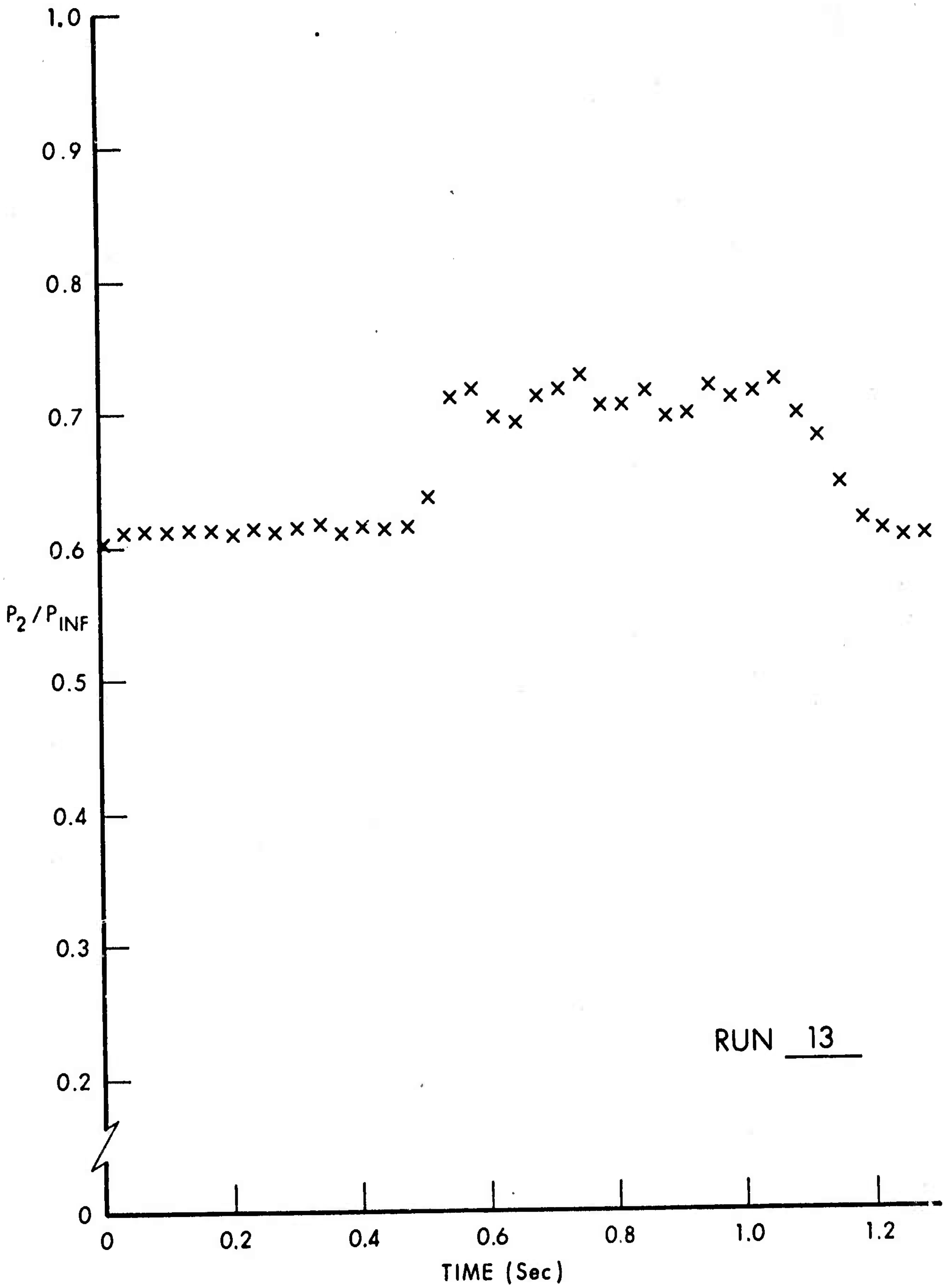
1.0
0.9
0.8
0.7
0.6
P_2 / P_{INF}
0.5
0.4
0.3
0.2
0
0
0.2
0.4
0.6
0.8
1.0
1.2
TIME (Sec)
RUN 13

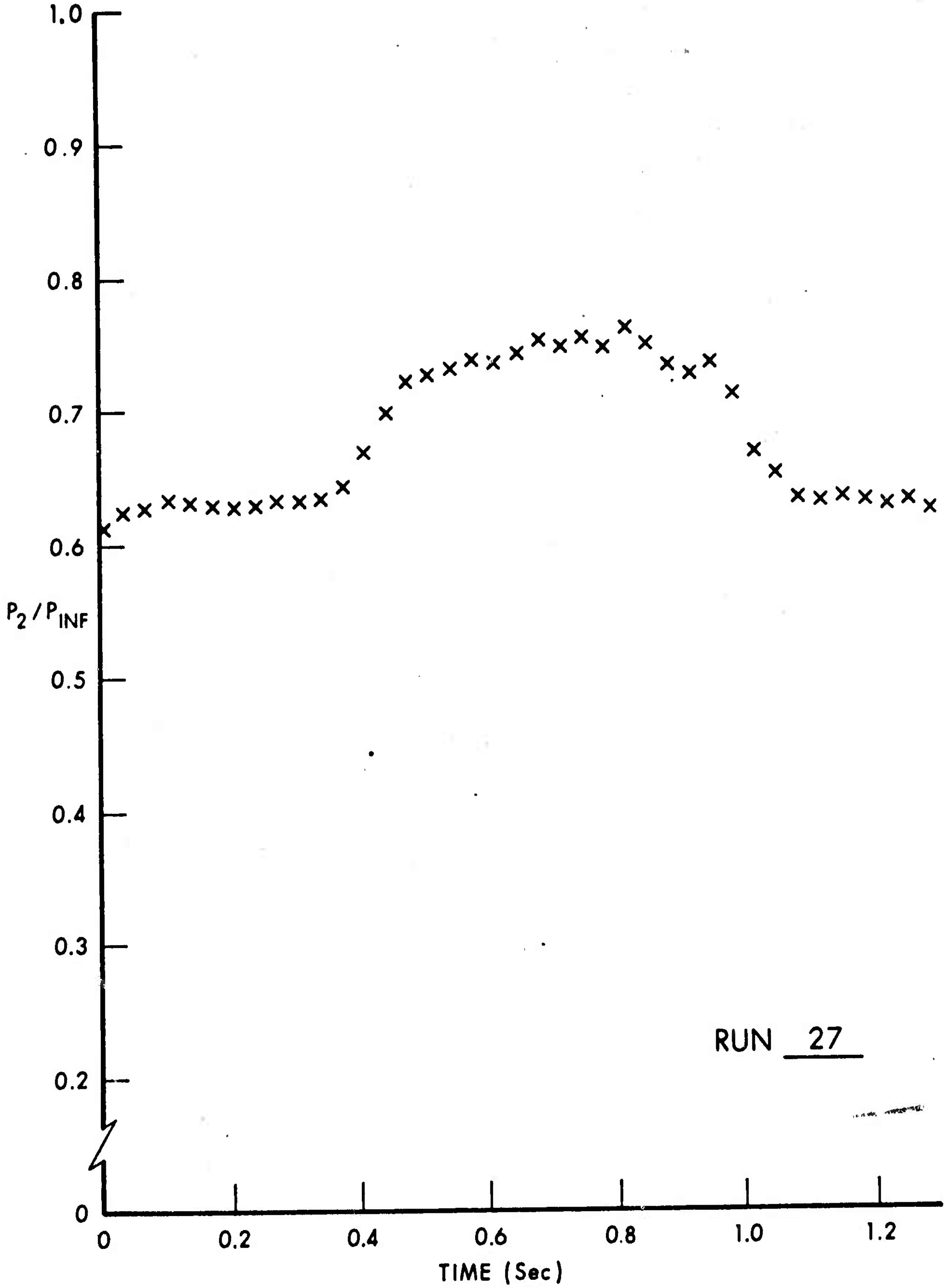
1.0
0.9
0.8
0.7
0.6
P2 / PINF
0.5
0.4
0.3
0.2
0
RUN 27
0
0.2
0.4
0.6
0.8
1.0
1.2
TIME (Sec)

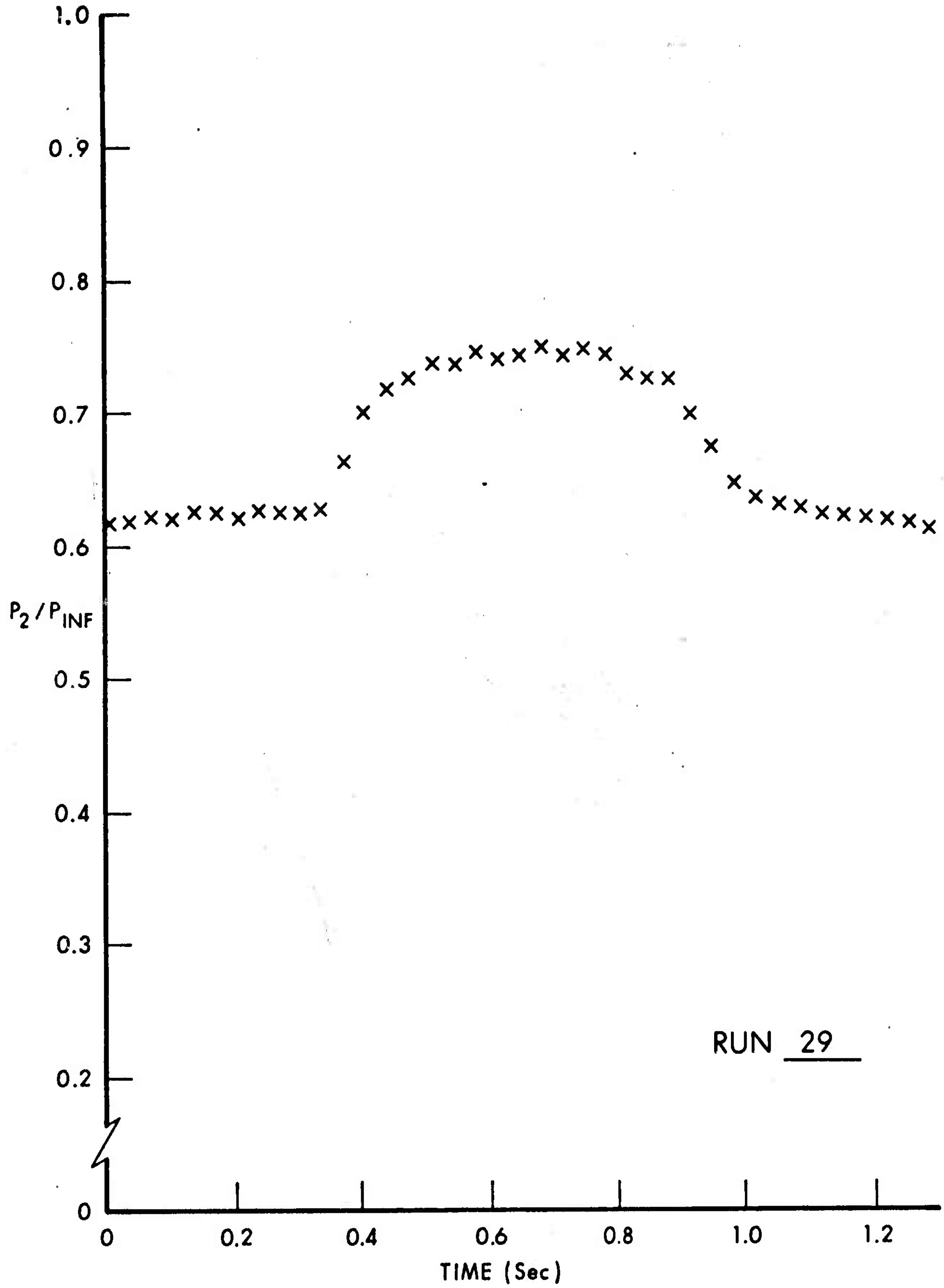
1.0
0.9
0.8
0.7
0.6
P_2/P_{INF}
0.5
0.4
0.3
0.2
0
0
0.2
0.4
0.6
0.8
1.0
1.2
TIME (Sec)
RUN 29

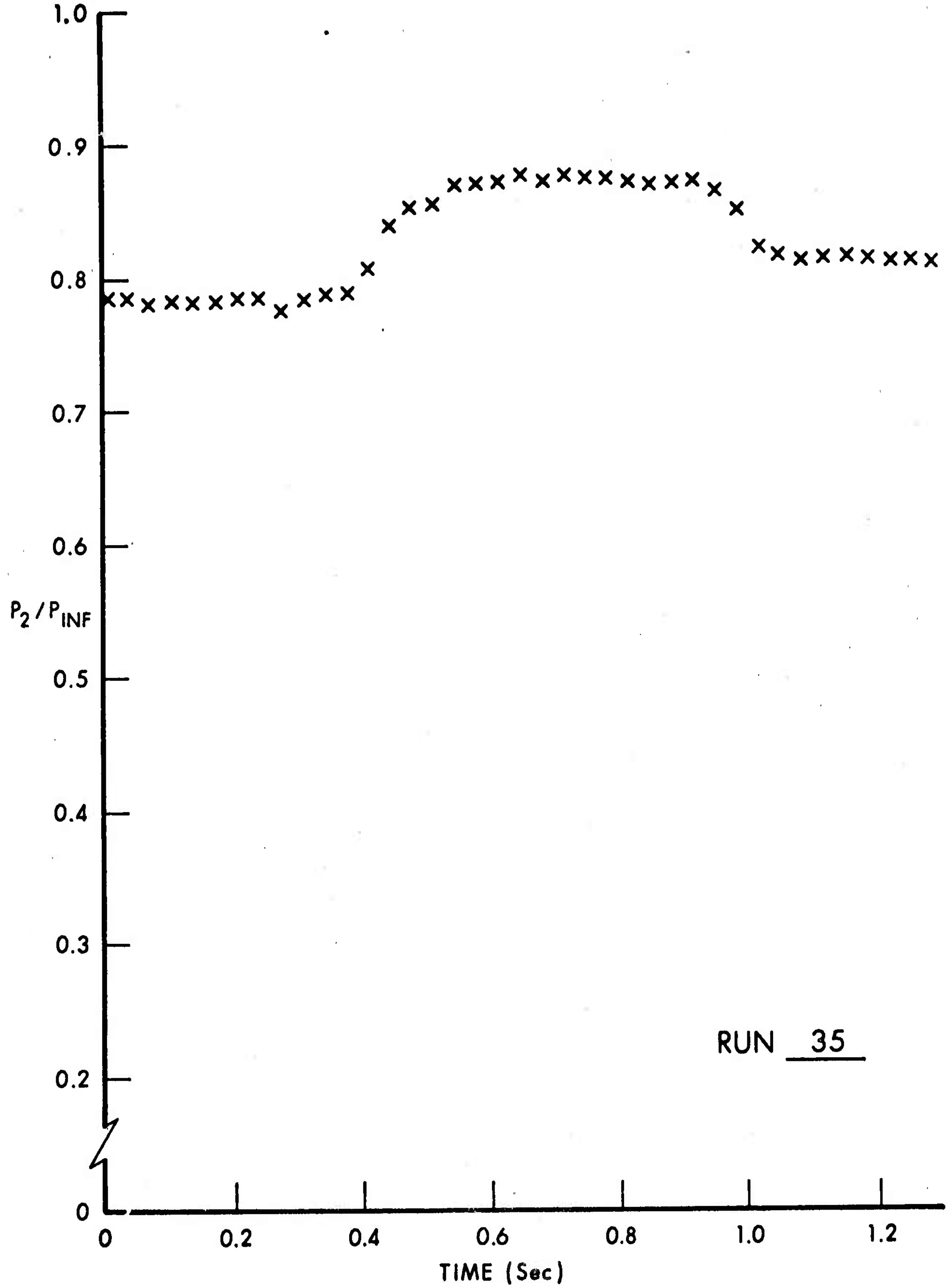
1.0
0.9
0.8
0.7
0.6
P_2/P_{INF}
0.5
0.4
0.3
0.2
0
0
0.2
0.4
0.6
0.8
1.0
1.2
TIME (Sec)
RUN 35

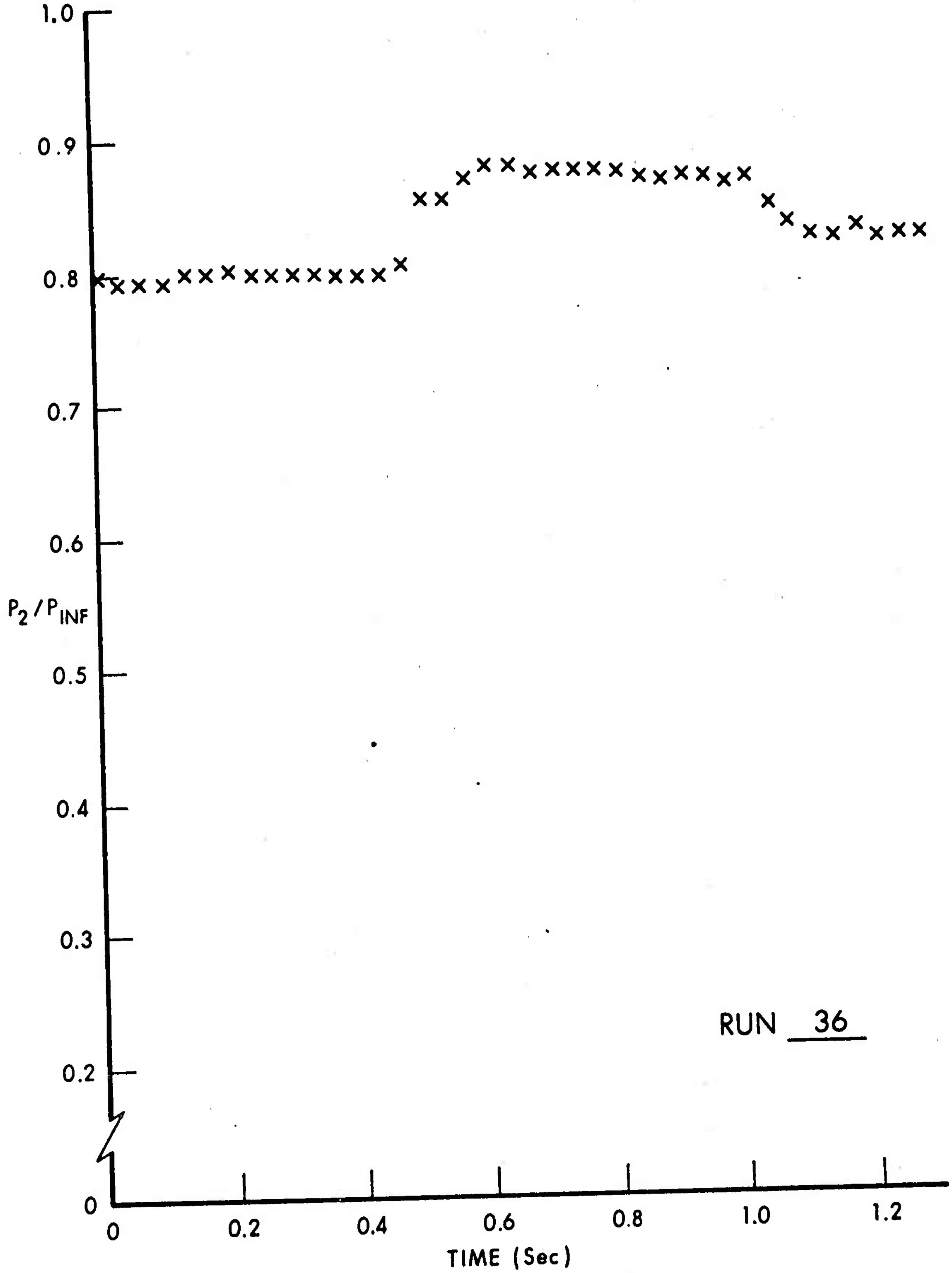

1.0
0.9
0.8
0.7
0.6
P2 / PINF
0.5
0.4
0.3
0.2
0
0
0.2
0.4
0.6
0.8
1.0
1.2
TIME (Sec)
RUN 36

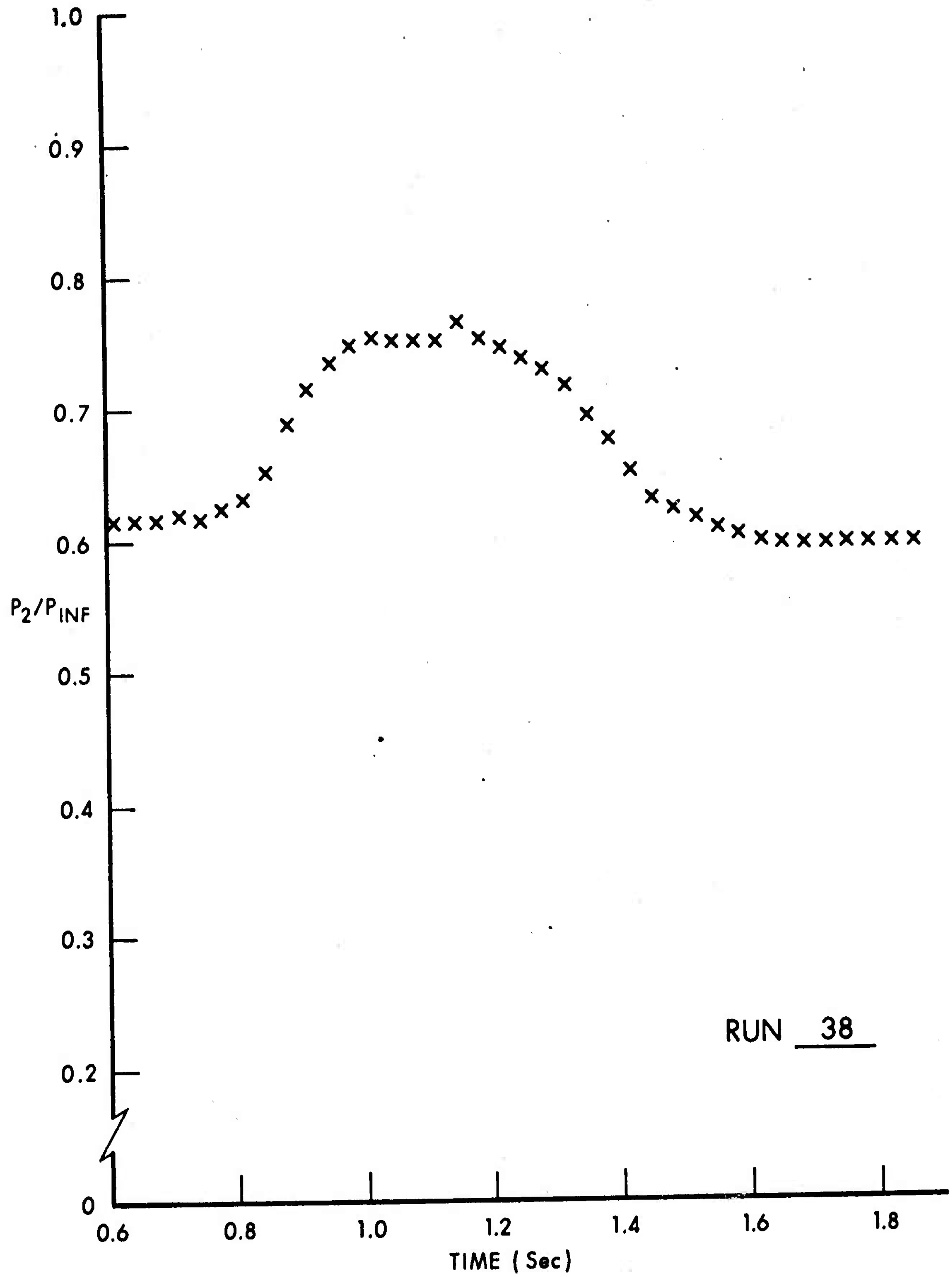
1.0
0.9
0.8
0.7
0.6
P2/PINF
0.5
0.4
0.3
0.2
0
RUN 38
0.6
0.8
1.0
1.2
1.4
1.6
1.8
TIME (Sec)

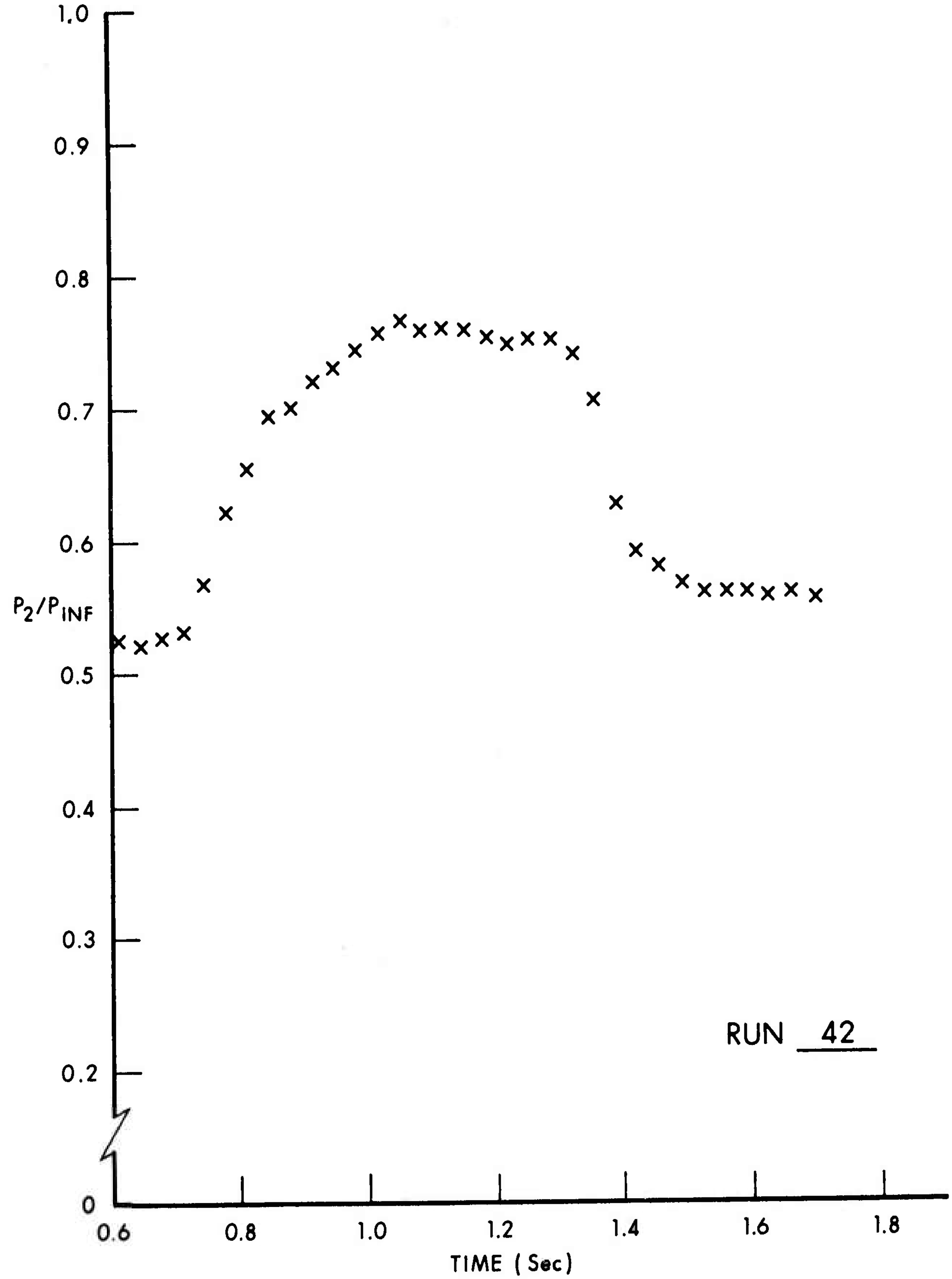
1.0
0.9
0.8
0.7
0.6
P_2/P_{INF}
0.5
0.4
0.3
0.2
0
0.6
0.8
1.0
1.2
1.4
1.6
1.8
TIME (Sec)
RUN 42

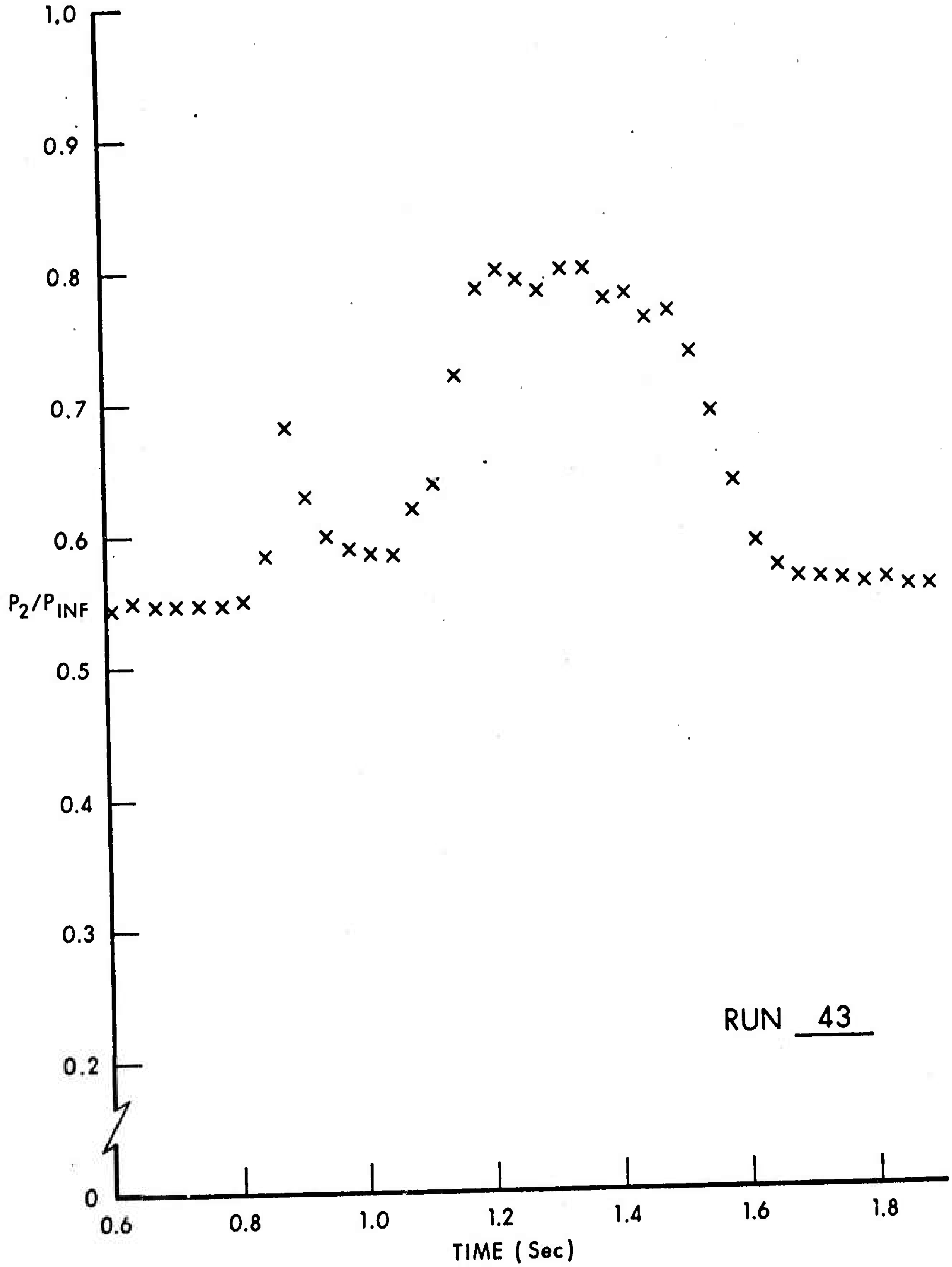
1.0
0.9
0.8
0.7
0.6
P_2/P_{INF}
0.5
0.4
0.3
0.2
0
0.6
0.8
1.0
1.2
1.4
1.6
1.8
TIME (Sec)
RUN 43

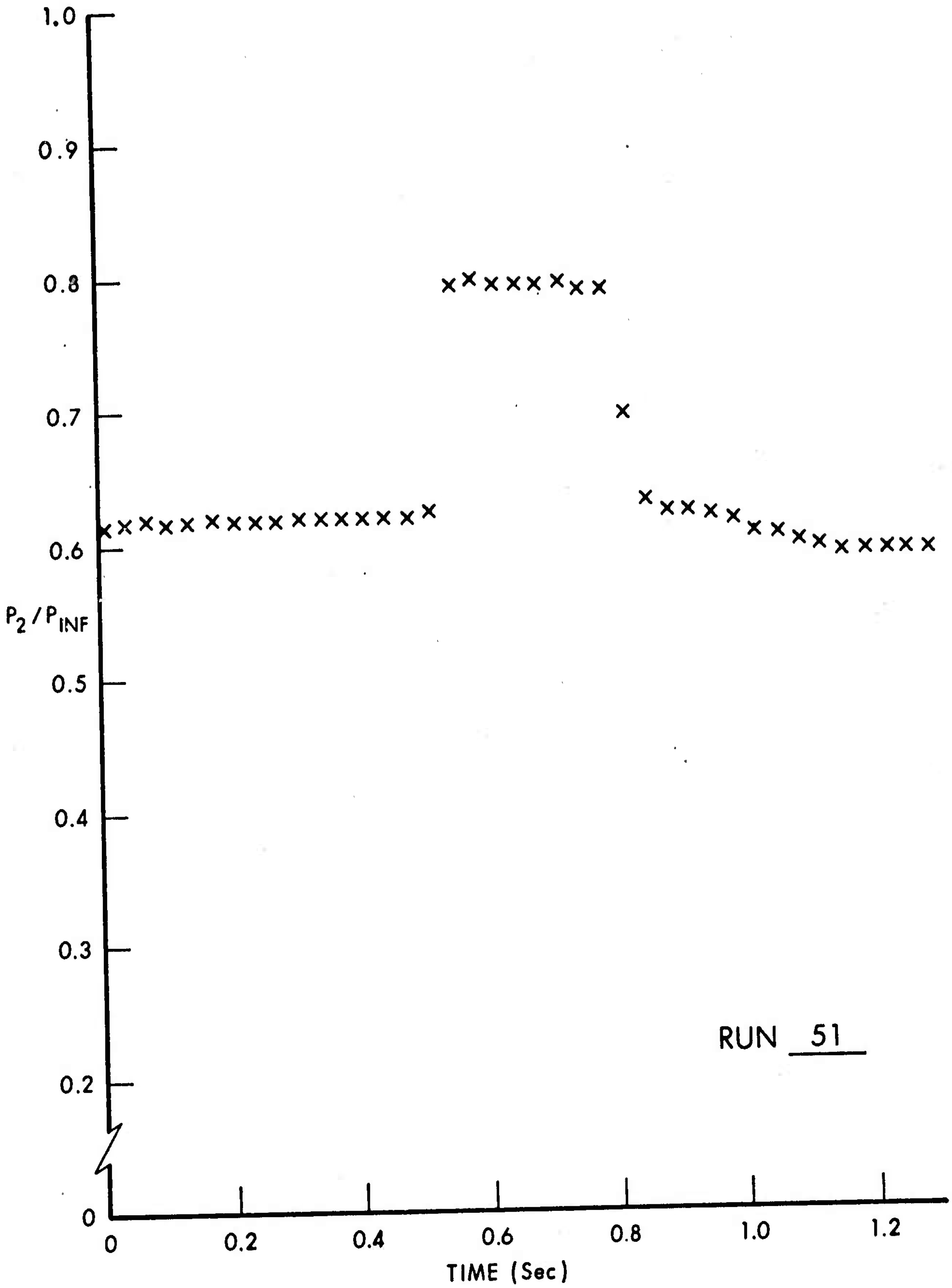
1.0
0.9
0.8
0.7
0.6
P2 / PINF
0.5
0.4
0.3
0.2
0
0
0.2
0.4
0.6
0.8
1.0
1.2
TIME (Sec)
RUN 51

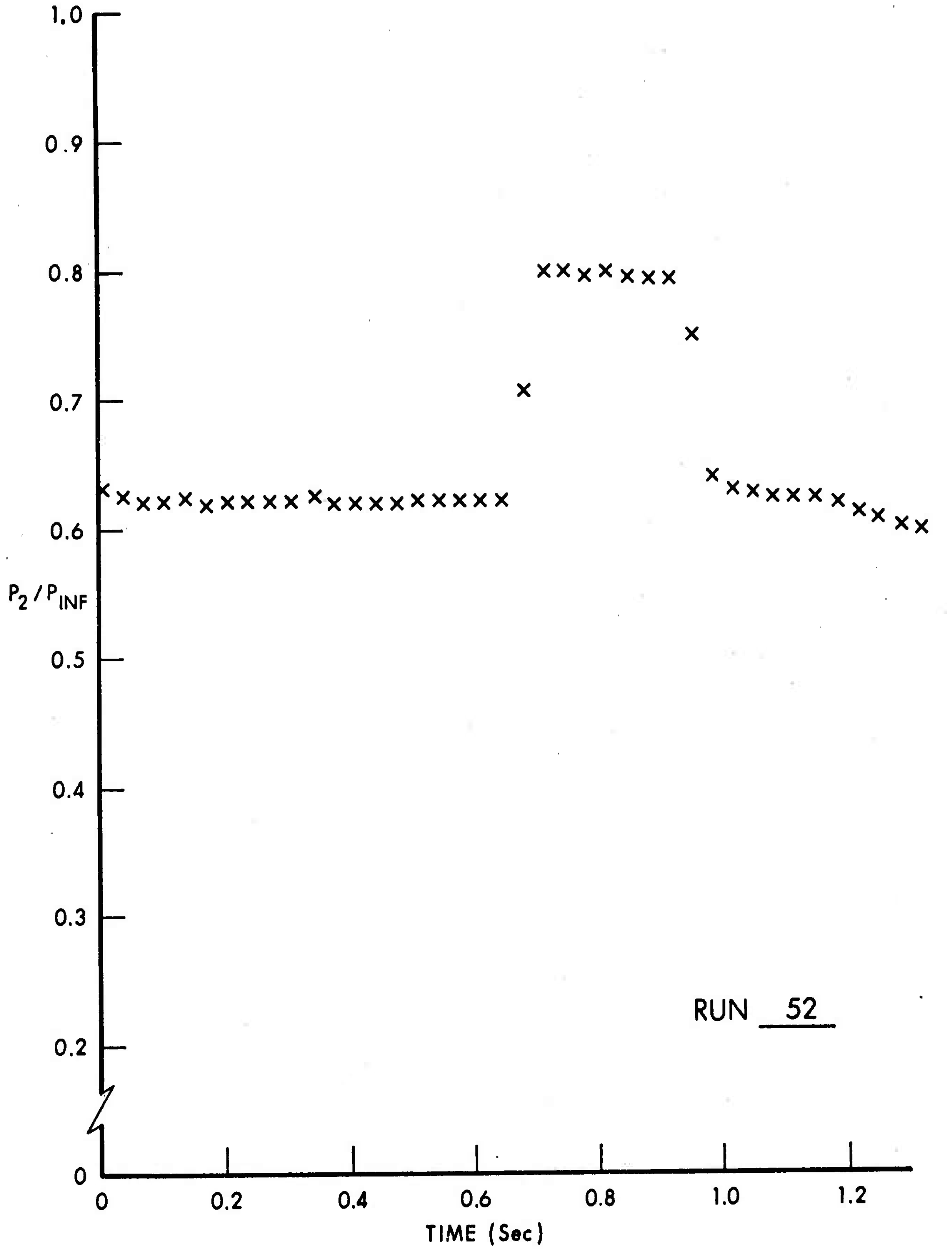
1.0
0.9
0.8
0.7
0.6
P_2 / P_{INF}
0.5
0.4
0.3
0.2
0
0
0.2
0.4
0.6
0.8
1.0
1.2
TIME (Sec)
RUN 52

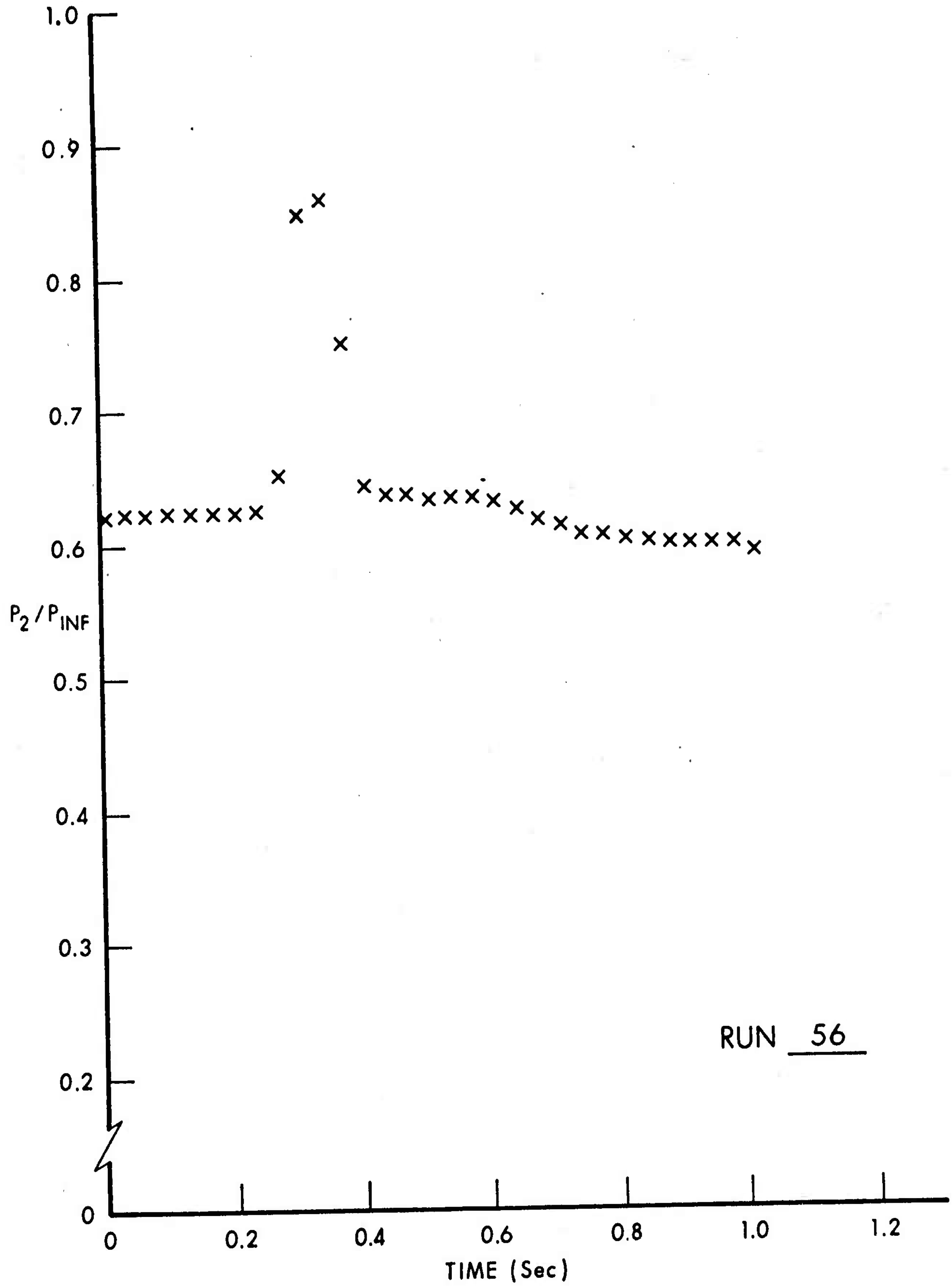
1.0
0.9
0.8
0.7
0.6
P_2 / P_{INF}
0.5
0.4
0.3
0.2
0
0
0.2
0.4
0.6
0.8
1.0
1.2
TIME (Sec)
RUN 56

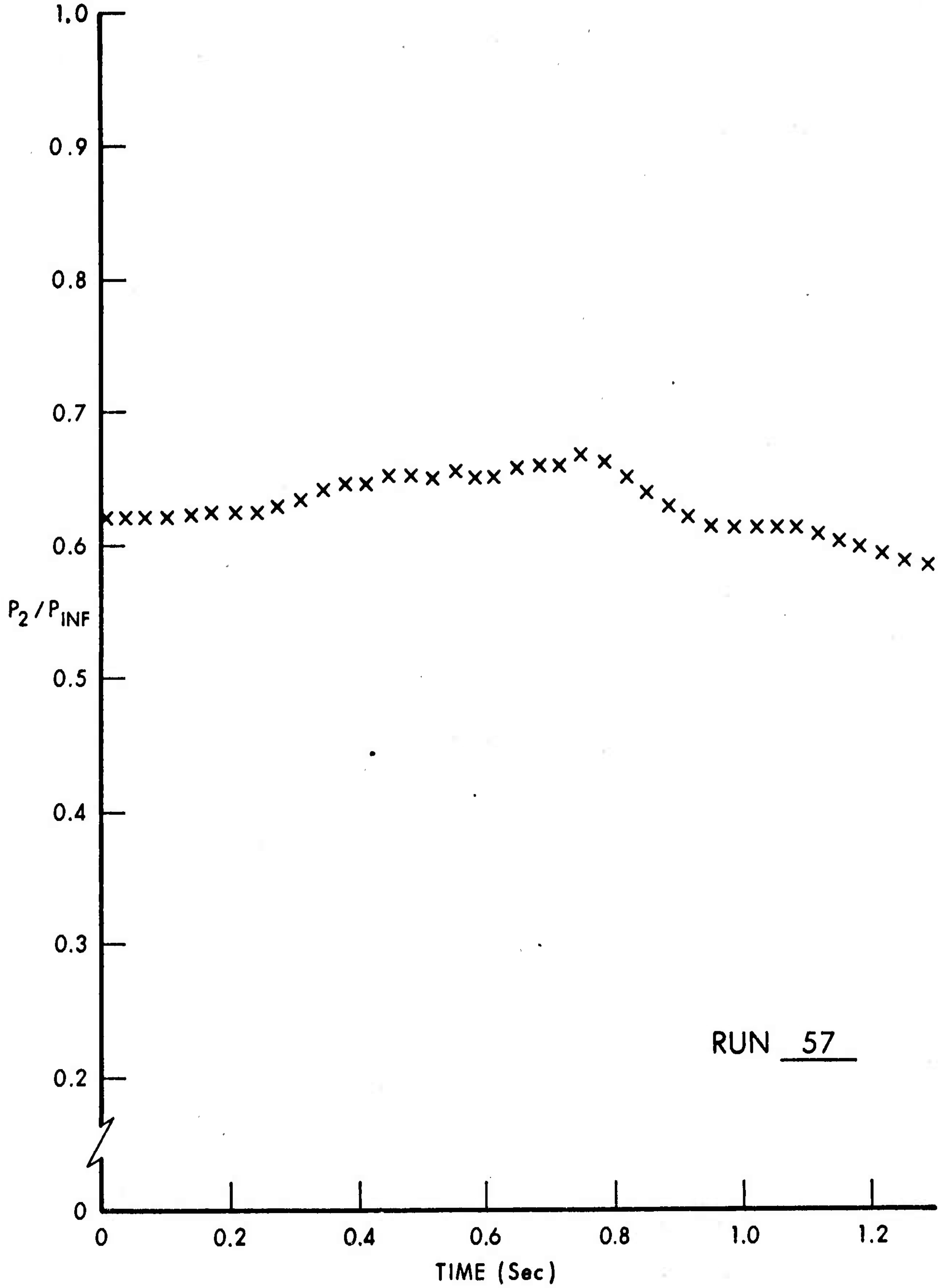
1.0
0.9
0.8
0.7
0.6
P2 / PINF
0.5
0.4
0.3
0.2
0
0
0.2
0.4
0.6
0.8
1.0
1.2
TIME (Sec)
RUN 57

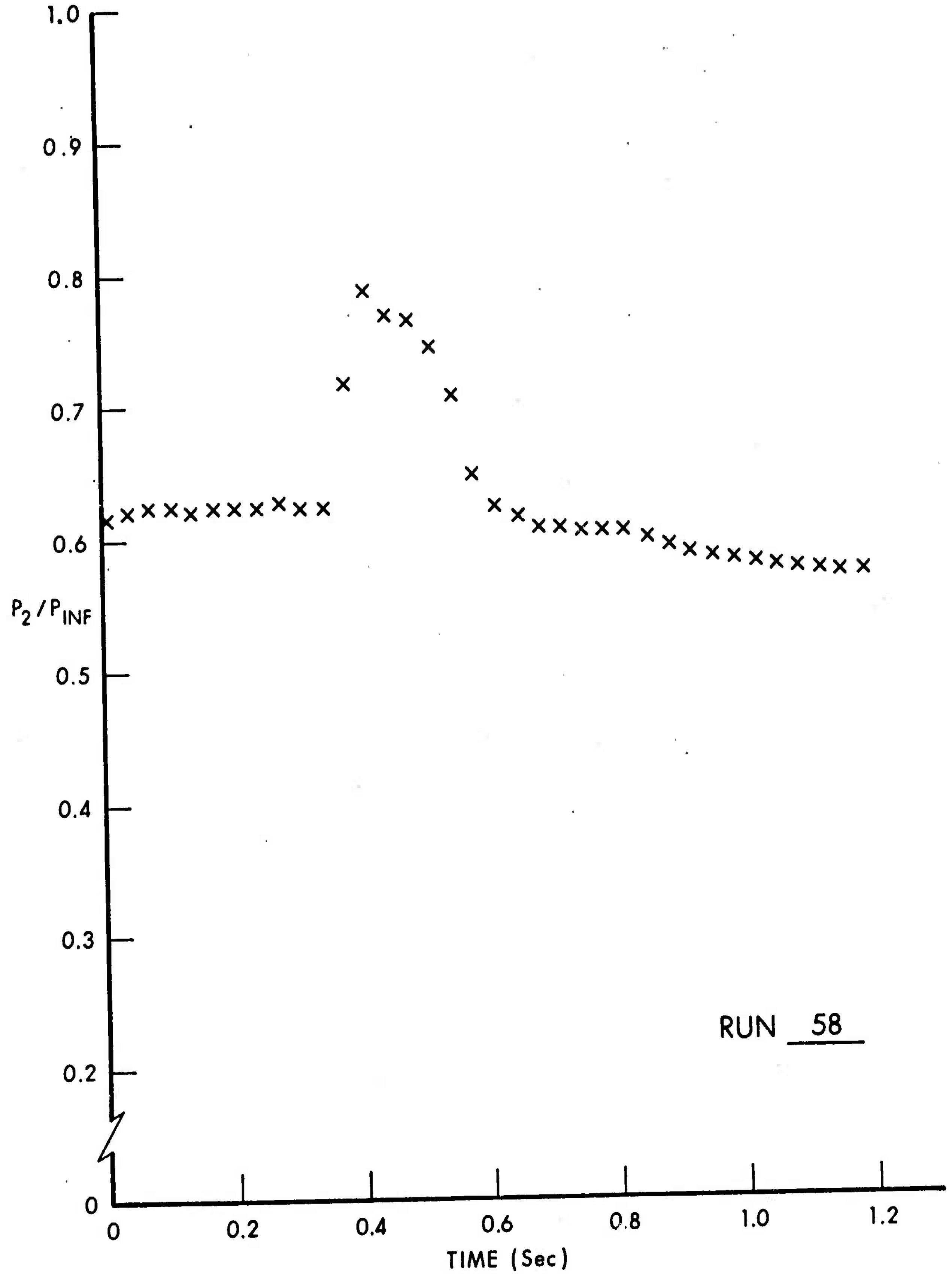
1.0
0.9
0.8
0.7
0.6
P_2 / P_{INF}
0.5
0.4
0.3
0.2
0
0
0.2
0.4
0.6
0.8
1.0
1.2
TIME (Sec)
RUN 58

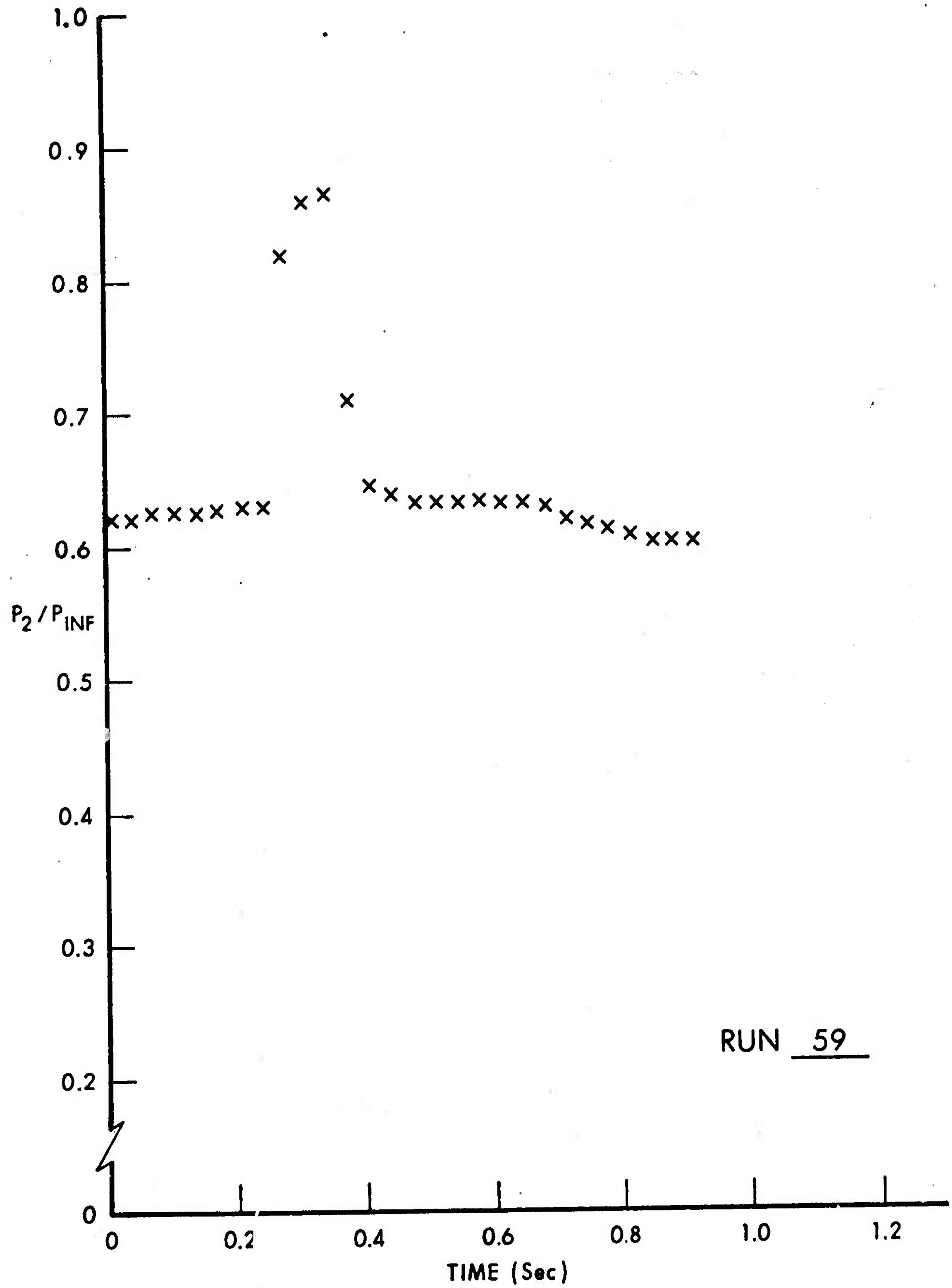
1.0
0.9
0.8
0.7
0.6
P_2 / P_{INF}
0.5
0.4
0.3
0.2
0
0
0.2
0.4
0.6
0.8
1.0
1.2
TIME (Sec)
RUN 59

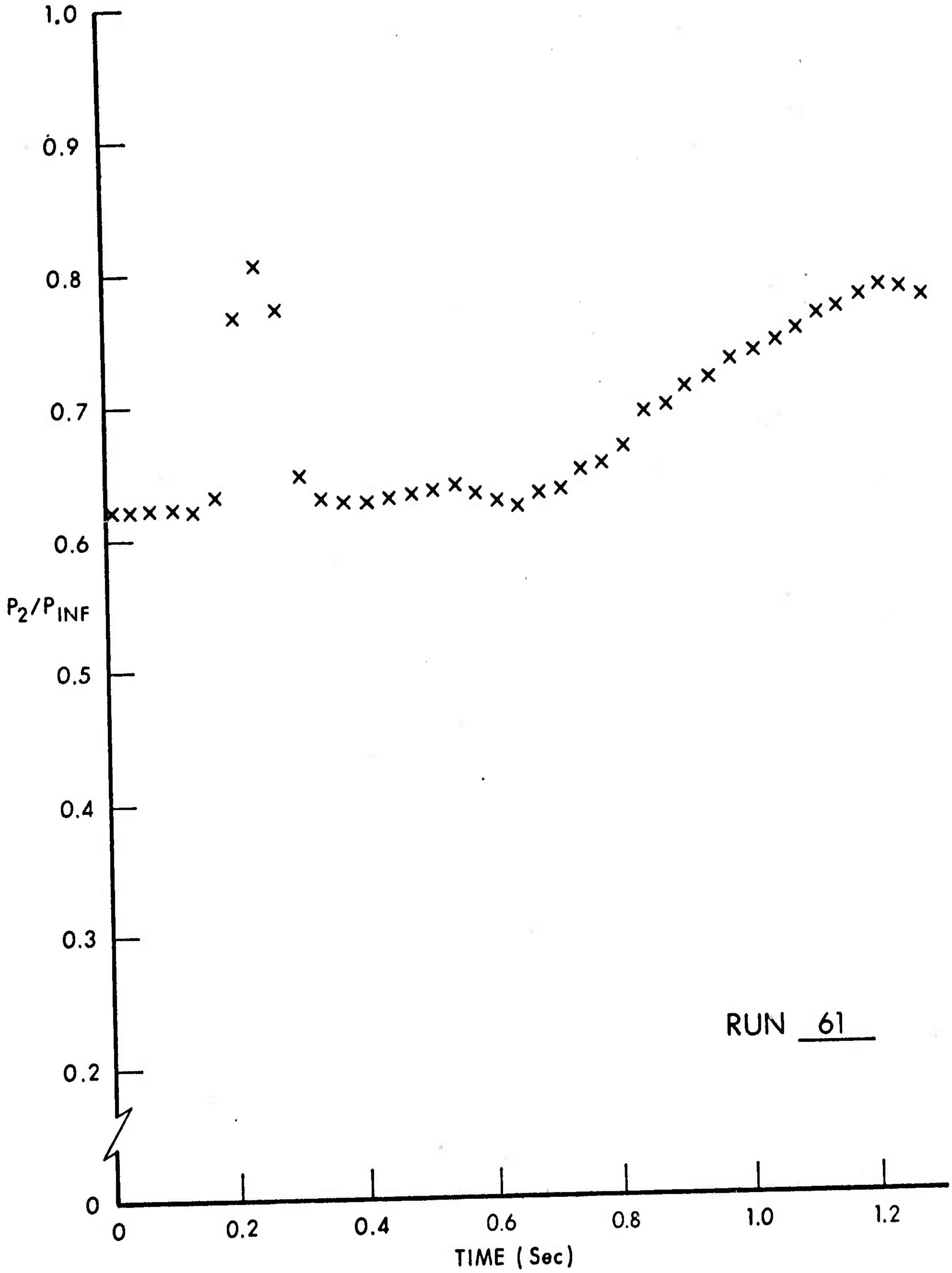
1.0
0.9
0.8
0.7
0.6
P_2/P_{INF}
0.5
0.4
0.3
0.2
0
RUN 61
0
0.2
0.4
0.6
0.8
1.0
1.2
TIME (Sec)

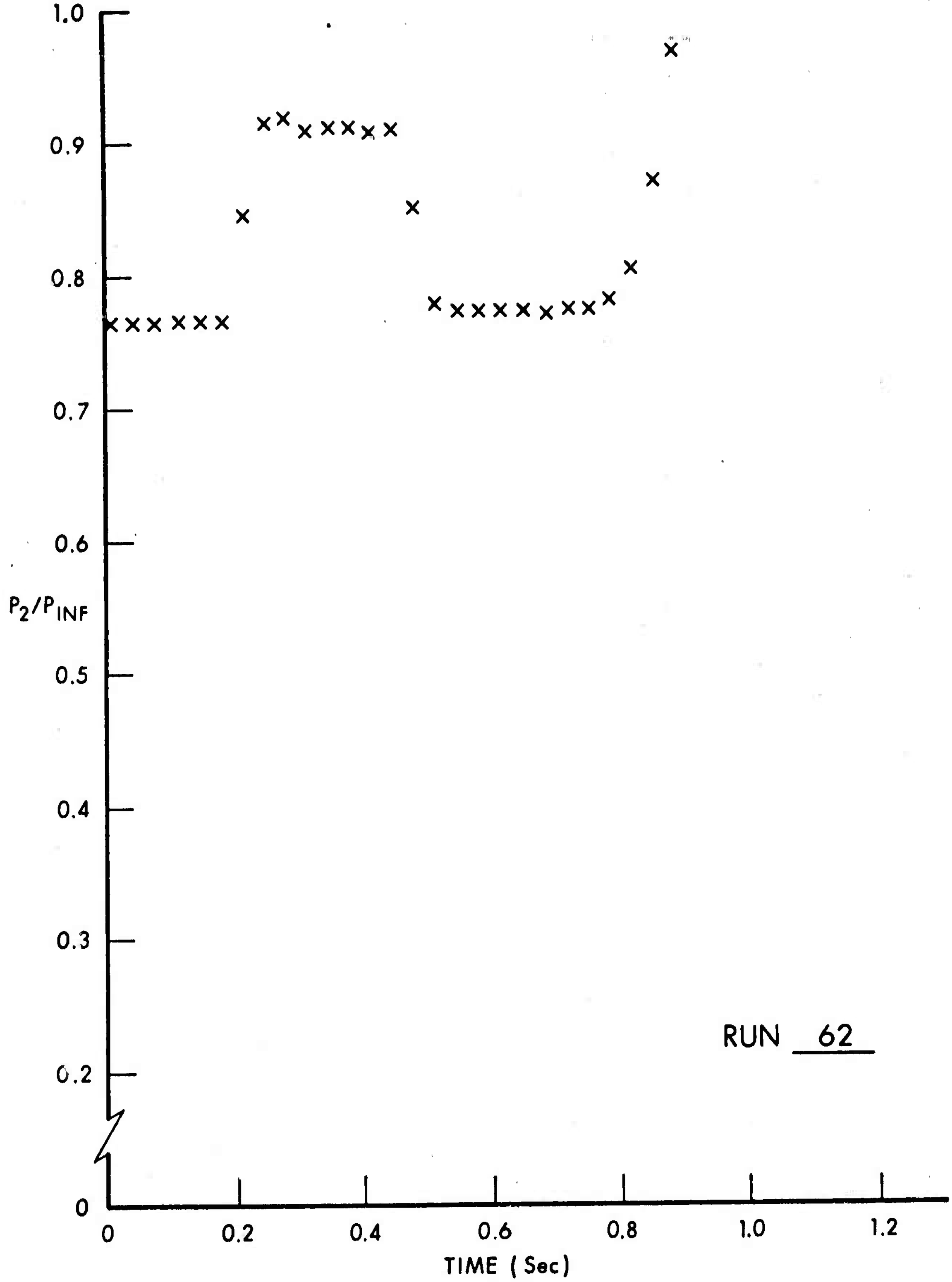

1.0
0.9
0.8
0.7
0.6
P2/PINF
0.5
0.4
0.3
0.2
0
0
0.2
0.4
0.6
0.8
1.0
1.2
TIME (Sec)
RUN 62

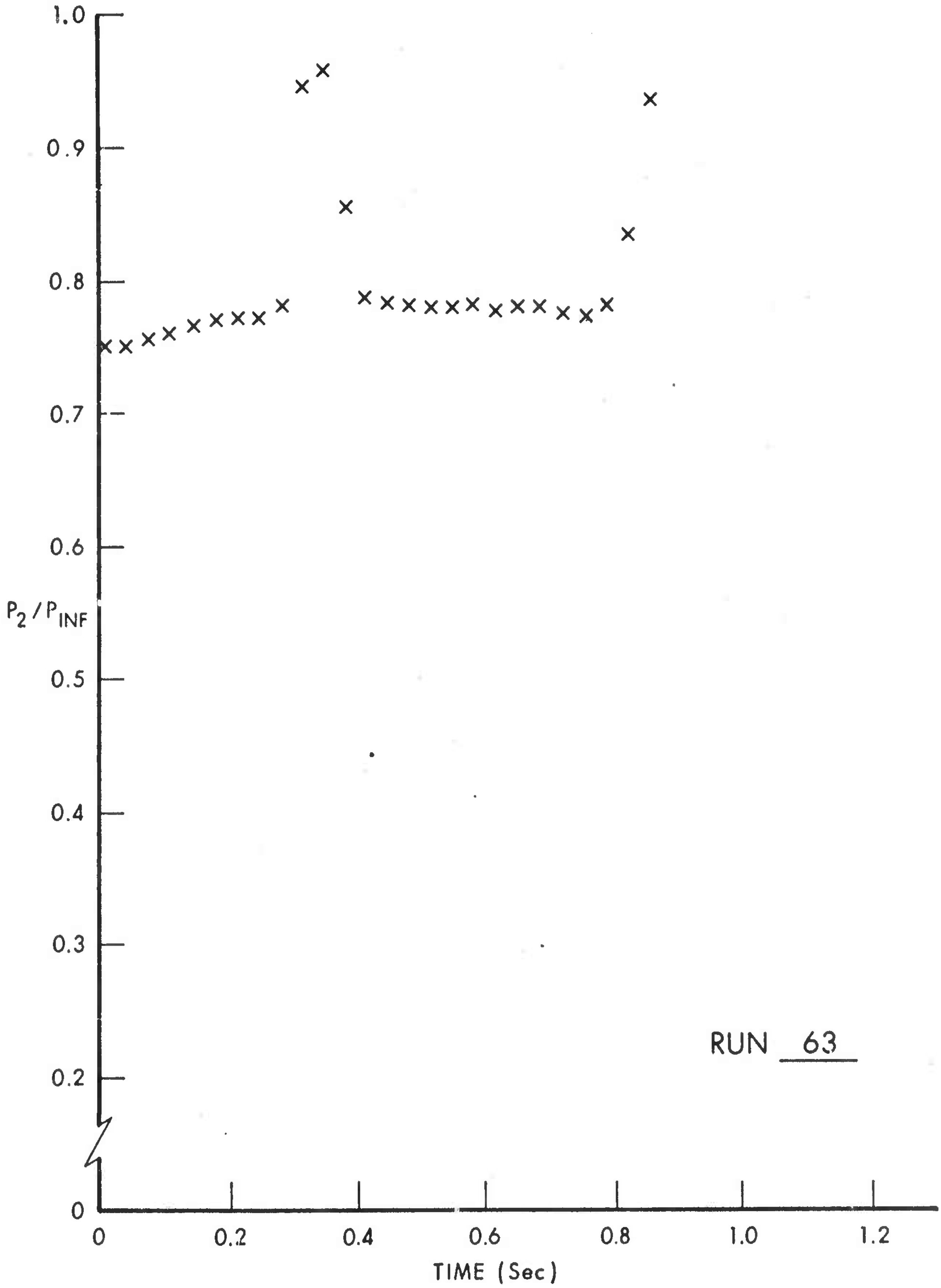
1.0
0.9
0.8
0.7
0.6
P_2 / P_{INF}
0.5
0.4
0.3
0.2
0
0
0.2
0.4
0.6
0.8
1.0
1.2
TIME (Sec)
RUN 63

APPENDIX B.

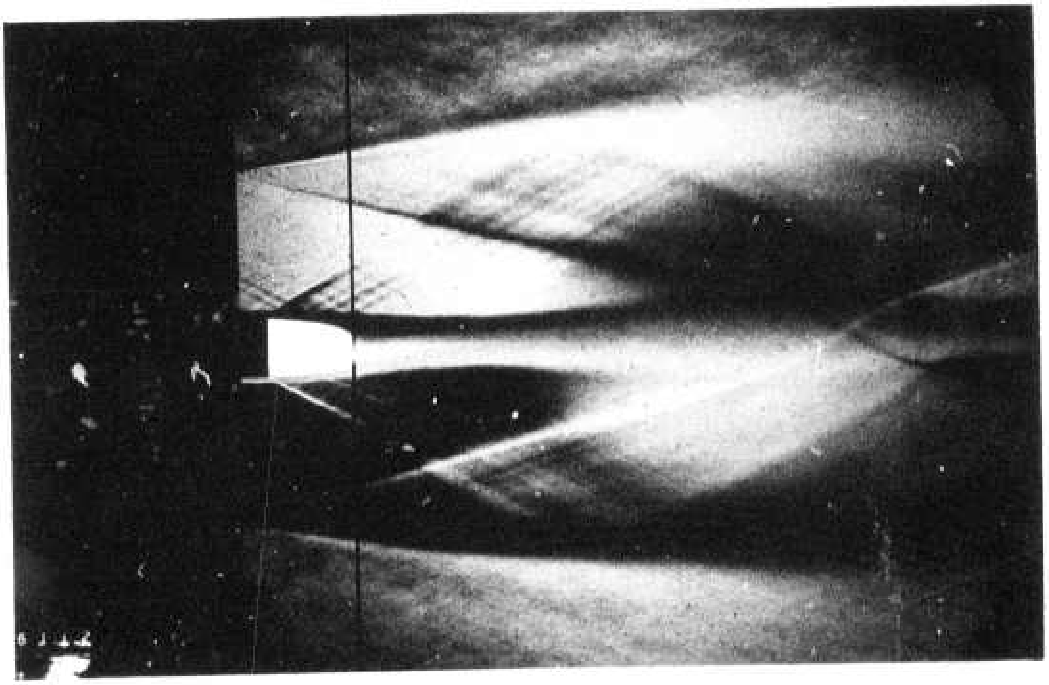

Run 1

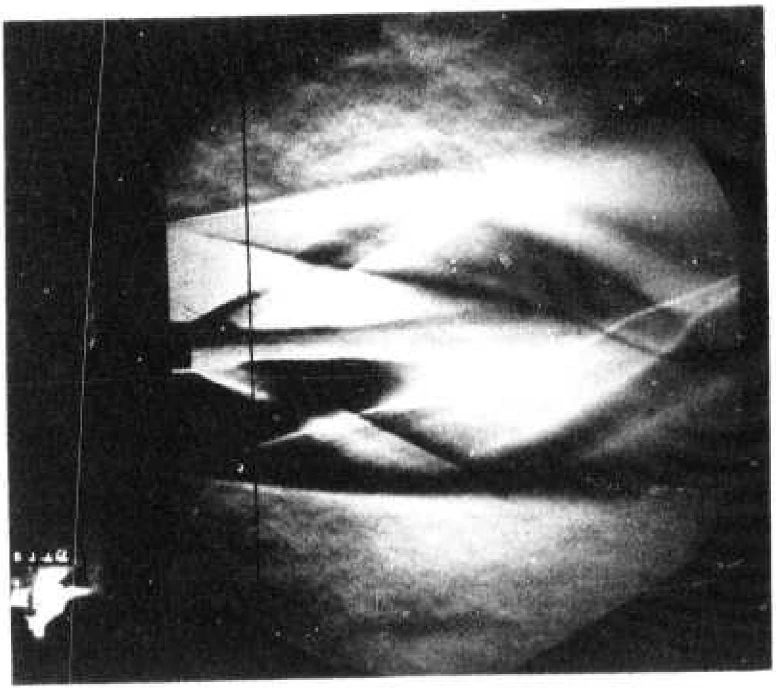

Run 1 (Post-Combustion)

SCHLIEREN PHOTOGRAPHS OF FLOW WITH COMBUSTION

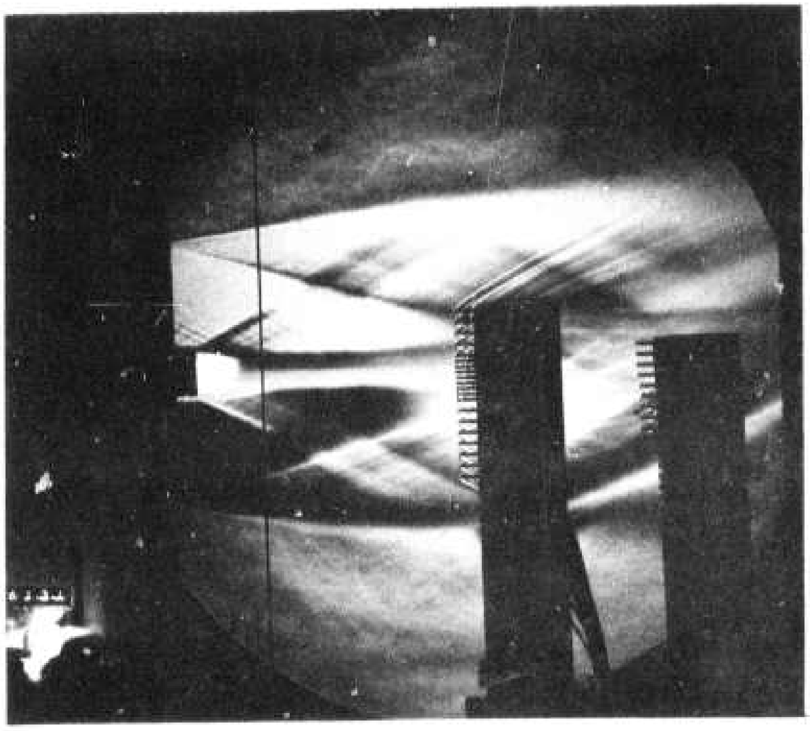

Run 2

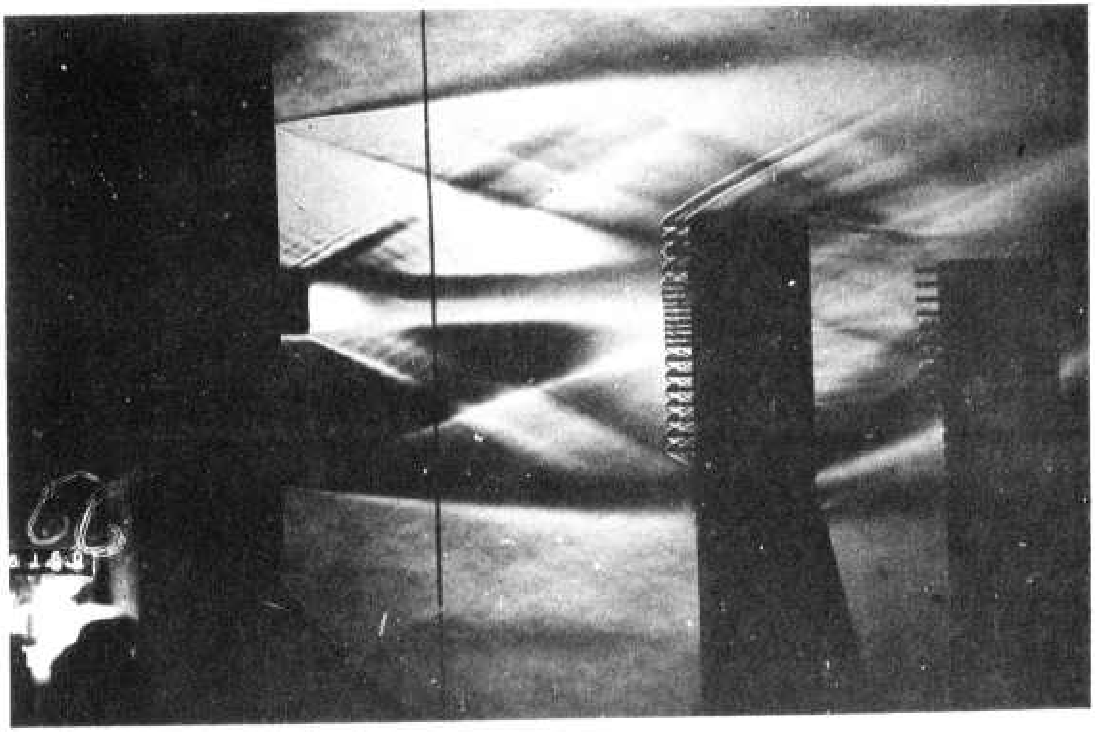

Run 10

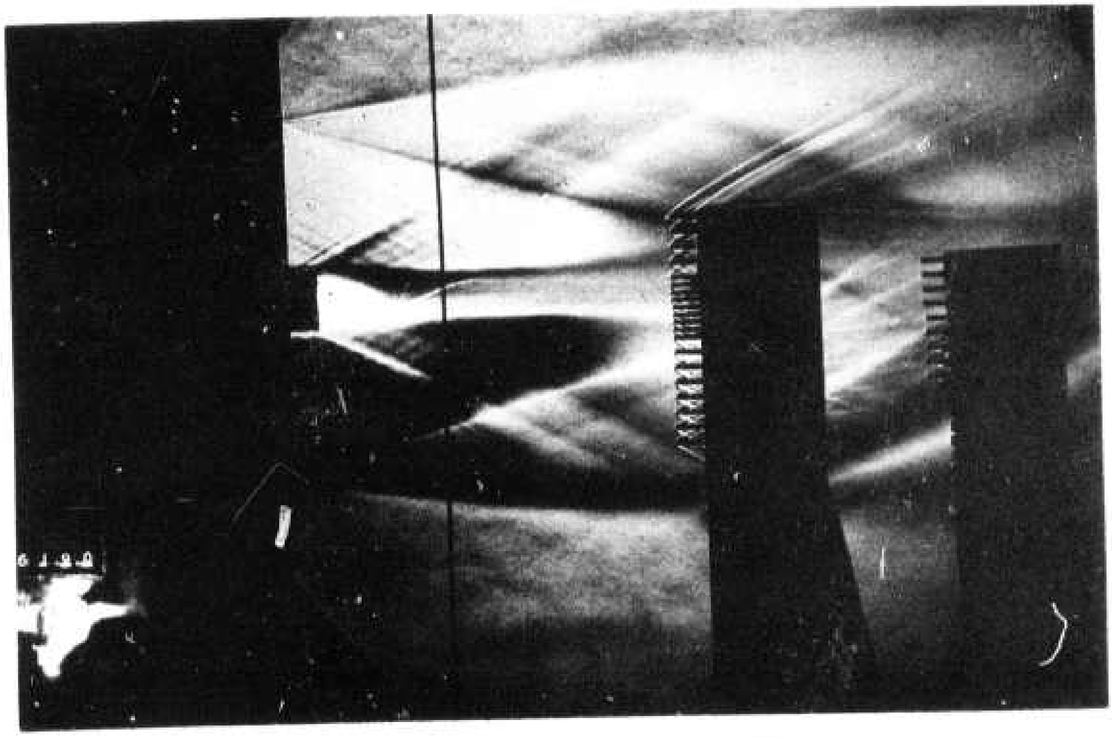

Run 12

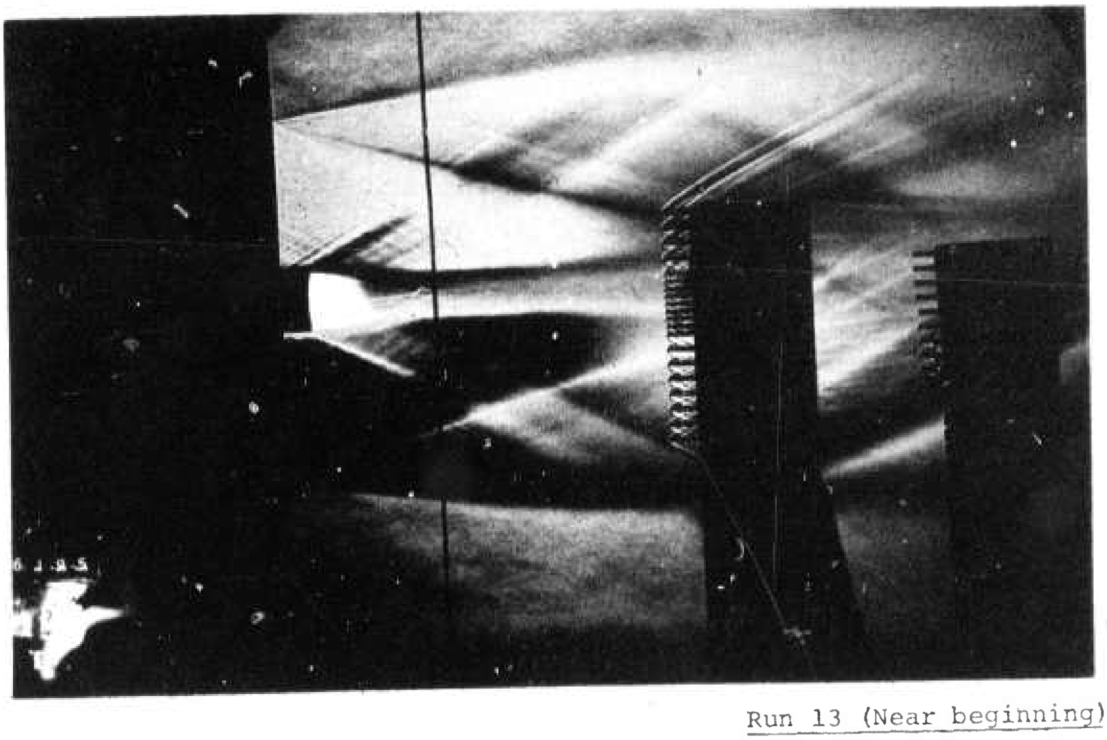

Run 13 (Near beginning)

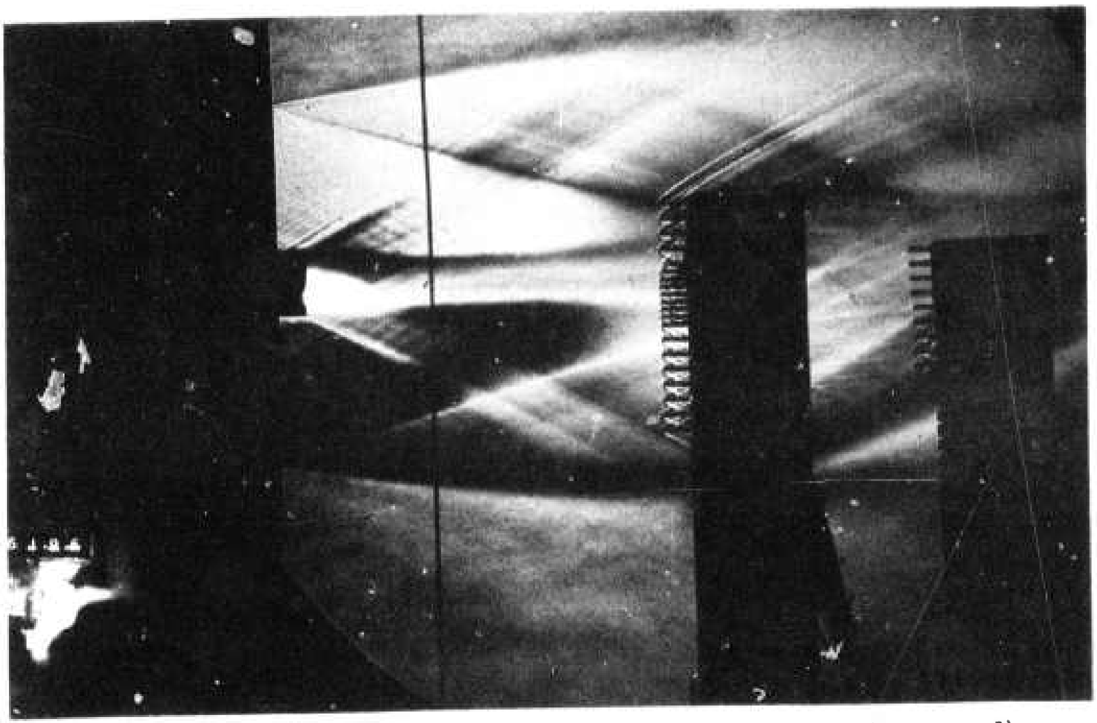

Run 13 (Near end)

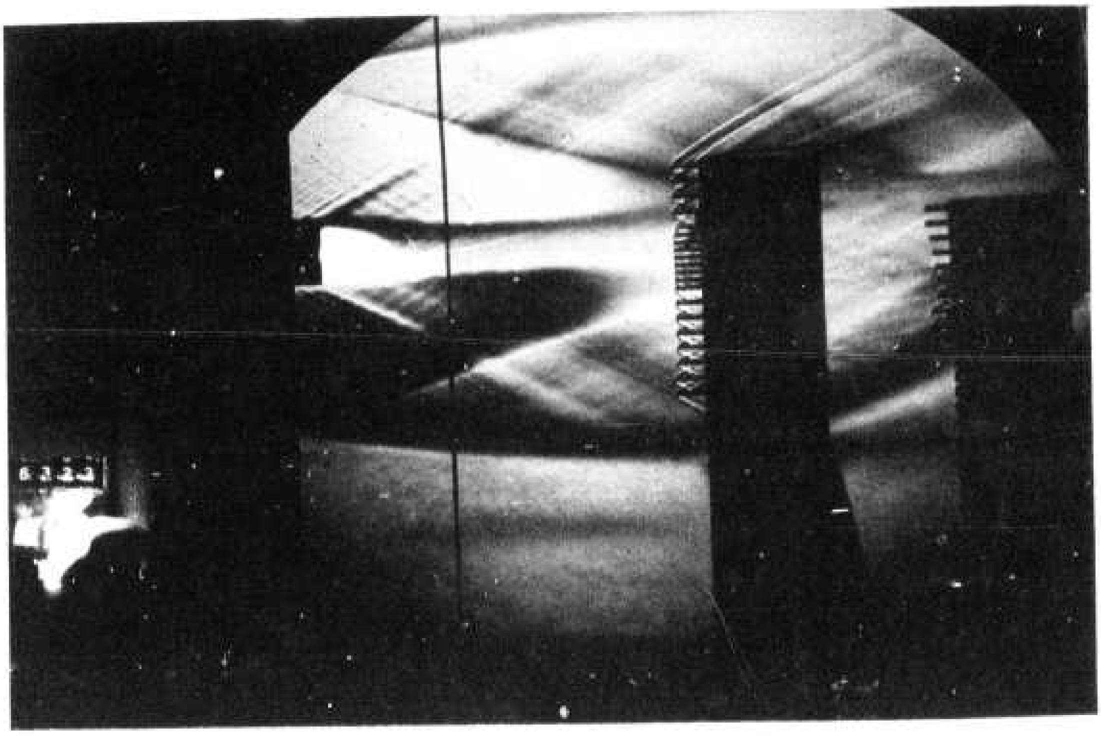

Run 27

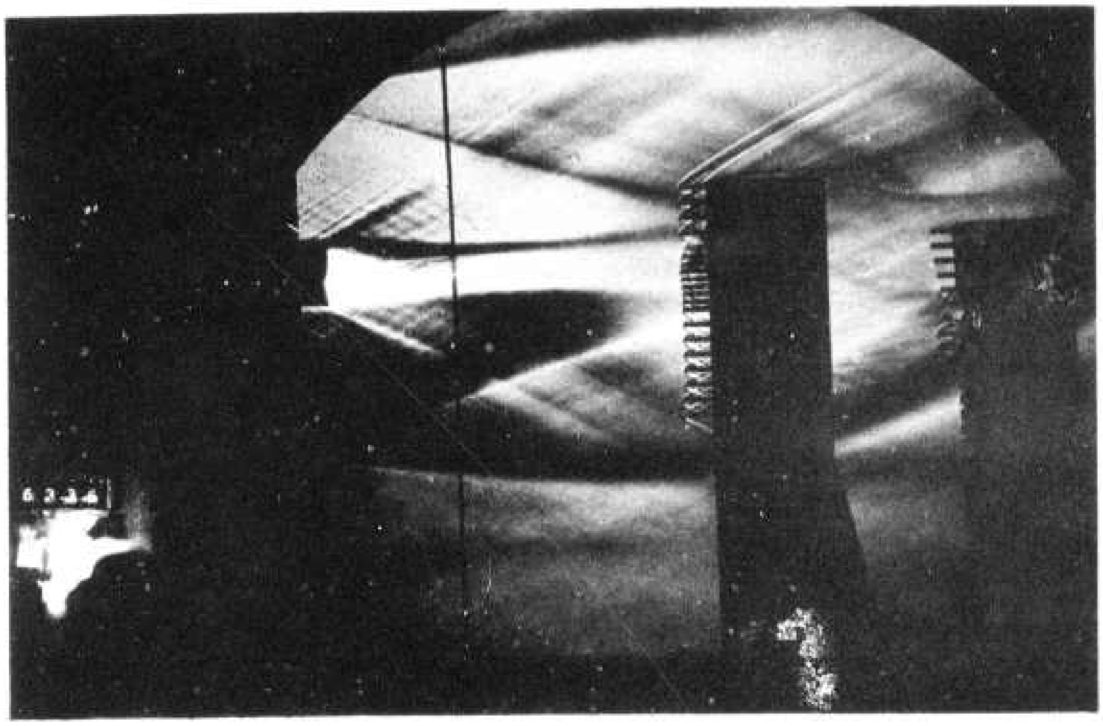

Run 29

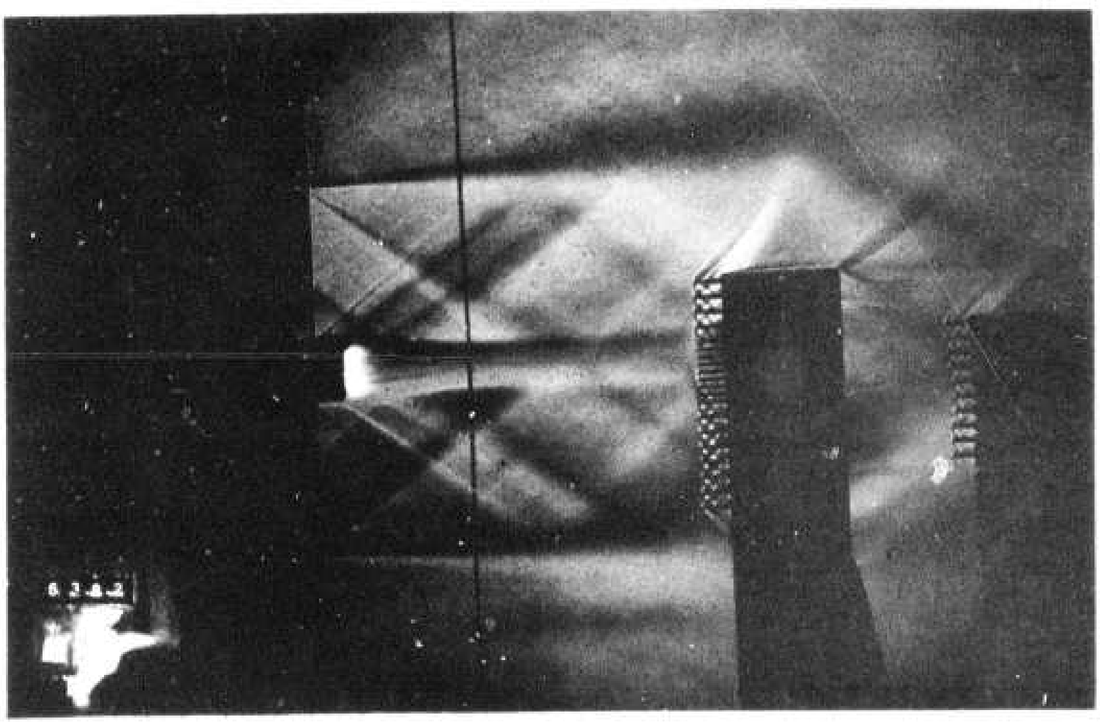

Run 35 (Beginning of Combustion)

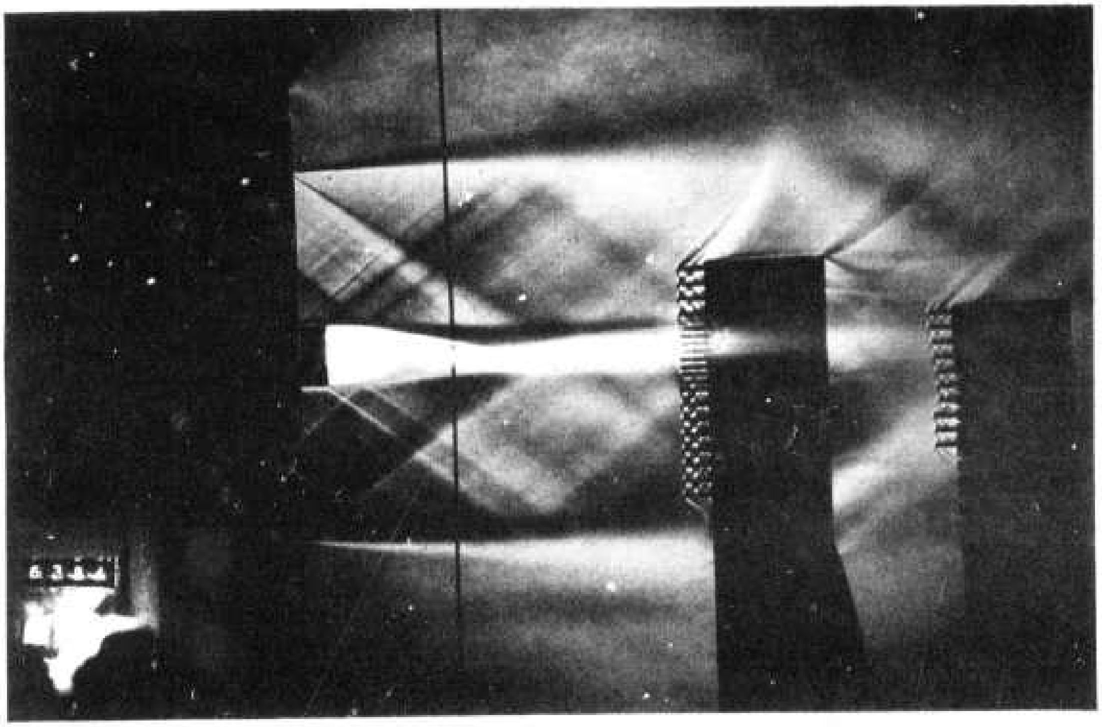

Run 35

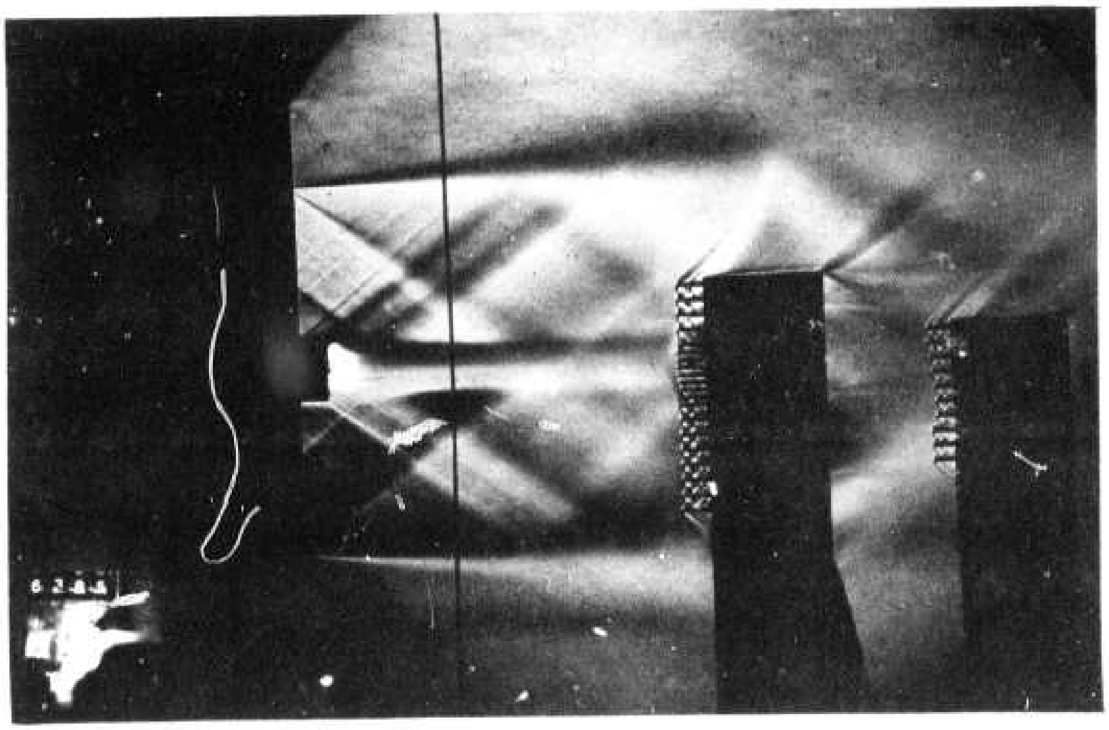

Run 35 (End of Combustion)

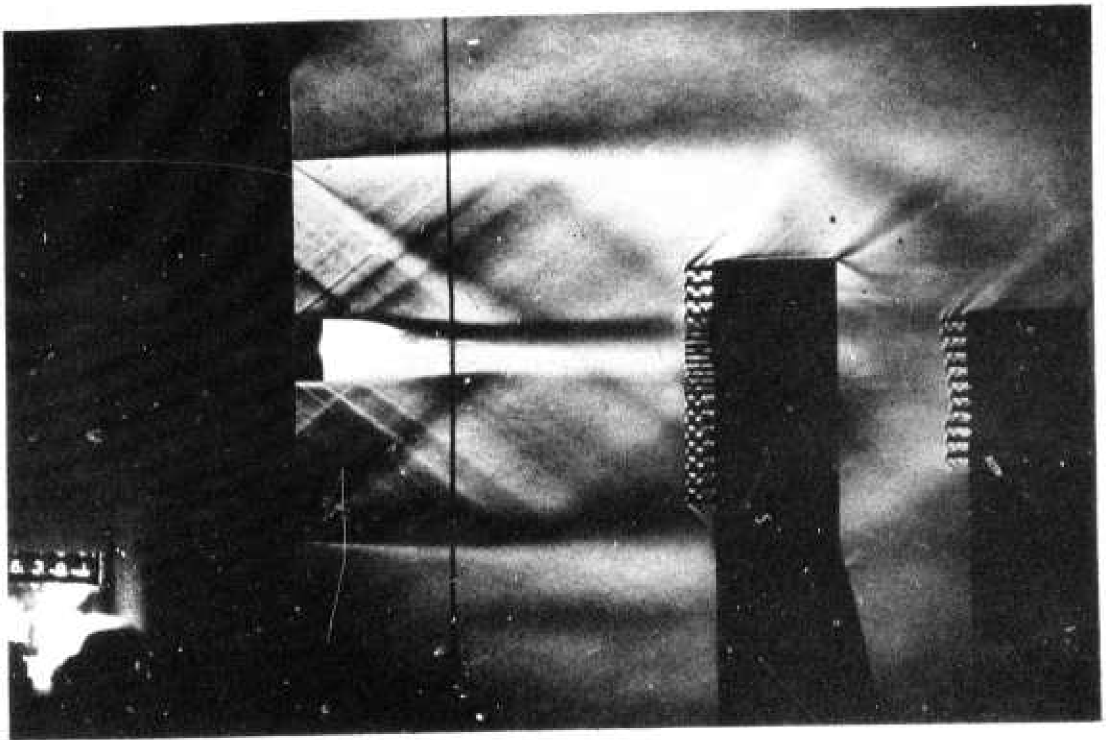

Run 36 (Beginning of Combustion)

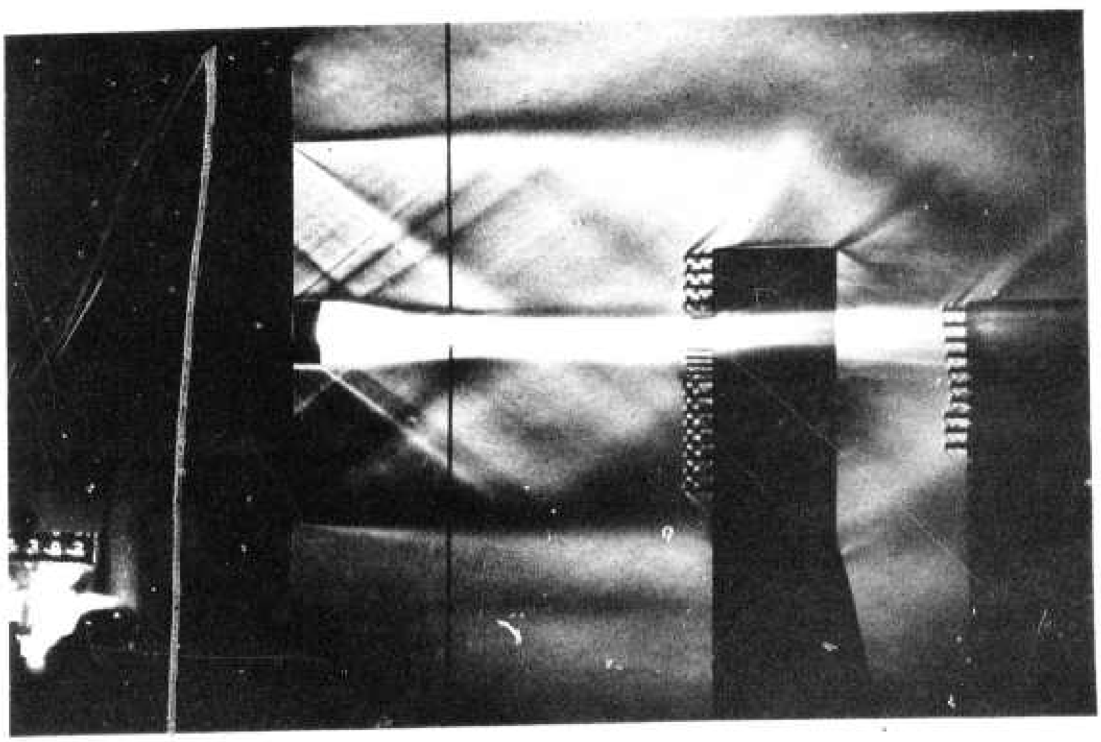

Run 36

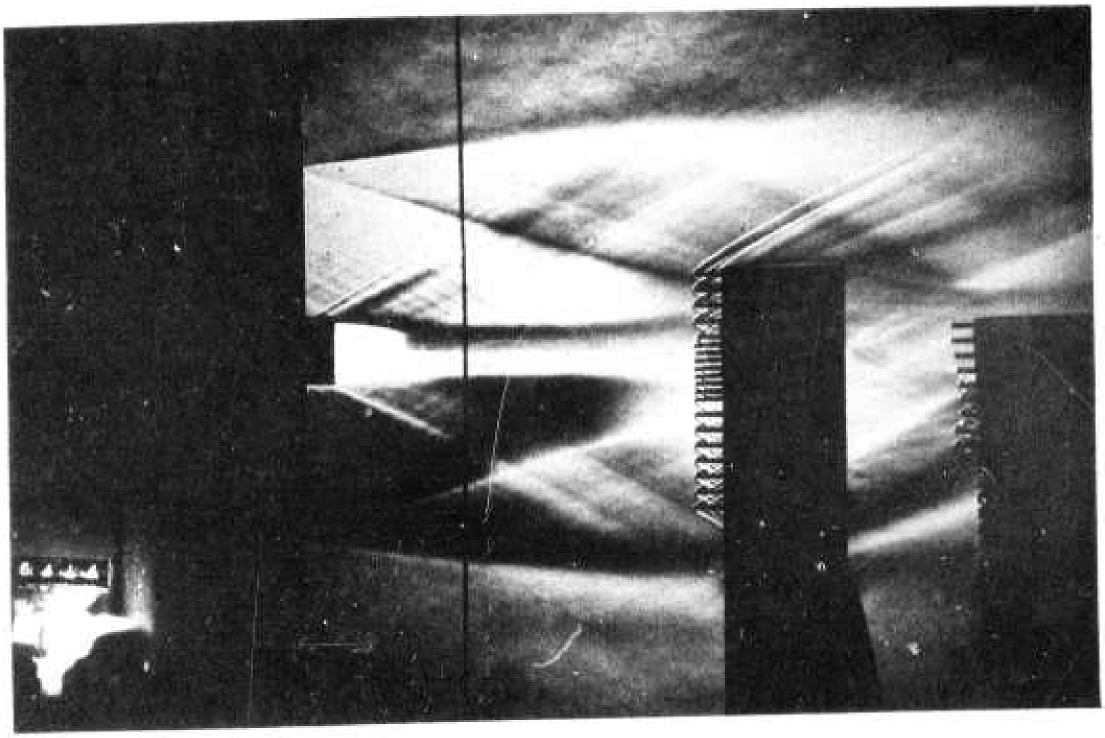

Run 38

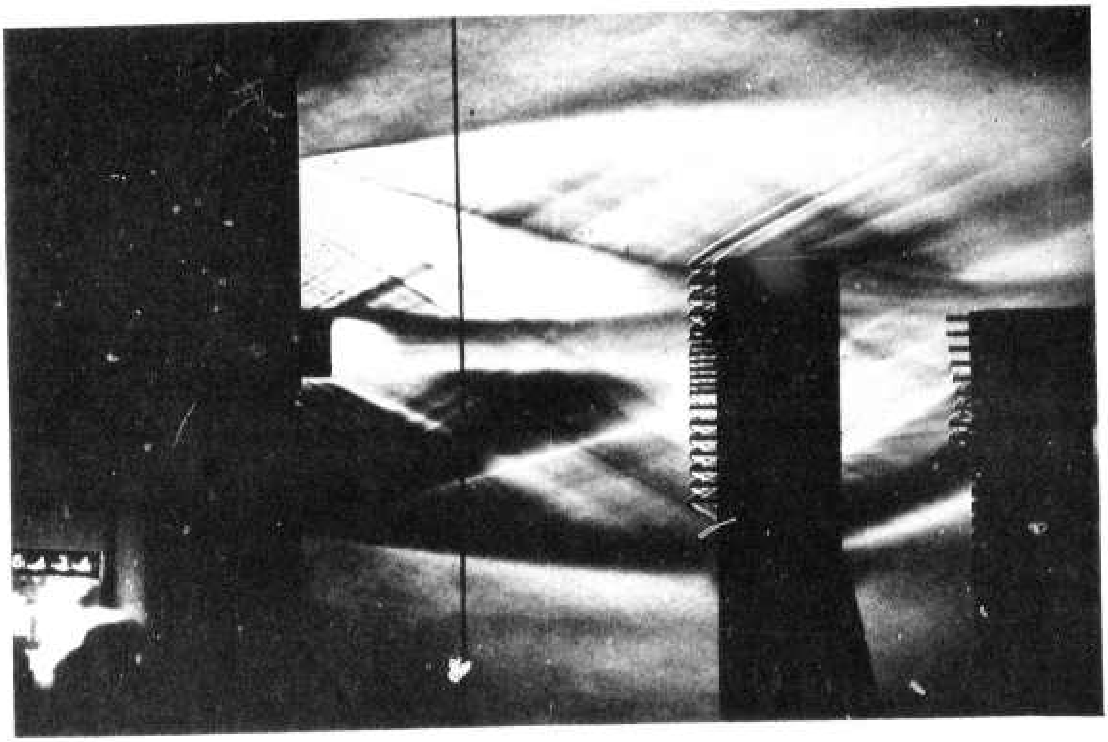

Run 41

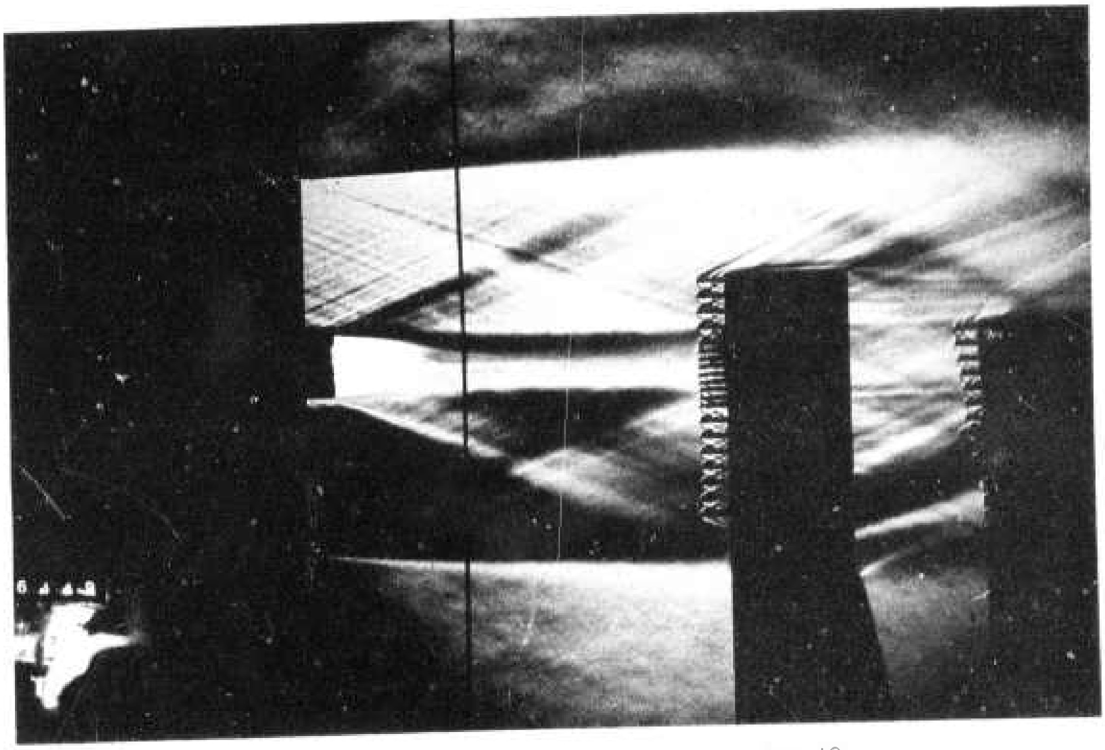

Run 42

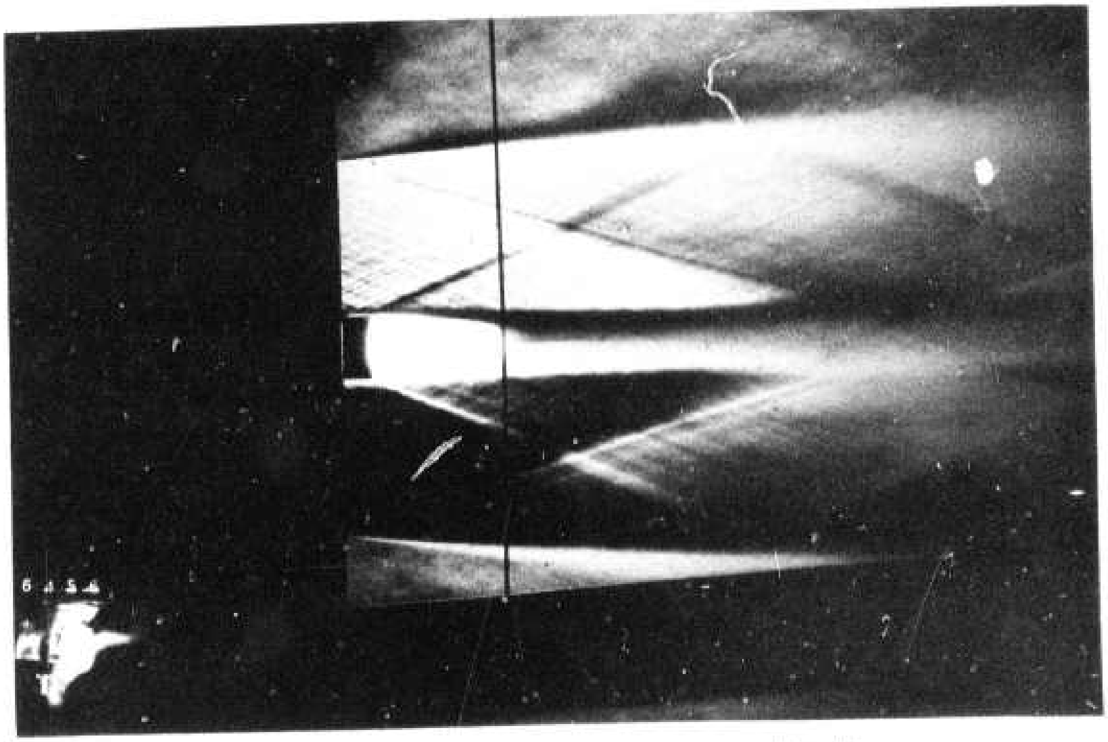

Run 43

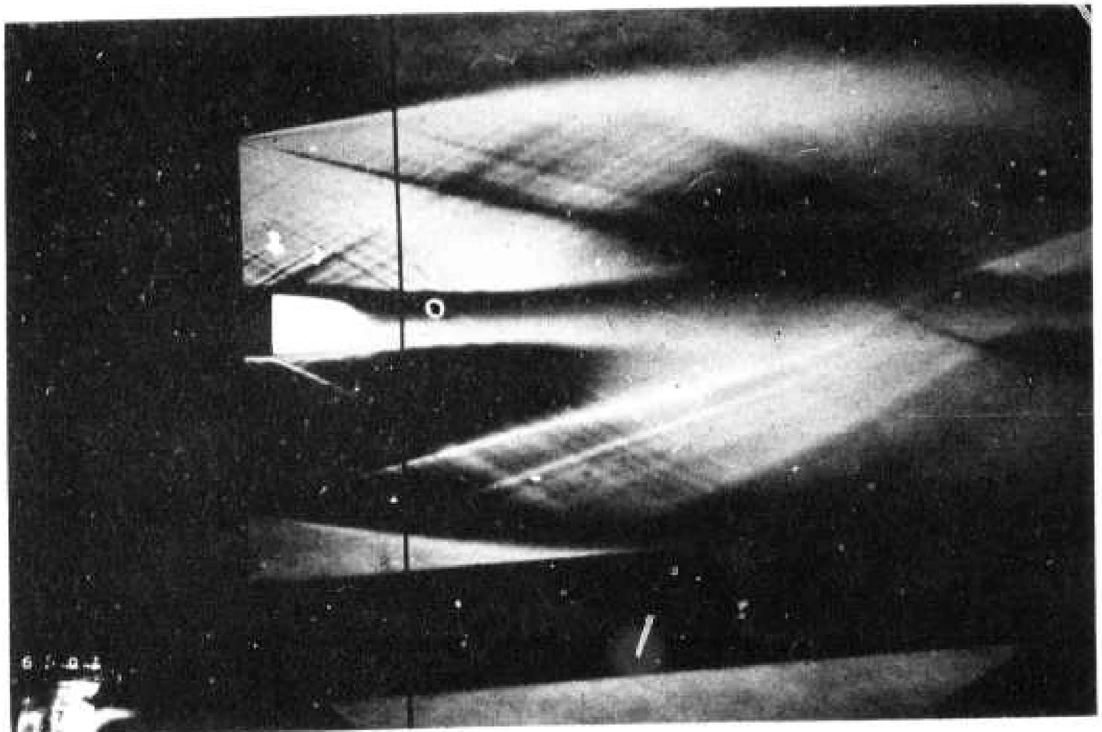

Run 51

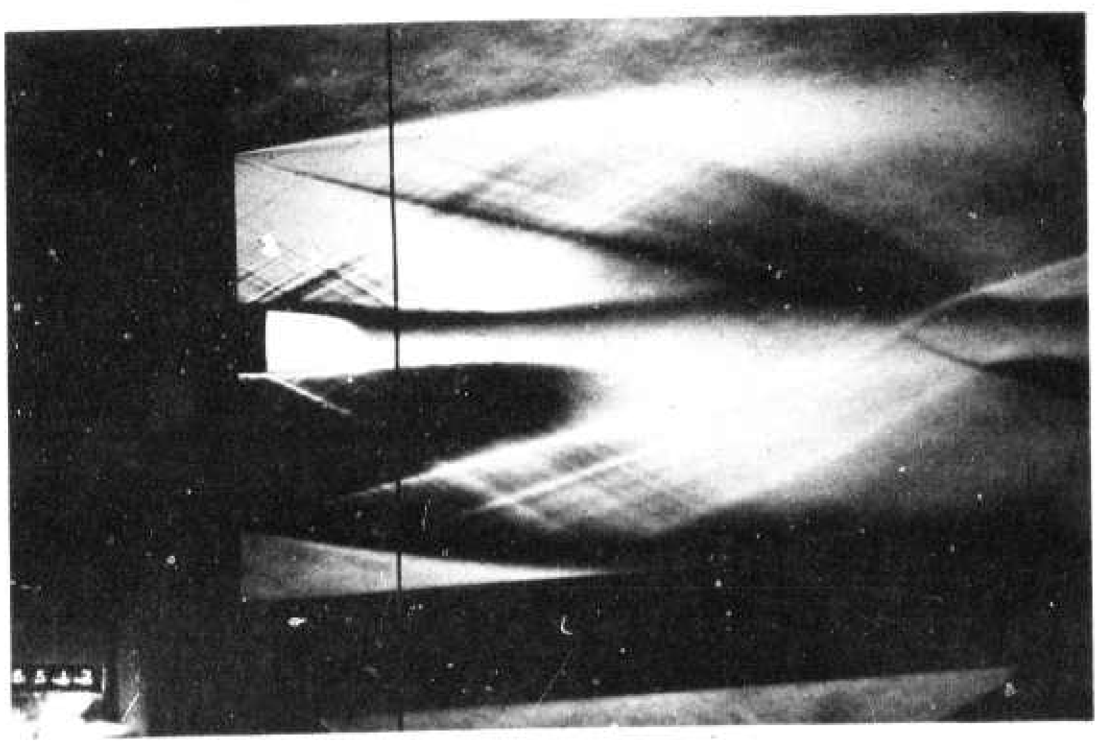

Run 52

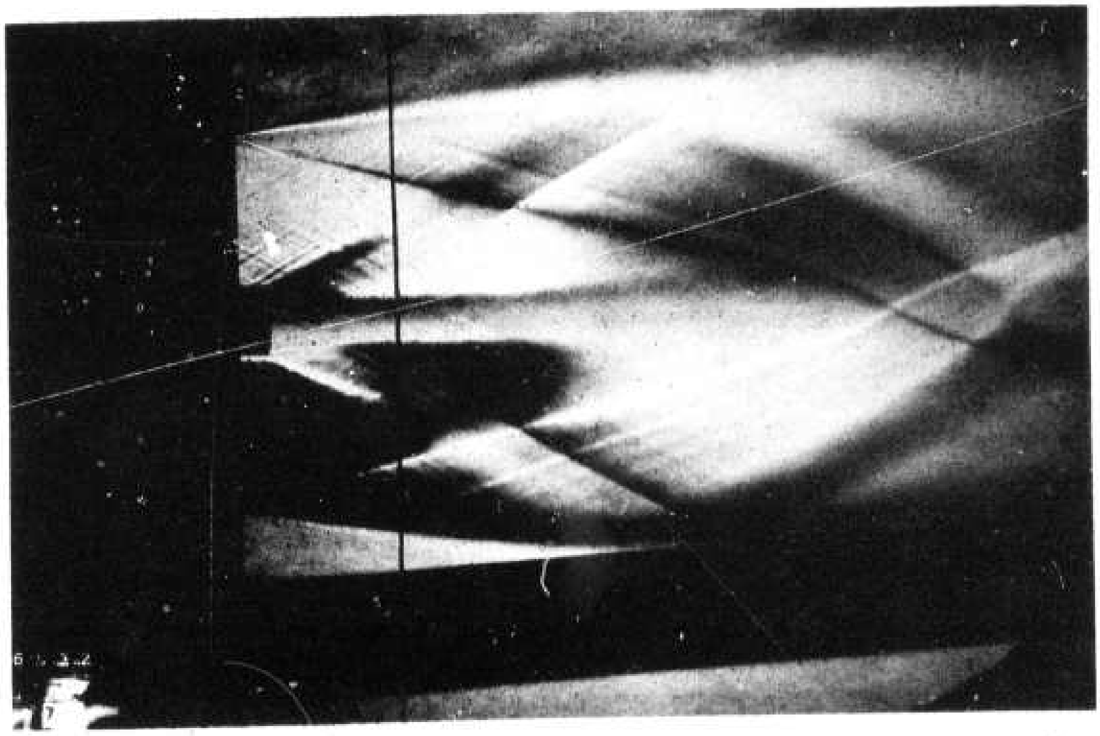

Run 56 (Pre-Combustion)

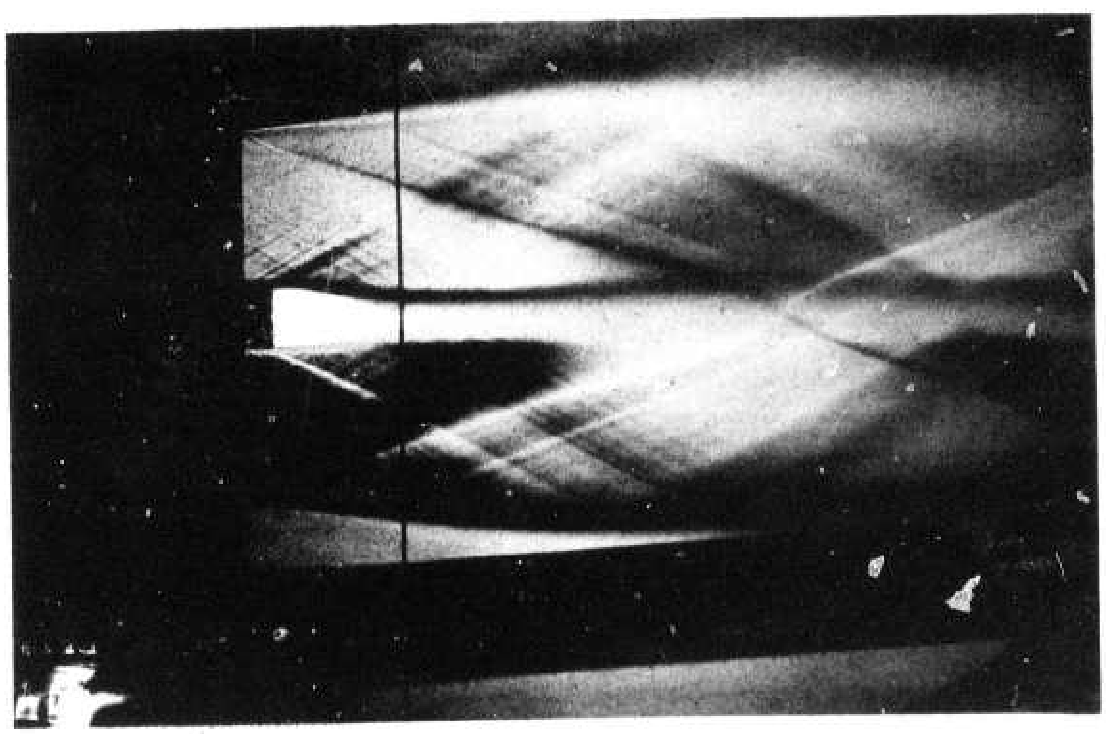

Run 58

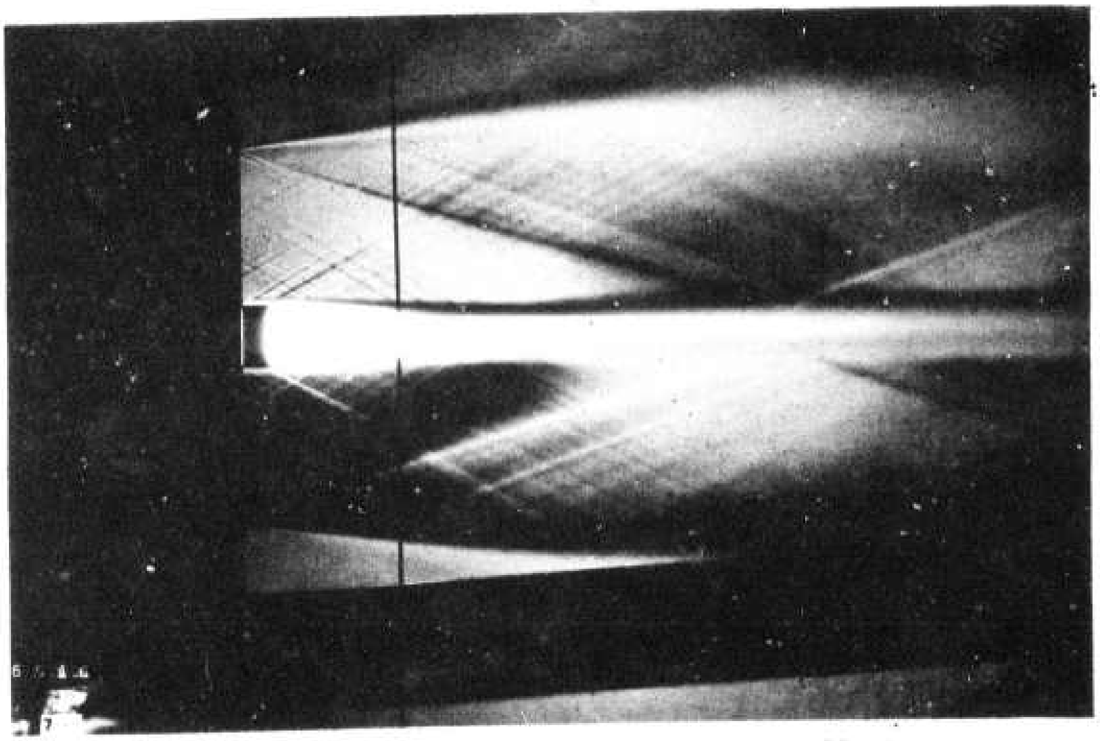

Run 59

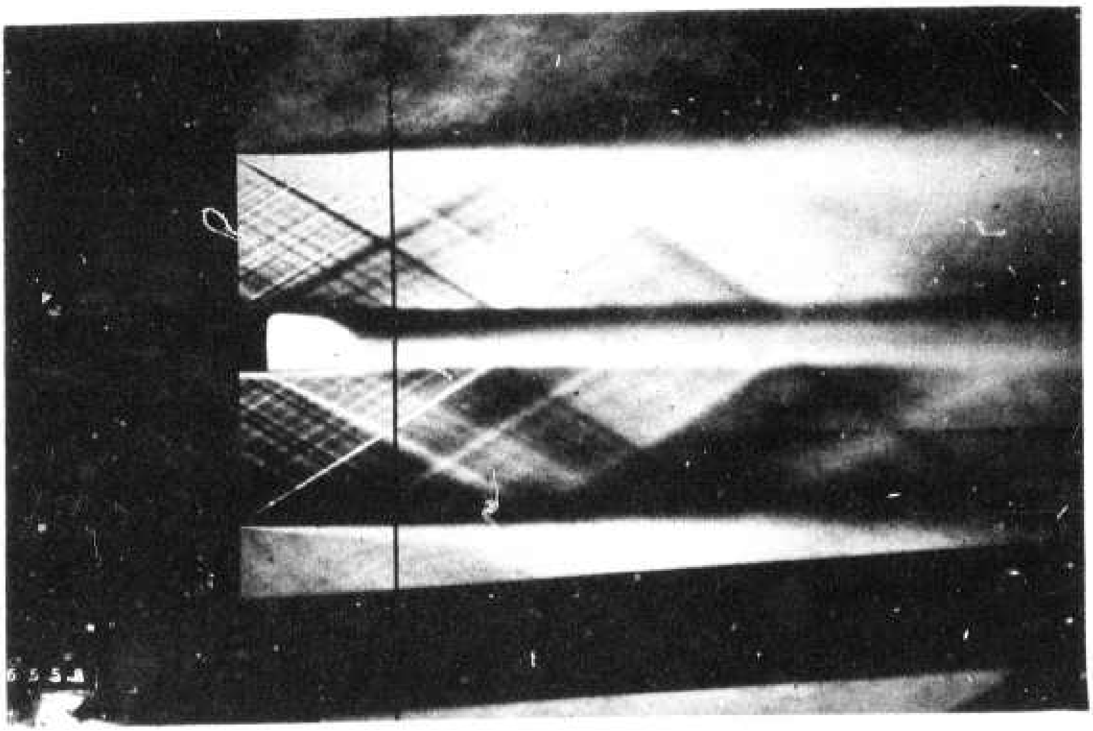

Run 61

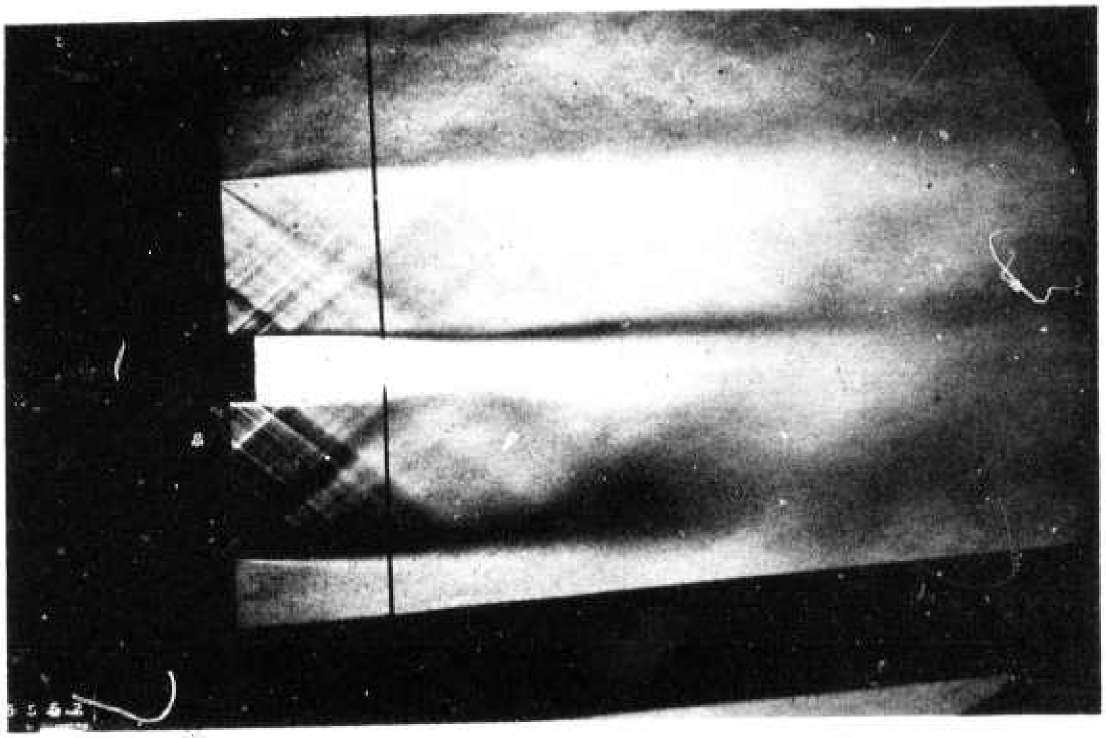

Run 62

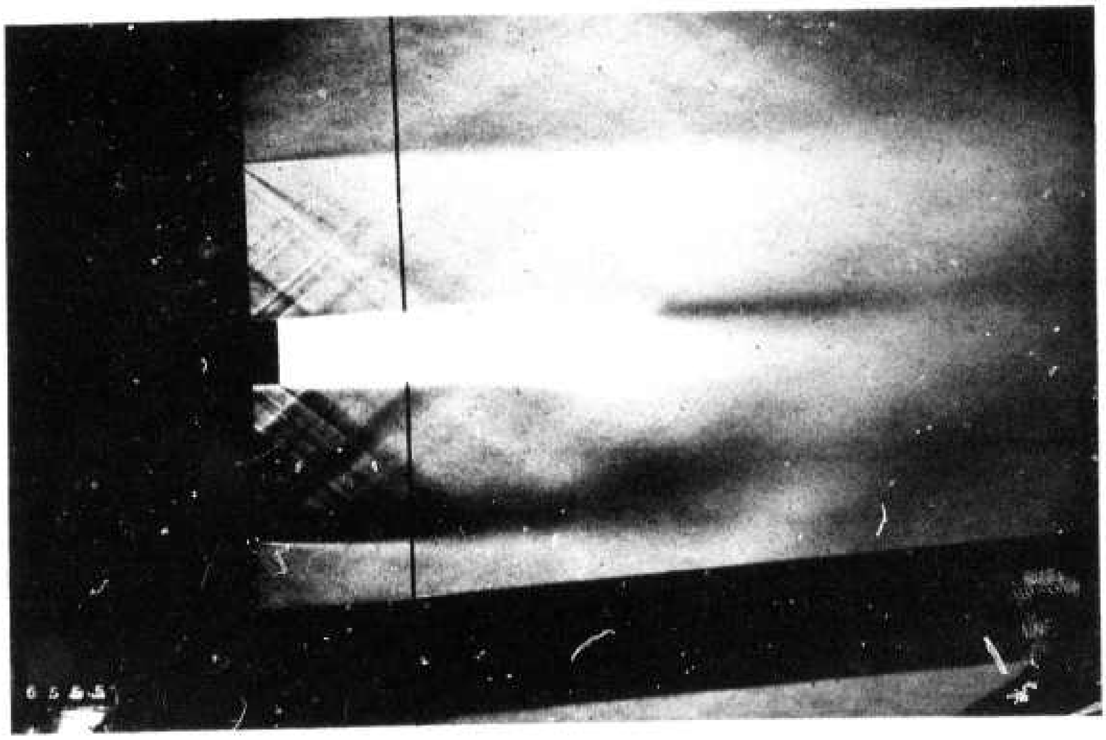

Run 63

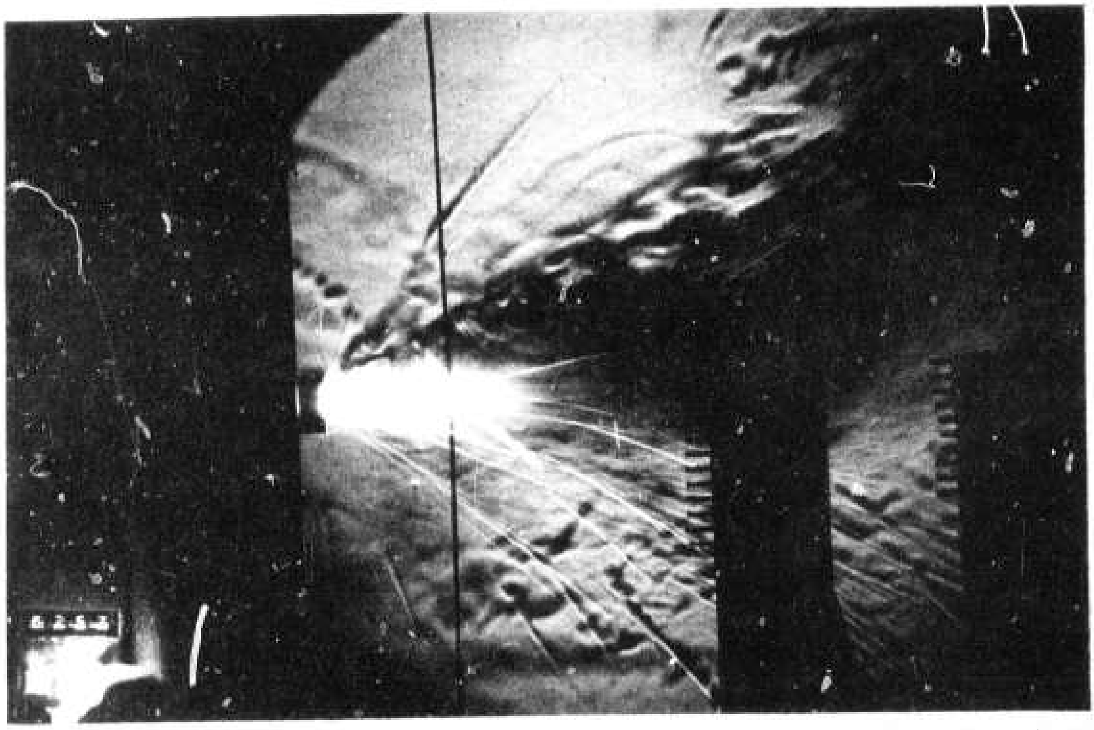

Run 1901 (No airflow)

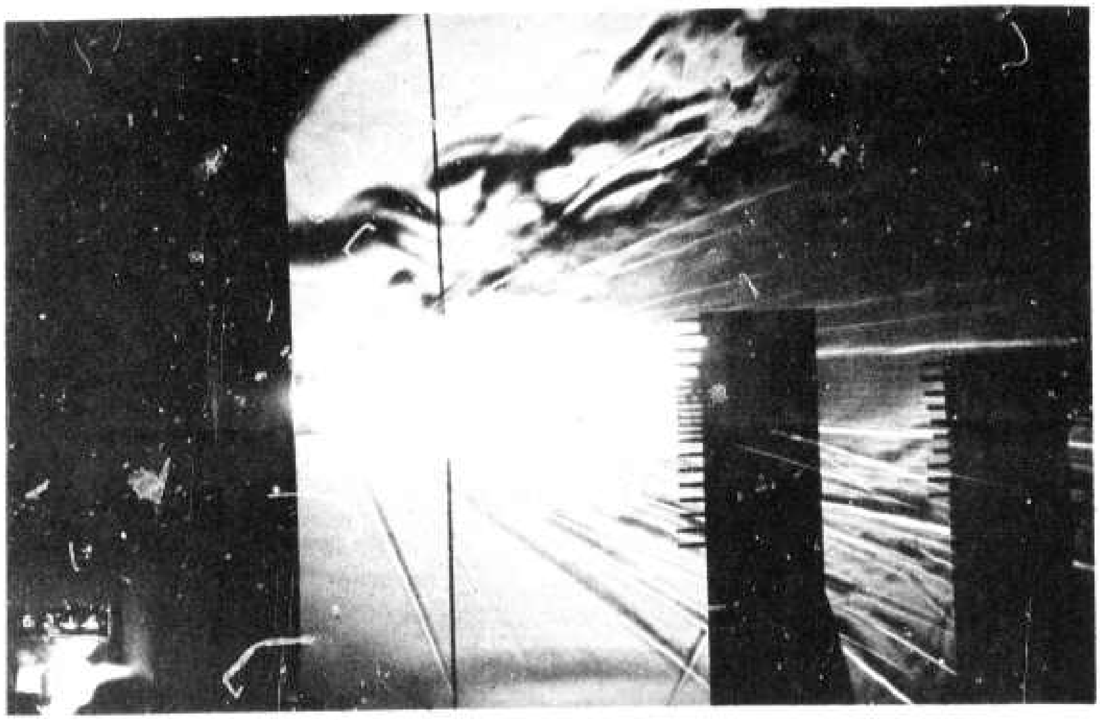

Run 2601 (No airflow)

DISTRIBUTION LIST

No. of Copies	Organization
2	Commander Defense Documentation Center ATTN: DDC-TCA Cameron Station Alexandria, Virginia 22314
1	Director Institute for Defense Analysis ATTN: Dr. H. Wolfhard 400 Army-Navy Drive Arlington, Virginia 22202
1	Commander U.S. Army Materiel Command ATTN: AMCDL 5001 Eisenhower Avenue Alexandria, Virginia 22333
1	Commander U.S. Army Materiel Command ATTN: AMCRD, BG H. A. Griffith 5001 Eisenhower Avenue Alexandria, Virginia 22333
1	Commander U.S. Army Materiel Command ATTN: AMCRD-T 5001 Eisenhower Avenue Alexandria, Virginia 22333
1	Commander U.S. Army Materiel Command ATTN: AMCDMA 5001 Eisenhower Avenue Alexandria, Virginia 22333
1	Commander U.S. Army Materiel Command ATTN: AMCRD-MT 5001 Eisenhower Avenue Alexandria, Virginia 22333

No. of Copies	Organization
1	Commander U.S. Army Aviation Systems Command ATTN: AMSAV-E 12th & Spruce Streets St. Louis, Missouri 63166
1	Director U.S. Army Air Mobility Research and Development Laboratory Ames Research Center Moffett Field, California 94035
1	Commander U.S. Army Electronics Command ATTN: AMSEL-RD Fort Monmouth, New Jersey 07703
4	Commander U.S. Army Missile Command ATTN: AMSMI-R AMSMI-RK Dr. R. Rhoades Mr. N. White Redstone Arsenal, Alabama 35809
1	Commander U.S. Army Tank Automotive Command ATTN: AMSTA-RHFL Warren, Michigan 48090
2	Commander U.S. Army Mobility Equipment Research & Development Center ATTN: Tech Docu Cen, Bldg. 315 AMSME-RZT Fort Belvoir, Virginia 22060
2	Commander U.S. Army Armament Command ATTN: G. Fischer J. Turkeltaub Rock Island, Illinois 61202

DISTRIBUTION LIST

No. of Copies	Organization
7	Commander U.S. Army Frankford Arsenal ATTN: SARFA-L1000 SARFA-J7200, C. Dickey Mr. R. Kwatnoski Ms. Elmendorf SARFA-J7100, G. Bornheim SARFA-J5300, W. Gadomski SARFA-8200, D.Mancinelli Philadelphia, Pennsylvania 19137
8	Commander U.S. Army Picatinny Arsenal ATTN: A. Beardell H. Hudgins D. Katz S. Kravitz J. Picard F. Taylor N. Weins D. Werbel Dover, New Jersey 07801
1	Commander U.S. Army White Sands Missile Range ATTN: STEWS-VT New Mexico 88002
1	Commander U.S. Army Harry Diamond Laboratories ATTN: AMXDO-TI Washington, DC 20438
1	Commander U.S. Army Materials and Mechanics Research Center ATTN: AMXMR-ATL Watertown, Massachusetts 02172

No. of Copies	Organization
1	Commander U.S. Army Natick Laboratories ATTN: AMXRE, Dr. D. Sieling Natick, Massachusetts 01762
2	Commander U.S. Army Research Office (Durham) ATTN: Mr. R. Heaston Tech Lib Box CM, Duke Station Durham, North Carolina 27706
3	Commander U.S. Naval Air Systems Command ATTN: AIR-604 Washington, DC 20360
3	Commander U.S. Naval Ordnance Systems Command ATTN: ORD-0632 ORD-035 ORD-5524 Washington, DC 20360
1	Chief of Naval Research ATTN: ONR-429 Department of the Navy Washington, DC 20360
1	Commander U.S. Naval Missile Center ATTN: Code 5632 Point Mugu, California 93041
4	Commander U.S. Naval Weapons Center ATTN: Code 608 Mr. E. Price Mr. J. Crump Code 753, Tech Lib Mr. J. Eisel China Lake, California 93555

DISTRIBUTION LIST

No. of Copies	Organization
2	Commander U.S. Naval Ammunition Depot ATTN: B. Douda J. Tanner Crane, Indiana 47522
1	Commander U.S. Naval Ordnance Laboratory ATTN: Code 730 Silver Spring, Maryland 20910
1	Director U.S. Naval Research Laboratory ATTN: Code 6180 Washington, DC 20390
1	Commander U.S. Naval Weapons Laboratory ATTN: Tech Lib Dahlgren, Virginia 22338
2	Superintendent U.S. Naval Postgraduate School ATTN: Tech Lib A. Fuhs Monterey, California 93940
2	Commander U.S. Naval Ordnance Station ATTN: Dr. A. Roberts Tech Lib Indian Head, Maryland 20640
1	AFSC (DOL) Andrews AFB Washington, DC 20331
1	AFOSR (SREP) 1400 Wilson Boulevard Arlington, Virginia 22209
2	AFRPL (RPMCP) ATTN: Dr. R. Weiss Dr. R. Schoner Edward AFB California 93523

No. of Copies	Organization
1	Director Hypersonic Research Lab (ARR) Aerospace Research Labs (OAR) Wright-Patterson AFB Ohio 45433
1	ARL (R. Tischer) Wright-Patterson AFB Ohio 45433
2	Headquarters National Aeronautics and Space Administration ATTN: RPS; RP Washington, DC 20546
1	Director NASA Scientific and Technical Information Facility ATTN: CRT P.O. Box 33 College Park, Maryland 20740
1	Director National Aeronautics and Space Administration George C. Marshall Space Flight Center ATTN: Tech Lib Huntsville, Alabama 35812
2	Director Jet Propulsion Laboratory ATTN: Dr. J. Strand Tech Lib 4800 Oak Grove Drive Pasadena, California 91103
1	Director, NASA John F. Kennedy Space Center ATTN: Tech Lib Kennedy Space Center Florida 32899

DISTRIBUTION LIST

No. of Copies	Organization
1	Director National Aeronautics and Space Administration Langley Research Center ATTN: MS-185, Tech Lib Langley Station Hampton, Virginia 23365
1	Director, NASA Manned Spacecraft Center ATTN: Tech Lib Houston, Texas 77058
2	Director National Aeronautics and Space Administration ATTN: MS-603, Tech Lib MS-86, Dr. Povinelli 21000 Brookpark Road Lewis Research Center Cleveland, Ohio 44135
1	Aerojet Solid Propulsion Co. ATTN: Dr. P. Micheli Sacramento, California 95813
1	ARO Incorporated ATTN: Mr. N. Dougherty Arnold AFS, Tennessee 37389
1	Atlantic Research Corporation ATTN: Tech Lib Shirley Highway at Edsall Road Alexandria, Virginia 22314
1	Dow Chemical Company ATTN: George Lane Midland, Michigan 48640
1	Explosives Corp of America ATTN: Patrick A. Yates P. O. Box 906 Redmond, Washington 98052

No. of Copies	Organization
1	General Electric Company Flight Propulsion Division ATTN: Tech Lib Cincinnati, Ohio 45215
2	Hercules Incorporated Allegany Ballistic Laboratories ATTN: Dr. R. Yount Tech Lib Cumberland, Maryland 21501
1	Hercules Incorporated Bacchus Division ATTN: Dr. M. Beckstead Magna, Utah 84044
1	Lockheed Palo Alto Research Laboratories ATTN: Tech Info Ctr 3251 Hanover Street Palo Alto, California 94304
2	Lockheed Propulsion Company ATTN: Dr. N. Cohen Dr. R. Derr P.O. Box 111 Redlands, CA 92373
1	McDonnell Douglas Corporation Missile and Space Systems Division ATTN: Tech Lib Santa Monica, California 90406
1	The Marquardt Corporation ATTN: Tech Lib 16555 Saticoy Street Van Nuys, California 91404
1	The Martin-Marietta Corporation Denver Division ATTN: Res Lib P.O. Box 179 Denver, CO 80201

DISTRIBUTION LIST

No. of Copies	Organization
1	MB Associates ATTN: Dr. A. McCone San Ramone, California 94583
2	North American Rockwell Corporation Rocketdyne Division ATTN: Dr. C. Oberg Tech Lib 6633 Canoga Avenue Canoga Park, California 91304
2	North American Rockwell Corporation Rocketdyne Division ATTN: Mr. W. Haymes Tech Lib McGregor, Texas 76657
2	Thiokol Chemical Corporation Elkton Division ATTN: Tech Lib E. S. Stern Elkton, Maryland 21921
3	Thiokol Chemical Corporation Huntsville Division ATTN: Dr. D. Flanigan Tech Lib E. Barnes Huntsville, Alabama 35807
1	Thiokol Chemical Corporation Longhorn Division ATTN: Dave Dillehay Marshall, Texas 79843
3	Thiokol Chemical Corporation Wasatch Division ATTN: Dr. M. Mihlfeith Graham Shaw Tech Lib P.O. Box 524 Brigham City, UT 84302
1	TRW Systems Group ATTN: Mr. H. Korman One Space Park Redondo Beach, California 90278
1	United Aircraft Corporation Pratt and Whitney Division ATTN: Tech Lib P.O. Box 2691 West Palm Beach, Florida 33402
1	United Aircraft Corporation Research Laboratories ATTN: Dr. R. Waesche East Hartford, CT 06108
2	United Technology Center ATTN: Dr. R. Brown Tech Lib P.O. Box 358 Sunnyvale, California 94088
1	Battelle Memorial Institute ATTN: Tech Lib 505 King Avenue Columbus, Ohio 43201
2	Brigham Young University Dept of Chemical Engineering ATTN: Prof. R. Coates Prof. M. Horton Provo, UT 84601
2	California Institute of Technology ATTN: Prof. F. Culick Tech Lib 1201 East California Blvd Pasadena, California 91102
1	Case Western Reserve University Division of Aerospace Sciences ATTN: Prof. J. Tien Cleveland, Ohio 44135

DISTRIBUTION LIST

No. of Copies	Organization
1	Calspan Corporation P.O. Box 235 Buffalo, New York 14221
2	Georgia Institute of Technology School of Aerospace Engineering ATTN: Prof. B. Zinn Prof. W. Strahle S. Pronchick Atlanta, Georgia 30333
1	IIT Research Institute ATTN: Prof. T. Torda 10 West 35th Street Chicago, Illinois 60616
1	Director Applied Physics Laboratory The Johns Hopkins University ATTN. Dr. R. Centrell 8621 Georgia Avenue Silver Spring, Maryland 20910
2	Director Chemical Propulsion Information Agency The Johns Hopkins University ATTN: Mr. T. Christian Tech Lib 8621 Georgia Avenue Silver Spring, Maryland 20910
1	Massachusetts Institute of Technology Dept of Mechanical Engineering ATTN: Prof. T. Toong Cambridge, Massachusetts 02139
1	Pennsylvania State University Dept of Mechanical Engineering ATTN: Prof. G. Faeth University Park, PA 16802

No. of Copies	Organization
3	Princeton University Dept of Aerospace and Mechanical Sciences ATTN: Prof. M. Summerfield Prof. I. Glassman Tech Lib James Forrestal Campus Princeton, New Jersey 08540
7	Purdue University School of Mechanical Engineering ATTN: Prof. J. Osborn Prof. S. N. B. Murthy John Andrews Duane Baker Prof. B. A. Reese Harry Bruestle Prof. D. E. Abbott Lafayette, Indiana 47907
1	Rutgers-State University Dept of Mechanical and Aerospace Engineering ATTN: Prof. S. Temkin University Heights Campus New Brunswick, New Jersey 08903
1	Stanford Research Institute Propulsion Sciences Division ATTN: Tech Lib 333 Ravenswood Avenue Menlo Park, California 94024
1	Stevens Institute of Technology Davidson Laboratory ATTN: Prof. R. McAlevy III Hoboken, New Jersey 07030
2	University of California Dept of Aerospace Engineering ATTN: Prof. S. Penner Prof. F. Williams La Jolla, California 92037

DISTRIBUTION LIST

No. of Copies	Organization
1	University of California Department of Chemistry ATTN: Prof. E. Peterson Berkeley, California 94704
2	University of Denver Denver Research Institute ATTN: R. M. Blunt Tech Lib P. O. Box 10127 Denver, Colorado 80210
2	University of Illinois Dept of Aeronautical Engineering ATTN: Prof. H. Krier Prof. R. Strehlow Urbana, Illinois 61803

No. of Copies	Organization
1	University of Minnesota Dept of Mechanical Engineering ATTN: Prof. E. Fletcher Minneapolis, Minnesota 55455
2	University of Utah Dept of Chemical Engineering ATTN: Prof. A. Baer Prof. G. Flandro Salt Lake City, Utah 84112

Aberdeen Proving Ground

Marine Corps Ln Ofc
Dir, USAMSAA